

Aus dem Institut für Stammzellforschung, Helmholtz-Zentrum München
Vorstand: Prof. Dr. Magdalena Götz
und dem Max-Planck-Institut für Psychiatrie, München
Arbeitsgruppe von Dr. Silvia Cappello

Modeling neuronal heterotopias using iPSC derived neural stem cells, neurons and cerebral organoids derived from patients with mutations in *FAT4* and *DCHS1*

Dissertation
zur Erlangung des Doktorgrades (Dr. rer. nat) der Fakultät für Medizin
an der Ludwig-Maximilians-Universität München

vorgelegt von
Johannes Klaus
aus Augsburg
– 2017 –

Mit Genehmigung der Medizinischen Fakultät
der Universität München

Betreuerin: Prof. Dr. Magdalena Götz

Zweitgutachter: Prof. Dr. Moritz Rossner

Dekan: Prof. Dr. med. dent. Reinhard HICKEL

Tag der mündlichen Prüfung: 09.10.2017

Eidestattliche Erklärung

Ich erkläre hiermit an Eides statt, dass ich die vorliegende Dissertation selbstständig verfasst, mich außer der angegebenen keiner weiteren Hilfsmittel bedient und alle Erkenntnisse, die aus dem Schriftum ganz oder annähernd übernommen sind, als solche kenntlich gemacht und nach ihrer Herkunft einzeln nachgewiesen habe.

Ich erkläre weiterhin, dass ich die hier vorgelegte Dissertation nicht in gleicher oder in ähnlicher Form bei einer anderen Stelle zur Erlangung eines akademischen Grades eingereicht habe.

München, den

Johannes Klaus

Table of Contents

Summary in German	7
Abstract	10
1 Introduction	12
1.1 Basic principles of cerebral development	12
1.1.1 Biology of radial glia	12
1.1.2 The generation of neurons	16
1.1.3 Neuronal migration	20
1.1.4 Malformations of the cortex	24
1.1.5 Typology of defects in neuronal migration	25
1.1.6 Contribution of radial glia scaffold stability	29
1.2 Fat4 and Dchs1 – two new players in cortical development	30
1.2.1 Drosophila Fat and Dachshous	30
1.2.2 Mammalian Fat4 and Dchs1	31
1.3 Question of this study	32
2 Results	35
2.1 Reprogramming patient fibroblasts into induced pluripotent stem cells	35
2.2 Generation of neural stem cells and human cerebral organoids from control and patient fibroblast derived iPSC	36
2.2.1 Neural progenitor cells derived from iPSC	36
2.2.2 Human cerebral organoids	37
2.2.3 Organisation of cortical zones and location of neurons in organoids from mutant cell lines	40
2.2.4 Proliferation of progenitors in mutant organoids	47

2.2.5	Polarity of radial glia in progenitor zones from mutant organoids	48
2.2.6	Morphology of radial glia in mutant organoids	51
2.3	Defects in migration of neurons with mutations in <i>FAT4</i> and <i>DCHS1</i>	56
2.4	The cytoskeleton and cytoskeletal genes are changed in mutant cells	59
2.4.1	Changes in the cytoskeleton of mutant cells	59
2.4.2	Single cell RNA sequencing of microdissected cortical zones	61
2.5	Summary	65
3	Discussion	67
3.1	IPSC based models of neurodevelopmental disease	67
3.2	Modeling neuronal migration disorders using organoids	67
3.2.1	Organoids as a model for development	69
3.2.2	Defects in organoids derived from <i>FAT4</i> and <i>DCHS1</i> mutated cells	70
3.2.3	Morphology of germinal zones in organoids	71
3.2.4	Radial glia in mutant organoids	72
3.3	Defects in neuronal migration	73
3.4	Mechanism behind the effects of <i>FAT4</i> and <i>DCHS1</i> defects on cerebral development	74
3.4.1	Role of the canonical functions of <i>FAT4</i> and <i>DCHS1</i>	74
3.4.2	Proliferation and Hippo signaling	75
3.4.3	Hints towards a molecular mechanism	77
3.5	Conclusion	78
4	Materials and Methods	80
4.1	Cell culture	80
4.1.1	Culture of human fibroblasts	81
4.1.2	Reprogramming of fibroblasts into induced pluripotent stem cells	81

4.1.3	Culture of iPSC	82
4.2	Generation of neural progenitor cells	82
4.2.1	Coating of culture dishes	82
4.2.2	Differentiation of iPSC into NPCs	83
4.2.3	Culture of NPCs	83
4.2.4	Time lapse imaging of neurons	84
4.3	Generation of cerebral organoids	85
4.3.1	Electroporation of organoids	86
4.3.2	Analysis of cerebral organoids	86
4.4	Immunohistochemistry	87
4.5	Quantification of PH3	87
4.6	In-situ hybridization	88
4.7	Generation of miRNAs	89
4.8	Plasmid preparation	90
4.8.1	Small scale plasmid preparation	90
4.8.2	Large scale plasmid preparation	90
4.9	qPCR	91
4.10	Western Blot	92
4.11	Single cell RNA sequencing	93
A	Tables for single cell RNA sequencing data	94
A.1	List of differentially expressed genes with a power greater than 0.4	94
A.2	GO terms related to the cytoskeleton (based on genes with a power greater than 0.4)	99

Zusammenfassung in deutscher Sprache

Die Entwicklung des Gehirns beruht auf genau regulierten und eng abgestimmten Prozessen der Proliferation, Differenzierung und Migration von Zellen. Im sich entwickelnden Neokortex werden Neurone von radialen Gliazellen produziert und migrieren dann entlang der Zellfortsätze der radial Gliazellen zu ihrer endgültigen Position. Die Zahl der Neurone wird durch die Proliferation und Differenzierung der radialen Gliazellen bestimmt, während für die Migration die Stabilität der radialen Zellfortsätze und die Motilität der Neurone selbst entscheidend sind.

Fehlbildungen des Kortex haben ihre Ursache in Störungen dieser Prozesse. Häufig sind es genetische Ursachen, die zur Entwicklung von Fehlbildungen führen, wie z.B. Punktmutationen in Genen, die diese Prozesse regulieren. Die Aufklärung der Ursachen kortikaler Fehlbildungen ist durch die Verwendung von Mausmodellen entscheidend voran gekommen. Allerdings weisen Mausmodelle Grenzen hinsichtlich der Modellierbarkeit menschlicher Entwicklungsprozesse auf, da der sich entwickelnde Kortex der Maus eine weniger komplexe Struktur aufweist.

Die Möglichkeit, induzierte pluripotente Stammzellen (iPSC) aus somatischen Zellen zu generieren eröffnet einen neuen Zugang zu menschlichen Zellen verschiedener Gewebetypen. iPSC können mittels geeigneter Protokolle in verschiedene Zelltypen differenziert werden. Durch diese Technologie ist es möglich, patientenspezifische Zellen zu generieren und durch Vergleich mit entsprechenden Kontrollzelllinien molekulare Mechanismen von Erkrankungen direkt an menschlichen Zellen zu studieren.

Bis vor Kurzem war es nur möglich, Zellen verschiedener Gewebetypen in einer zweidimensionalen Monolayer-Kultur zu generieren. Neuere Protokolle zur Generierung dreidimensionaler Gewebestrukturen, sogenannter Organoiden, eröffnen neue Möglichkeiten, Zellen in einem dreidimensionalen Gewebekontext zu untersuchen. Speziell zur Untersuchung der Entwicklung des Gehirnes gibt es die Möglichkeit, zerebrale Organoiden zu erzeugen. Zerebrale Organoiden bilden tubuläre Strukturen aus, in denen sich radiale Gliazellen, verschiedene Progenitorotypen und Neurone in einer Anordnung befinden, wie man sie auch im Embryo vorfinden würde. Menschliche zerebrale Organoiden können spezifisch menschliche Prozesse widerspiegeln, die sich in der Maus nicht finden.

Die vorliegende Arbeit untersucht die Rolle von *FAT4* und *DCHS1* in der Entwicklung von neuronalen Migrationsstörungen bei Patienten mit *van Maldergem Syndrom*, einer genetischen Erkrankung mit einer großen Zahl verschiedener Symptome, zu denen das Auftreten von neuronalen Migrationsstörungen gehört. Schon in der Maus konnte eine Rolle von *Fat4* und *Dchs1* in der Entwicklung des Kortex gezeigt werden. Diese Studie macht sich die Verfügbarkeit von Fibroblasten von Patienten mit *van Maldergem Syndrom* zunutze. Die Fibroblasten wurden zu iPSC reprogrammiert, und dann in neurale Progenitorzellen (NPCs) differenziert oder zur Generierung von zerebralen Organoiden verwendet.

Die Analyse zerebraler Organoiden mit Hilfe von Immunfärbungen zeigte Unterschiede in der Organisation von kortikalen Strukturen zwischen Kontrollorganoiden und Organoiden, die aus mutierten Zellen generiert wurden. In Kontrollorganoiden findet sich eine klare Trennung der neuronalen Zellschicht von der Zellschicht der Progenitoren, während in mutierten Organoiden diese Trennung nicht scharf ist. In Organoiden von *DCHS1*-mutierten Zellen finden sich außerdem Veränderungen an den Neuriten der Neurone. In *FAT4* mutierten Organoiden kann gezeigt werden, dass radiale Gliazellen weniger gerade Zellfortsätze haben und die Zellen zum Teil delaminieren.

Um zu untersuchen, ob Neurone außerdem einen intrinsischen Migrationsdefekt zeigen, wurde *time lapse imaging* mit isolierten Neuronen durchgeführt. In der Tat kann gezeigt werden dass Neurone mit Mutationen in *DCHS1* oder *FAT4* Veränderungen in ihrem Migrationsverhalten zeigen. Sie bewegen sich langsamer, sprunghafter und weniger direkt.

Durch Western-Blot-Analyse von Zellextrakten aus neuronalen Progenitorzellen zeigt sich, dass die Expression von stabilisierten Mikrotubuli, Komponenten des Zytoskeletts, in *FAT4*-mutierten Zellen erniedrigt ist. Durch *single-cell RNA sequencing* von Zellen aus Organoiden, einer Technologie zur Bestimmung des Transkriptom einzelner Zellen, kann gezeigt werden, dass in Zellen mit Mutationen in *DCHS1* oder *FAT4* Komponenten des Zytoskeletts dereguliert sind. Vor allem Tubuline zeigen Veränderungen, was auf eine zentrale Rolle des Zytoskeletts bei der Entwicklung der Fehlbildungen bei Patienten mit *van Maldergem Syndrome* hinweist.

Diese Arbeit stellt einen der ersten Versuche dar, humane neuronale Migrationsstörungen in zerebralen Organoiden zu modellieren. Dabei zeigen sich in der Tat spezifische Phänotypen für Migrationsstörungen in zerebralen Organoiden. Aber auch Neurone, die mit Hilfe eines Protokolls zur Differenzierung von Zellen in

Monolayer-Kultur generiert wurden, zeigen spezifische Defekte. Die Ergebnisse dieser Arbeit legen nahe, dass die Entwicklung von neuronalen Migrationsstörungen in Patienten mit *van Maldergem Syndrom* ihre Ursache in Defekten sowohl in radialen Gliazellen als auch in Neuronen hat.

Abstract

Malformations of the brain are the result of disturbances in the regulation of proliferation, differentiation and migration of cells in the developing central nervous system. In the cortex, malformations often become apparent as mislocalized neuronal tissue, so-called *heterotopias*. In mouse models, neuronal heterotopias could be shown to be the consequence of either disturbed migration of neurons or instability of the scaffold of radial glia processes which neurons use as a guide during migration.

Mouse models revealed many aspects of the mechanism underlying the formation of cortical malformations, however, their use is limited due to structural and functional differences between mouse and humans. Induced pluripotent stem cells (iPSC) offer a promising way to derive human cells of any tissue of interest from patients and control individuals to study the phenotype of cells affected by disease causing mutations. These protocols, however, usually yield two-dimensional monolayer cultures, and do not allow insights into the effects of three-dimensional tissue context on cellular processes. Organoids offer a possibility to overcome this problem, since they represent three-dimensional, embryonic structures which reflect the three-dimensional structure of organs. Cerebral organoids in particular have been shown to reflect the three-dimensional organization, cell type composition, and transcriptional footprints of the developing brain. This work made use of the availability of fibroblasts derived from patients with *van Maldergem Syndrome*, a disease which often comprises the development of neuronal heterotopia and which has been shown to be caused by mutations in *FAT4* or *DCHS1*, to investigate possible mechanisms leading to the development of heterotopia seen in patients. To do this, iPSC were generated from the fibroblasts and differentiated to neural progenitor cells (NPCs) and neurons or three-dimensional cerebral organoids to analyze effects of the mutations on progenitor cells or cortical structures in a three-dimensional context.

Analysis of organoids revealed differences between control cell derived organoids and mutant cell derived organoids in the organization of cortical zones. The separation of the neuronal layer and the progenitor layer was less clear, and nodules of neurons appeared in the progenitor zone. In *DCHS1* mutant derived organoids, neurites of neurons showed a changed morphology.

Especially *FAT4* mutant derived organoids showed changes in the morphology

of radial glia cells, which possess less straight and often truncated processes and often were delaminate from the apical surface. These results could be further supported by knockdown of *FAT4* in control organoids, which revealed a similar phenotype.

To see whether neurons in isolation also show defects, their movement behavior was analyzed by time lapse imaging, which revealed that indeed neurons derived from mutant iPSC cells showed changes in their migration: they moved more slowly, less straight and in a more saltatory fashion.

Finally, single cell RNA sequencing of cells from organoids, which allows for analysis of the transcriptome of single cells, revealed striking changes in cytoskeletal genes in both *DCHS1* and *FAT4* mutant cells. Specifically the expression of tubulins was changed, demonstrating changes in the cytoskeleton, which is a promising candidate to explain the changes seen in organoids and neurons. This is further underlined by western blot analysis of cell extracts from neural progenitor cells which showed changes in the expression of stabilized microtubules, hinting towards a generalized change in the regulation of the microtubule cytoskeleton.

Taken together, this work is one of the first to model neuronal heterotopia in cerebral organoids. It further shows that the phenotype seen in patients is most likely is the result of disturbances in neurons as well as in progenitor cells. Furthermore, it suggests that the mutations analyzed lead to changes in the regulation of the cytoskeleton, which suggests a new function of *FAT4* and *DCHS1* in regulating processes important for neural development.

1 Introduction

1.1 Basic principles of cerebral development

The development of the central nervous system (CNS), as complex and intangible as it may seem, begins with a surprisingly simple embryonic structure, the neural tube. The neural tube is the primordial structure which gives rise to all parts of the CNS. The neural tube is made up of the neuroepithelium, which is constituted by *neuroepithelial cells* (Götz and Huttner 2005), elongated, bipolar cells which span the whole width of the neuroepithelium.

Neuroepithelial cells do not persist, however: they give rise to a more specialized type of cell, designated *radial glia cells* (Paridaen and Huttner 2014; Götz and Huttner 2005). While these cells share a lot of characteristics with neuroepithelial cells, they are distinct from them in marker expression and identity (Kriegstein and Noctor 2004; Florio and Huttner 2014). Radial glia cells have long been thought to be a mere structural aid, namely for migrating neurons. However, they are now recognized to be the prime stem cell of the CNS, generating almost all the cells present in the adult brain (Malatesta et al. 2007). For this reason, they are also called *neural stem cells* (NSC).

The appearance of radial glia opens up the way for more profound transformations of the neuroepithelium. As their biology is central to these transformations, and to the development of the CNS, it will be described in the section to follow, focusing mainly on the development of the cerebral cortex.

1.1.1 Biology of radial glia

As they are derived from neuroepithelial cells, radial glia cells still retain many features of neuroepithelial cells. They are in contact with the luminal side of the neural tube, their cilium reaching into the lumen, and they extend a process up to the basal side (also called *pial surface*) of the neural tube (Schmechel and Rakic 1979). Furthermore, like neuroepithelial cells, they express markers such as Nestin (Hartfuss et al. 2001; Park et al. 2009).

However, radial glia are also distinct in many respects. As is implied by their name, they show many features of glial cells. For example, they express glial markers such as Blpb or Glast (Hartfuss et al. 2001; Kriegstein and Götz 2003)

and show microscopical characteristics of astroglia (Choi and Lapham 1978). It should be mentioned in this context that the glial nature of radial glia, together with the fact that (astro)glia can act as neural stem cell in certain areas of the adult brain, suggests a more profound connection between glia biology and the ability to act as a stem cell (Doetsch 2003).

Neuroepithelial cells possess tight junctions to connect the cells to each other. During their transition to radial glia, tight junctions are replaced by adherent junctions, only retaining the expression of ZO-1, which translocates to adherent junctions (Aaku-Saraste et al. 1996). Adherent junctions are thought to play a crucial role in the biology of radial glia, as they are strongly connected to upholding their apico-basal polarity (Florio and Huttner 2014).

Apico-basal polarity

Already their morphology suggests that radial glia are highly polarized cells, as their morphology is distinctly bipolar. For example, the cilium of radial glia cells is strictly maintained at the apical side, protruding into the lumen of the neural tube (Kriegstein and Götz 2003). Their high degree of polarity is reflected on the molecular level, as many molecules in radial glia are localized differently along their apico-basal axis. For instance, the Notch pathway can show such a polarized pattern, the Notch protein being present at the apical tip of the cell, as has been shown for developing zebrafish retina, for instance (Del Bene et al. 2008).

Radial glia express known regulators of apico-basal polarity, like members of the apical complex, namely Par3, Par6 and aPKC, as well as proteins belonging to the Crumbs complex, such as Crb, Pals, and others (Manabe et al. 2002; Bultje et al. 2009; Imai 2006). Small GTPases like Cdc42 function in this context as well. Cdc42, in particular, regulates adherent junctions of radial glia, which are important in the regulation of cell polarity (Cappello et al. 2006).

The importance of adherent junctions is underlined by the fact that polarity proteins localize in the vicinity of adherent junctions and are in part recruited by them (Singh and Solecki 2015). Adherent junctions in radial glia comprise several proteins, among them N-Cadherin, β -Catenin and α -E-Catenin, the latter being important for the connection between adherent junctions and the cytoskeleton (Junghans et al. 2005; Kadowaki et al. 2007; Harris and Tepass 2010). In addition to cadherins, Nectins are also part of the adherent junctions, binding Afadin,

which is important for establishing connections to the actin cytoskeleton (Takai et al. 2008).

There are several examples of the functional relevance of radial glia cell polarity. Many polarity proteins seem to be involved in the regulation of proliferation, differentiation and fate choices of radial glia (Costa et al. 2007; Bultje et al. 2009; Shen et al. 2002). In this context, one plausible, but still debated model links fate choices of radial glia to the asymmetric inheritance of polarity proteins during cell division. Depending on the orientation of the mitotic spindle, proteins at the apical side of the cell could be distributed asymmetrically, leaving the two daughter cells with different molecular characteristics, which could lead to different fate choices. A mechanism like this is inherently linked to the spatial constraint a radial glia cell is subjected to (Götz and Huttner 2005; Lancaster and Knoblich 2012). That the spatial and physical conditions of a cell are indeed linked to its biological behavior is exemplified by Cdc42 knockout in radial glia, which leads to their delamination by loss of their adherent junctions, followed not only by their translocation away from the apical surface, but also a change of fate (Cappello et al. 2006).

Adherent junctions are highly involved in effects like this, as interfering with components of adherent junctions leads to drastic changes in cerebral development. In most of these cases, the integrity of radial glia is disturbed, leading to massive changes in development with resulting malformations in mouse models (Yamamoto et al. 2015; Schmid et al. 2014; Kadowaki et al. 2007). Adherent junction proteins can also directly be involved in signaling: β -Catenin, a component of adherent junctions, is involved in Wnt-signaling, and β -Catenin bound at adherent junctions has been shown to be recruited for Wnt-signaling in radial glia cells (Kurabayashi et al. 2013).

Interkinetic nuclear migration

While mitosis of radial glia exclusively take place at the ventricular surface, their nuclei are also found at non-ventricular positions, giving the ventricular zone (VZ) of the developing cortex, the layer that is constituted by the nuclei of radial glia, a *pseudostratified* appearance. This is possible because the nuclei move up- and down while going through the cell cycle, a process called *interkinetic nuclear migration* (INM). INM is synchronized with the cell cycle, such that mitosis can take place at the ventricular surface, while the other phases of the cycle are passed while the nucleus is moving up- and down.

While the function of INM can only be speculated on (see below), many parts of its mechanism could be illuminated in recent years. One striking feature of INM is that the protein machinery mediating the apically directed movement is distinct from the one mediating the basally directed movement (Taverna and Huttner 2010). Knockdown of Dynein, a minus-end directed microtubule motor, leads to inhibition of the apically-directed movement, but not the basal one (Tsai et al. 2010). In contrast, interference with Kinesins, such as Kif1a, leads to inhibition of the basally-directed movement (Tsai et al. 2010). Both proteins are microtubule motors, underlining the importance of microtubules for INM. However, actomyosin motors have also been implicated in INM (Schenk et al. 2009). Furthermore, the functional role of centrosomal proteins, such as Cep120, has been recently described (Xie et al. 2007).

The synchronization with the cell cycle might suggest a tight link between INM and the cell cycle, such that inhibiting INM would block mitosis. Of note, at least in mouse models, interfering with INM does not prevent mitosis, contradicting this hypothesis (Taverna and Huttner 2010). When cells are forced to undergo mitosis at basal locations after blockage of INM, the centrosome is displaced from its physiological position and translocated to the nucleus.

However, under physiological conditions, the centrosome is located apically, and it is thought that one important function of INM is to make the centrosome available for the nucleus at the time of mitosis. This could simply be done by just keeping the nuclei at the apical surface. In this case, however, space would be very limited. For this reason, the hypothesis goes, nuclei currently not in M-Phase move away from the ventricular surface to make space for the ones that undergo mitosis. INM would then be a way to increase the number of cells that the ventricular surface can harbor, given the constraint of centrosomal location (Miyata et al. 2015; Fish et al. 2008; Smart 1972).

In addition, one model suggests that the localization of the nucleus during INM, together with the time spent at certain locations, influences cell fate. As certain factors could be localized differently along the apico-basal axis of the cell, the time the nucleus spends at certain positions along the apico-basal axis during INM could have a differential effect. While far from formally proven, there is indeed data from zebrafish suggesting that such a mechanism could be true (Del Bene et al. 2008).

Radial glia and their tissue context

It should have become clear that the biology of radial glia crucially depends on their spatial context in the neural epithelium. Their polarity is strongly connected to their adherent junction belt, tethering them to neighboring cells. While data suggests that factors segregated along their apico-basal polarity can influence their fate, the cilium is maintained apically, protruding into the ventricle, where it can sense signals from the CSF (Johansson et al. 2013).

That radial glia are spatially very well defined is also of importance in connection with the model described in section 1.1.1, which tries to explain fate choices of radial glia with asymmetric distribution of cellular components after cell division. These components can be proteins localized at the apical tip, but it can also be mediated by asymmetric inheritance of the basal process after division, which leads to two different daughter cells, endowing them with different biological behaviors (Miyata et al. 2001). It should be noted in this context, however, that symmetric inheritance of the basal process by splitting has also been observed (Kosodo et al. 2008).

By differential fate choices after division, radial glia can give rise to a variety of cell types, including several types of progenitors with different biological properties, some of which have only recently been characterized.

1.1.2 The generation of neurons

Long thought of as mere structural aid in the developing brain, radial glia cells are now recognized to be the prime stem cells of the developing CNS (Malatesta et al. 2000; Noctor et al. 2001). At the beginning of cerebral development, radial glia undergo symmetric, proliferative divisions, but soon switch to an asymmetric division mode (Götz and Huttner 2005). They can generate neurons directly, but more common is the generation of subsequent progenitor cells that, in turn, can generate neurons by themselves (Florio and Huttner 2014). The following sections will describe the most important of these progenitor cells.

Short neural precursors and intermediate progenitors

Radial glia cells are also considered *apical progenitors* because of their apical contact and the location of their mitosis at the ventricular surface. They also generate another type of apical progenitor, *short neural precursors* (SNP). SNPs are,

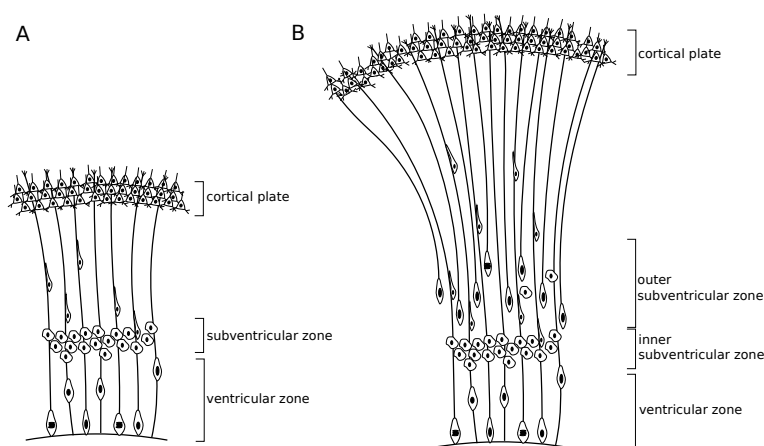


Figure 1.1: Schematic representation of the histology of the developing cortex in mouse (A) and humans (B).

like radial glia, bipolar cells and retain their apical attachment. However, they have lost their basal process. SNPs differ from radial glia in marker expression, as they do not express *Blpb* and *Glast* (Gal 2006; Tyler and Haydar 2013). Although they usually do not receive much attention, they are very abundant in the murine developing cortex (Gal 2006). SNPs are considered to be mainly neurogenic, i.e. they divide to generate a pair of neurons (Stancik et al. 2010), which also has led to a newer name, *apical intermediate progenitor* (Florio and Huttner 2014).

Not only apical progenitors can be observed in the developing cortex, but also cells dividing at a more basal location, where they form a distinct progenitor zone, the *subventricular zone* (SVZ) (Haubensak et al. 2004; Noctor et al. 2004). It is populated by multipolar cells which have delaminated from the apical surface, lost their expression of *Pax6* and upregulated *Tbr2* (Englund 2005). This type of progenitor cells is called *intermediate progenitor* or *basal intermediate progenitor* (Florio and Huttner 2014). They either divide to generate neurons directly, or they amplify to increase the neuronal output (Miyata 2004; Noctor et al. 2004).

Basal radial glia

An additional type of progenitors was discovered by analyzing the developing human fetal cortex, which revealed interesting differences to the developing rodent cortex. Only at early stages they are very similar, with a ventricular zone containing radial glia cells, and a subventricular zone populated by intermediate progenitors. At later stages, the cortex of humans rapidly expands radially, and a massive increase in thickness of the proliferative layers can be observed (Hansen

et al. 2010) and as a consequence, additional proliferative layers emerge. They are constituted by radial glia-like cells, which have a basal process, but usually lost their apical contact (Hansen et al. 2010; Fietz et al. 2010) (Fig. 1.1). These cells are called *basal radial glia* (bRG) or *outer radial glia* (oRG).

It turns out bRGs are not only found in humans, but in many other primates (Betizeau et al. 2013), and even in non-primate species like the ferret (Reillo et al. 2010). What these species have in common is a more complex cortical structure, which includes the formation of gyri, a consequence of the need to accommodate an increased number of neurons.

BRGs have been shown to generate neurons (Hansen et al. 2010), but they can also self-renew and expand their own population (Hansen et al. 2010). In ferret, it has been shown that there is a dedicated time-window for the generation of bRGs by apical radial glia cells, after which they sustain their population by self-renewing divisions (Martínez-Martínez et al. 2016). Analogous to the nuclear movement of radial glia cells, bRGs undergo a similar movement called mitotic somal translocation (MST), which is the upward movement of their nucleus just prior to mitosis (Hansen et al. 2010; Ostrem et al. 2014).

The existence of bRGs in many species, including humans, introduces a lot more of heterogeneity into the landscape of progenitors. Indeed, bRGs themselves seem to display a greater heterogeneity than previously thought, at least with respect to morphology and cell cycle kinetics (Betizeau et al. 2013). Basal radial glia, like radial glia, even generate IPs, adding to the complexity of the developing cortex (Betizeau et al. 2013). In addition, apical radial glia change after the appearance of their basal counterparts, both in gene expression profile as well as in respect to their morphology, which seems to involve truncation of their basal process (Nowakowski et al. 2016).

Molecular control of neurogenesis

Naturally, the molecular machinery that controls the generation of different progenitor subtypes and neurons is complex. Generally, it can be differentiated between effectors that instruct radial glia identity, and keep radial glia in a more proliferative state, and effectors that induce the generation of either subtypes of progenitors or the differentiation to neurons. The *Notch* signaling pathway, for instance, has been shown to be important for the transition from neuroepithelial cells to radial glia (Hatakeyama 2004). Impairment of Notch-signaling in radial

glia leads to premature commencement of neurogenesis (Hatakeyama 2004), while its activation suppresses the generation of basal progenitors from radial glia cells (Mizutani et al. 2007). Premature activation of Notch leads to induction of RG markers in neuroepithelial cells (Gaiano et al. 2000). These data imply that Notch is capable of instructing radial glia fate and regulating the generation of downstream cell types.

Other factors regulate the generation of subsequent progenitor types or the differentiation to neurons. For example, basal progenitors are increased in number upon downregulation of *Trnp1* in the mouse developing cortex (Stahl et al. 2013). It should be mentioned in this context that *Trnp1* has been also implied in the generation of gyri (Stahl et al. 2013), promoting the idea that basal progenitor numbers and function are linked to gyrification.

There are also many transcription factors that are able to regulate the generation of basal progenitors. Notable examples are Insulinoma-1, Neurogenin-2 and AP2 γ . All these three factors induce the expression of *Tbr2*, a transcription factor being important in basal progenitors (Pinto et al. 2009; Miyata 2004; Farkas et al. 2008). Factors like these have been mainly described in mouse, and for their capacity to generate basal progenitors in the SVZ.

Factors that regulate the generation of basal progenitors, have turned out to be important for understanding species difference in cortical architecture. Notably, a human specific duplicated version of *ARHGAP11A*, *ARHGAP11B*, has been shown to increase the generation of basal progenitors, and, like *Trnp1*, is able to induce folding of the cortex when overexpressed in mouse (Florio et al. 2015).

It is still an open question, however, how the generation of *basal radial glia* in species where these cells are more numerous is regulated. One hint comes from a study in ferret, showing that basal radial glia are generated in a dedicated, short time-window, where *Cdh1*, an adherent junction protein, is found to be able to regulate the production of basal radial glia (Martínez-Martínez et al. 2016). The exact molecular action is not clear, but it is feasible to assume that it is part of regulating the delamination of apical radial glia cells in order to generate a basal radial glia.

In fact, it is an interesting feature of the developing cortex that physical delamination from the ventricular zone, for example by interfering with adherent junctions, can lead to at least a partial induction of fate change. One example, the effect of downregulating *Cdc42* in mouse, has already been mentioned (Cappello et al. 2006). This phenomenon underlines the fundamental property of neurogenesis

already hinted to (see section 1.1.1), namely the functional role of spatial location and physical confinement in specifying cell behavior.

Finally, a set of transcription factors has been found that instruct neuronal differentiation. Pax6 is a generic widely expressed determinant of neurogenesis, but it has a very complex role, as it, for instance, also regulates dorsal versus ventral identity of progenitor cells (Quinn et al. 2007). However, it is able to induce neuronal fate in astrocytes (Heins et al. 2002). Neurogenin-1 and -2, for example, specify glutamatergic neuronal subtypes, and Ascl1, on the other hand, is important for the specification of interneurons. Strikingly, some of these factors can induce neuronal fate in cells from a completely different lineage. Ascl1, for example, induces neuronal fate in fibroblasts (Vierbuchen et al. 2010).

1.1.3 Neuronal migration

After different subtypes of progenitors appeared, what started out with a homogeneous sheet of neuroepithelial cells has transformed into a multilayered structure, the developing cortical wall. The progenitor cells reside in different proliferative zones. The neurons that are generated from these progenitors are

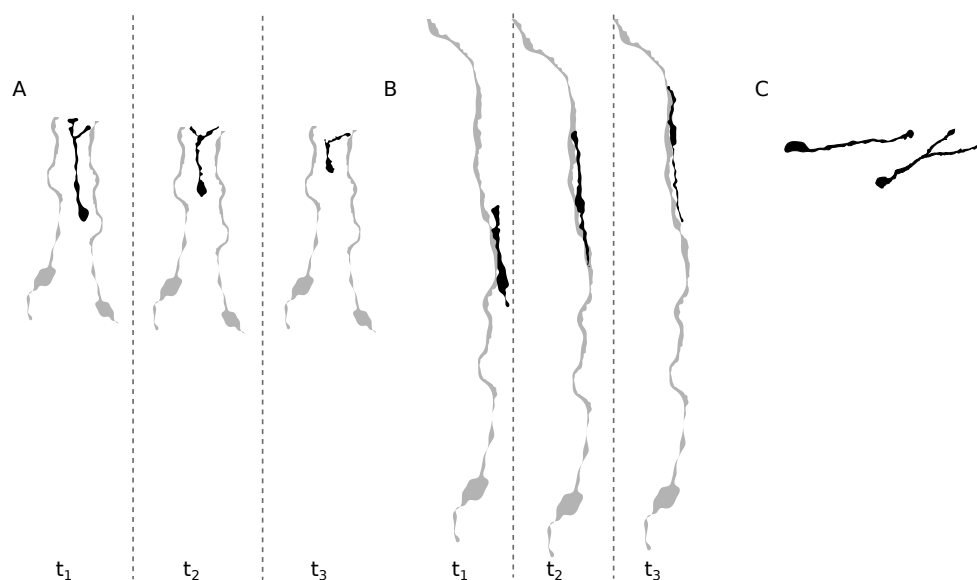


Figure 1.2: Schematic silhouettes of the morphology of neurons during migration with different migration modes. Somal translocation of an excitatory neurons, independent of radial glia (A, radial glia in grey). Radial glia guided locomotion of an excitatory neuron, migrating along a radial glia cells (B, radial glia in grey). Morphology of an migrating interneuron during tangential migration (C). Note the branching process.

not born at their final position, but have to migrate to their destination, either taking a radial route in case of excitatory neurons born in the VZ of the cortical wall, or an even more complicated and longer, tangential, route in the case of interneurons, which are generated in the ventral portion of the telencephalon.

Excitatory neurons born in the ventricular zone can undergo two modes of migration, somal translocation or radial glia guided locomotion (Evsyukova et al. 2013) (Fig. 1.2,A,B). At the beginning of neurogenesis, when the cortex is still relatively small, somal translocation is thought to be the primary mode of movement. During somal translocation, the cell remains attached to the basal surface, and pulls itself up by its basal process (Fig. 1.2, A) (Miyata et al. 2001; Nadarajah 2003).

Later, cells switch to radial glia guided locomotion. Here, the neuron has a bipolar morphology, the leading process extending into the direction of movement, and a thin, short trailing process at the rear. While migrating, the cell is attached to the basal process of a radial glia cell, which it uses as a guide (Rakic 1972; Noctor et al. 2001) (Fig. 1.2, B).

Radial glia guided locomotion

That neurons can use radial glia as guides for their migration has first been suggested in fixed tissue, showing neurons being apposed to a radial glia fiber (Rakic 1972). The dynamics of their migration, however, could only be illuminated by time-lapse imaging studies, which allowed to follow single neurons over time. Migrating neurons, it became clear, change the dynamics of their migration during their journey, and the radial migration of an excitatory neuron can be divided into distinct phases (Noctor et al. 2004).

The first phase is a short radial migration up to the SVZ or the intermediate zone (IZ), which lies just basal to the SVZ (Noctor et al. 2004; Tabata et al. 2009). There, the neuron enters the second phase, the multipolar phase. During this phase, the neuron adapts a multipolar morphology, showing only little movement and extending processes in various directions (Tabata and Nakajima 2003). After this phase, the neuron finally assumes a bipolar morphology, attaches to a radial glia fiber and migrates to the cortical plate. At the cortical plate, the neuron enters its final phase, usually undergoing somal translocation to reach its final position (Evsyukova et al. 2013).

The function of the multipolar phase is still enigmatic. One can speculate that it

might have to do with a need to polarize the cell, inducing neuritogenesis and the growth of an axon (Tabata and Nakajima 2003). This is suggested, for example, by the fact that Cdk5 is needed during the multipolar phase of neuronal migration, and Cdk5 is also important for dendritic development (Ohshima et al. 2007). Specifically, Cdk5 acts in polarizing the cell, which might be necessary before the neuron can commence proper radial migration. Also, other proteins, such as N-Cadherin, Reelin, and the small GTPase Rap1 have been found to be important for orienting the neuron during its multipolar phase (Jossin and Cooper 2011). In addition, the multipolar phase might also play a role in specifying layer identity (Miyoshi and Fishell 2012).

After leaving the multipolar phase, the neuron is polarized, having a leading process and a thin trailing process, which will be its future axon (Barnes and Polleux 2009; Noctor et al. 2004). The movement pattern of radially migrating neurons is saltatory, and it follows a cyclic pattern: the leading process extends and shows a characteristic swelling, the nucleus is pulled up to the leading process, and finally, the trailing process retracts. After retraction of the trailing process, the cycle begins again. The pattern of nuclear movement is called *nucleokinesis*. It is thought to be an upward pull mediated by the centrosome, which is ahead of the nucleus during migration (Ayala et al. 2007).

Microtubules and microtubule motors play very likely a role in this process. It is thought that microtubules, originating at the centrosome, extend posteriorly to the nucleus, engulfing it in a microtubule cage, and anteriorly into the leading process (Tsai and Gleeson 2005). The nucleus is tethered to the microtubule by a complex involving Dynein (Tanaka et al. 2004). As a result, a pulling force can be transmitted to the nucleus, leading to an upward movement.

In addition to microtubules and microtubule binding proteins, actin and actomyosin motors have also been implicated in nucleokinesis during radial migration (Ayala et al. 2007). It is thought that actomyosin, being localized at the rear part of the migrating cell, contracts in order to exert a pushing force on the nucleus (Schaar and McConnell 2005).

The existence of more diverse set of progenitors in many species complicates neuronal migration. While apical radial glia may acquire a truncated morphology (Nowakowski et al. 2016), neurons can migrate along a greater diversity of paths by following different bRG processes. Indeed, in ferret, a species with abundant bRGs, neuronal migration follows complicated patterns (Gertz and Kriegstein 2015). The increase in migration pathways accessible to neurons in species with

a higher number of bRGs could be a way to increase the complexity of cortical architecture that can result from these developmental processes.

The migration of interneurons

Interneurons are not generated in the ventricular zone of the cortex, but in the ventral portions of the telencephalon, the ganglionic eminences (Anderson et al. 2001) (Fig. 1.3). Specifically, most interneurons arise from the medial ganglionic eminence and the caudal ganglionic eminence, while only few interneurons arise from the preoptic area (Marín 2013). In order to reach the cortex, they have to migrate significantly greater distances and follow a more convoluted path. Their mode of migration is called *tangential migration*. Upon reaching the cortex, they abandon their tangential mode of movement and switch to radial migration, sometimes undertaking a short detour to the apical surface before turning around and moving up to the cortical plate (Marín 2013).

When crossing the pallial-subpallial boundary, interneurons do not enter the cortical plate as one single stream of cells, but rather come separated in two streams (Fig. 1.3). One stream is located just below the cortical plate, crossing

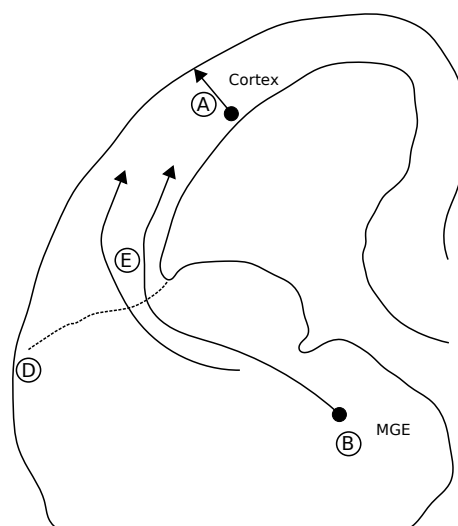


Figure 1.3: Schematic representation of a coronal section of a mouse forebrain (approx. E14) with migration paths of cortical neurons and interneurons. Exemplified here is the generation of interneurons in the MGE (B) and their migration across the pallial-subpallial boundary (D, dotted line) in two different migratory streams (E). Cortical neurons are generated in the VZ of the cortex and take a radial path to the cortical plate (A).

through the marginal zone (MZ), while the second stream crosses through the SVZ (Marín 2013). It is interesting in this context that interneurons in the lower, SVZ-crossing, stream seem to be attracted by Tbr2+ IPs (Sessa et al. 2010), a striking example of the kind of tissue interactions that help shaping the cortex.

While migrating, interneurons are polarized in the direction of movement, extending a leading process and pulling a trailing process behind (Fig. 1.2,C). In contrast to excitatory neurons, the leading process of interneurons shows continuous branching. All but one of the branches will collapse, the remaining one determining the direction of movement. This process, which resembles axonal pathfinding is thought to be important for sensing guidance cues (Marín 2013).

Guidance cues are important for determining the path of interneurons to the cortex. For instance, they have to be repelled by ventral structures, such as the striatum. Cues mediating this repellent effect are, for example, Ephrin-A5/EphA4R interactions (Zimmer et al. 2008) or Semaphorins (Marin 2001). There also are attractive cues that direct the migration of interneurons to the cortex. One example would be Neuregulin-1 (Flames et al. 2004). Neuregulin-1 exists in two isoforms, one of them being a membrane-bound form, acting as local guidance cue and forming a permissive corridor for migration. The other isoform is secreted and acts as a long-range guidance molecule (Flames et al. 2004)

1.1.4 Malformations of the cortex

The processes described in the last sections are the basis for the development of a properly formed and well-functioning cortex. Perturbations, either by environmental insults or due to mutations, lead to the development of cortical malformations. The different kinds of malformations that can be seen are of course numerous, depending on the particular process or system affected.

Some malformations affect the size of the brain, or the cortex in particular, as does, for instance, *microcephaly*. People suffering from this condition have a drastically reduced brain size that goes hand in hand with a reduced size of their heads and severe mental disabilities. *Megencephaly*, in contrast, would belong to the opposite type, as patients display a massive increase in size of one or both hemispheres, leading to a variety of symptoms, including epilepsy (Leventer et al. 2008). The size of the brain is affected by many genes that are involved in spindle regulation, and many genes mutated in patients with microcephaly

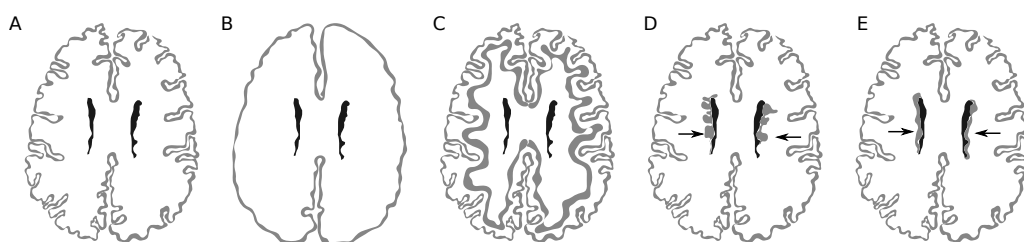


Figure 1.4: Schematic representation of different types of neuronal migration defects, as they would present in a MRI scan. A normal brain is depicted in (A). Lissencephaly type I (B). Subcortical band heterotopia (C). Periventricular heterotopia of the nodular type (D) and the laminar type (E).

belong to this group, such as *ASPM* and *CENPJ* (Faheem et al. 2015). On the other hand, megalencephalies can be caused by mutations in RTK-PI3K-AKT signaling, a downstream effector of FGF-2 (Hevner 2015).

One class of malformations is called *neuronal migration disorders*, as from their phenotype it seems that the migration of neurons during development is impaired (see section 1.1.3). Usually, these diseases are characterized by abnormally localized neurons, which form nodules or sheets at locations normally devoid of gray matter. The symptoms of patients with this kind of malformations differ, and they range from almost symptomless cases to severe forms with intellectual disabilities and epilepsy. The following section will describe the most important types of neuronal migration disorders in detail

1.1.5 Typology of defects in neuronal migration

One hallmark of the human cortex is its pronounced degree of gyrification, in contrast to, say, rodents, whose cortical surface has a smooth appearance, i.e. they are *lissencephalic*. There are, however, malformations of the human brain where the number and morphology of gyri in humans is changed. On the one hand, diseases like *polymicrogyria* show a highly increased number of gyri, while patients with *lissencephaly* have a smooth cortex without any gyrification (Fig. 1.4, B).

Lissencephaly is classified as a neuronal migration disorder, although the connection is at first sight not obvious (Walsh 1999; Leventer et al. 2008). However, from both a pathological as well as a mechanistic point of view, neurons do show indeed a defect in migration.

There are two classes of lissencephaly, *type II cobblestone lissencephaly* and the

“classical” *type I lissencephaly*. The former shows cobblestone-like outgrowths at the pial surface, which is thought to result from defects in the integrity of the pia (Walsh 1999). *Type I lissencephaly*, however, is characterized by a reduction or absence of gyri with a completely smooth surface. In this type of lissencephaly, the structural aberrations are more profound and widespread, and also affect the layering of the cortex, which sometimes only has four instead of six layers and other deficits (Leventer et al. 2008). Patients often suffer from epilepsy and severe forms of intellectual disabilities.

Patients suffering from *subcortical band heterotopia* (SBH), which sometimes is also referred to as *double cortex*, have a more clear displacement of neurons (Leventer et al. 2008). They show a second sheet of neurons below the proper, normotopic cortex, being separated from the ventricle by white matter (Fig. 1.4, C) (Leventer et al. 2008). This makes it look like a second cortex being located below the first one, which is the reason for the term “double cortex”. However, the second cortex does not show the degree of organization the normal cortex would have, therefore, *subcortical band heterotopia* should be the preferred term (Leventer et al. 2008).

The symptoms of SBH are usually milder intellectual disabilities than in lissencephaly patients, but very often they suffer from epilepsy, too (Leventer et al. 2008).

The hallmark of SBH is the sheet of white matter that separates the neurons from the ventricle. In many cases of malformations, heterotopic neurons are found directly at the ventricle, with no white matter separating them from the surface. This kind of malformations are referred to as *periventricular heterotopias* (PH) (Fig. 1.4, D,E). Depending on the morphology of the heterotopic neuronal tissue, they are referred to as *periventricular laminar heterotopia* (Fig. 1.4, D) or *periventricular nodular heterotopia* (Fig. 1.4, E) (Leventer et al. 2008). Patients with PH can be completely without symptoms, but very often, they suffer from epileptic seizures.

Genetic causes of cortical malformations

In recent years, many mutations that cause cortical malformations have been identified. Their identification not only helps to understand the pathogenesis of cortical malformations, but also offers new insights into the processes of the development of the cortex.

Neuronal migration disorders in particular show a specific pattern: genes that

are functionally involved in the regulation of the cytoskeleton stick out (Liu 2011). The cytoskeleton play a central role in many processes involved in the development of the cortex, such as stabilization radial glia (see section 1.1.1) or neuronal migration (see section 1.1.3), so this may not seem surprising. The following section describes some important genes found to be causative for defects in neuronal migration.

Microtubules and microtubule-associated proteins

Mutations or deletions of *LIS1* (*PAFAH1B1*) explain about 50% of cases of lissencephaly (Walsh 1999). Most patients show deletions, sometimes of larger chromosomal regions that comprise other genes, but point mutations are reported as well (Walsh 1999).

Hints to the way *LIS1* functions come from its ortholog in *Aspergillus Nidulans*, nudF. NudF in *Aspergillus* is important for the translocation of the nucleus, and this depends on the interaction with nudA, which is encoded by the ortholog of *DYNEIN* in mammalian cells. Dynein is a microtubule-minus-end directed motor. That *LIS1* is involved in the function of microtubules is underlined by the fact that it precipitates with microtubules and regulates their stability (Sapir 1997). The interaction between nudF in *Aspergillus* is conserved in mammalian cells, where *LIS1* interacts with Dynein (Sasaki et al. 2000).

The *LIS1*-Dynein complex is thought to be involved in organizing the spindle apparatus (Wang et al. 2013; Vallee et al. 2000), and as such, *LIS1* might play a role in regulating spindle orientation and mitosis in neural progenitors. Furthermore, the *LIS1*-Dynein complex localizes to the centrosome and seems to be important for the coupling between centrosome and nucleus (Tanaka et al. 2004). This not only plays a crucial role for interkinetic nuclear migration in progenitors (see section 1.1.1), but also for nucleokinesis in neuronal migration (see section 1.1.3), hence being a possible explanation for a migration defect in neurons.

There are mouse mutants of *Lis1*. Their phenotypes vary depending on the gene dosage left. The homozygous null mouse is not viable, the heterozygous null shows a disorganized cortex as well as defects in the hippocampus (Wynshaw-Boris et al. 1998).

Lissencephalies are also caused by mutations in another gene, *DCX*. *DCX* is located on the X chromosome, hence, there is a disparity between male and female phenotypes: male patients display lissencephaly, while females, who are mosaics

for the mutation due to random X inactivation, usually show the phenotype of SBH (Walsh 1999). However, it is not clear how mosaicism contributes to the disparity between the two phenotypes.

DCX encodes Doublecortin (*DCX*), a microtubule associated protein. It precipitates with microtubules, and it is localized on the microtubule cage that is formed around the nucleus during nucleokinesis in migrating neurons (see section 1.1.3) (Walsh 1999; Tanaka et al. 2004). Functionally, it has been shown that *DCX* functions together with *LIS1* in centrosome-nucleus coupling (Tanaka et al. 2004).

The knockout of *Dcx* in mouse does not recapitulate the phenotype seen in humans, but interestingly, acute knockdown using RNAi in rats (but not in mice) does show a phenotype similar to the human disease (Nosten-Bertrand et al. 2008; Ramos 2005). Besides a possible species difference, this hints to the not uncommon situation that a constitutive knockout does not show a phenotype, while acute intervention does. However, it should be noted that the *Dcx* knockout mouse does show a defect in the hippocampus (Nosten-Bertrand et al. 2008).

There are also other microtubule genes associated with neuronal migration disorders, namely some tubulins themselves, such as *TUBA1A*, *TUBB3* or *TUBBG1* (Liu 2011). They cause varying syndromes and defects. Mutations in *TUBA1A* cause lissencephaly in humans, while, reminiscent of the situation with *DCX*, a mouse mutant of a GTP-binding site in *TUB1A1* shows aberration in the hippocampus, but no cortical defects (Liu 2011). Generally, this points to an important role of the microtubule cytoskeleton in the processes associated with neuronal migration and maturation. However, also the actin cytoskeleton has been implicated in the pathogenesis of cortical malformations.

Actin cytoskeleton-related genes

The actin-binding protein Filamin A (*FLNA*) has been strongly implicated in periventricular heterotopia (Walsh 1999), accounting for roughly 25% of all cases of periventricular nodular heterotopia (Liu 2011). *FILAMIN A* is X-linked, and mutations are usually lethal in males, while periventricular heterotopia occurs in females.

Filamins are actin-binding and cross-linking proteins (Feng and Walsh 2004). Their function in cross-linking actin is important for cell migration in different cell types (Cunningham et al. 1992; Xu et al. 2010). Specifically, Filamins could mediate cell stiffness and spreading in migrating cells, as well as adhesive in-

teractions with the substrate (Nakamura et al. 2011). In addition, it has been suggested that Filamin A might be required for establishing polarity in migrating neurons (Nagano 2004).

There is a knockout mouse model for *FILAMIN A*, but it once more does not show a phenotype reminiscent of periventricular heterotopia. RNAi in the rat cortex seems to lead to ectopic neurons (Carabalona et al. 2011). Interestingly, in these experiments, the authors could see disruptions of the radial glia scaffold, hinting to a possible role of Filamin A not only in migrating neurons, but also in neural progenitors (Carabalona et al. 2011).

1.1.6 Contribution of radial glia scaffold stability

From the examples given in the section above, it should have become clear that genes mutated in patients with malformations can function in both, radial glia as well as neurons. In principle, one can hypothesize that neuronal migration defects can arise due to two defects: disintegration of the scaffold of radial glia would deprive neurons of their guide for migration, leaving them stalled, or making them migrate in the wrong direction. On the other hand, many defects can be imagined where the radial glia scaffold is left intact, however the neuron is unable to migrate due to intrinsic, cell autonomous defects.

There are mouse models that model aspects of neuronal migration disorders, such as SBH or PH, by disturbing genes that, until now, have not been shown to be mutated in patients. One striking example is the conditional knockout of RhoA, which shows SBH (Cappello et al. 2012). The role of RhoA could, in this case, be clearly assigned to radial glia, as RhoA $-/-$ knockout neurons migrate normally in a wild type context (Cappello et al. 2012). Specifically, the radial scaffold disintegrates due to the instability of its processes, and due to the dismantling of adherent junctions. As a consequence, rosette-like structures are formed, and neurons generated in this environment migrate either, as they are supposed to, to the cortical plate, or they catch a ventricular-oriented process and migrate apically, leading to the appearance of two layers of neurons (Cappello et al. 2012).

A similar disruption of adherent junctions can be seen in knockout mice of α -E-Catenin, which leads to gross disturbances of radial glia structure and misdirected migration of neurons (Schmid et al. 2014). The same is true of Afadin, another protein involved in adherent junctions formation, whose knockout leads to the formation of a double cortex in mouse (Yamamoto et al. 2015). As mentioned,

some data in humans indicates the involvement of radial glia in the pathogenesis of malformations as well (Carabalona et al. 2011; Ferland et al. 2008).

These models indicate that gross disturbances of the radial scaffold do lead to neuronal heterotopia in mice, but still leaves the question of the contribution of different cell types to the pathology in human patients unanswered.

1.2 Fat4 and Dchs1 – two new players in cortical development

From what has been described so far, genes involved in neuronal migration disorders are often connected to the cytoskeleton. However, there are also genes where this connection does not seem so obvious. Recently, patients suffering from *Van Maldergem Syndrome* have been described to also suffer from cortical malformations, such as PH (Mansour et al. 2012). Mutations in *FAT4* or *DCHS1* could be identified as being causative, but until now, it is not known how these two genes cause cortical malformations (Cappello et al. 2013).

The exact role of *FAT4* and *DCHS1* in mammals is unclear, but more and more things could be clarified in recent years. Much more is known about their orthologs in *Drosophila*, *Fat* and *Dachsous*, which will be described in the following section.

1.2.1 Drosophila Fat and Dachsous

Drosophila *Fat* (*Ft*) and *Dachsous* (*Ds*) are giant protocadherin proteins, belonging to the cadherin superfamily of proteins. They have a large extracellular domain with many cadherin repeats, followed by a transmembrane and an intracellular domain. *Ft* and *Ds* form heterophilic complexes across cell borders (Matakatsu 2004).

Ft and *Ds* have two main functions in *Drosophila*: the first is the regulation of *planar cell polarity* (PCP), the second is the regulation of growth by modulating the *Hippo* signaling pathway (Matakatsu 2004).

PCP refers to the polarization of a sheet of cells along its tangential axis. The directional information that is created by PCP is crucial for many developmental processes, including the proper orientation of stereocilia in the cochlea, the movement of fluids by directional beating of cilia and the function of the kidney (Vladar et al. 2015; Papakrivopoulou et al. 2013; Jones and Chen 2007). In

Drosophila, PCP is regulated by two pathways: the first one, called the *core pathway*, is based on Frizzled (Fz) signaling components, while the second one is mediated by Ft and Ds. Ft-Ds mediated PCP signaling is thought to interact with the core pathway, but this must be in an indirect manner, as Ft-Ds can still induce polarity in the absence of the core pathway (Thomas and Strutt 2011).

The mechanism behind Ft-Ds induced planar polarity includes a third protein, Four-jointed (Fj). While Ft is expressed homogeneously across tissues, Ds and Fj are expressed in gradients (Thomas and Strutt 2011). As Fj modulates the interaction between Ft and Ds, it is thought that Ft-Ds-complex formation is polarized across the mediolateral axis of cells (Thomas and Strutt 2011).

Besides the regulation of PCP, Ft and Ds are modulating *Hippo*-signaling. The Hippo pathway mediates the phosphorylation of the transcription factor York1 (Yki) by Warts, which leads to the deactivation of Yki (Halder and Johnson 2010). As Yki induces the transcription of genes important for proliferation, Hippo signaling has a negative effect on proliferation and growth (Halder and Johnson 2010).

There is an interesting hypothesis that tries to link PCP and the regulation of Hippo by Ft and Ds (Lawrence et al. 2008). This hypothesis assumes that the steepness of the gradient of Ft-Ds complex formation in the context of PCP signaling also modulates Hippo signaling, such that the steeper the gradient, the less Hippo is activated. As steepness decreases with increasing organ size, Hippo would be activated from a certain threshold size on, halting growth of an organ at an appropriate size (Lawrence et al. 2008).

1.2.2 Mammalian Fat4 and Dchs1

There are several mammalian orthologs for Ft and Ds. Four different Fat genes found in mammals, *Fat1-3* and *Fat4*, *Fat4* being the closest to Ft. The orthologs of Ds in mammals are *Dchs1* and *Dchs2*, while Fj has only one ortholog, *Fjx1*. The functions of the proteins these genes code for is largely unclear, but *Fat4* and *Dchs1* are thought to interact, like Ft and Ds, and to regulate PCP as well as Hippo signaling (Saburi et al. 2008; Mao et al. 2011).

Knockout mice of *Fat4* and *Dchs1* indeed show defects that can be attributed to defective PCP regulation and partly to disturbances in growth. Pups are born in mendelian ratios, however, they stop to grow and die soon after birth (Saburi et al. 2008; Mao et al. 2011). They show changes in the orientation of stereocilia in

the cochlea and cystic dilations of the kidneys, both phenotypes being indicative of PCP defects (Saburi et al. 2008; Mao et al. 2011). In addition, bones are changed in shape and size, and many organs are smaller (Saburi et al. 2008; Mao et al. 2011).

Knockout mice do not seem to show pronounced defects in the CNS, however. This is surprising, because, besides the fact that mutations in *Fat4* and *Dchs1* do lead to malformations in the cortex, *Fat4* and *Dchs1* are expressed in the ventricular zone of mice, localizing close to the adherent junctions (Ishiuchi et al. 2009). In another region, *Fat4* and *Dchs1* have been shown to be important for migration of facial-branchiomotor neurons, which depends on the regulation of PCP (Zakaria et al. 2014). Interestingly, in this system, there is a gradient of expression of both *Fat4* and *Dchs1*, unlike to the situation in *Drosophila*, where only *Dchs1* shows a graded expression (Zakaria et al. 2014), indicating that the mechanism of action of *Fat4* and *Dchs1* is not identical to the one of *Ft* and *Ds* in *Drosophila*.

While the PCP dependent disturbances of the migration of facial-branchiomotor neurons are highly indicative of a functional role of *Fat4* and *Dchs1* in migration per se, it should be noted that the type of migration affected in this system is tangential migration. Patients with van Maldergem Syndrome show cortical heterotopias, which are supposed to be the result of defective radial migration. The knockout mouse does not show defects in the cortex like those seen in patients, however, acute knockdown by in-utero electroporation of shRNAs leads to over-proliferation of progenitors, which could be linked to changes in Hippo signaling (Cappello et al. 2013). In postnatal stages, heterotopic neurons could be found in electroporated mice. But how exactly these two phenomenons are connected remains enigmatic. Especially, it is not clear whether knockdown of *Fat4* and *Dchs1* in neurons leads to an intrinsic migration defect in those neurons, or if the effect is based on the disruptions or the mislocalized proliferation of progenitors.

1.3 Question of this study

The sections above have illustrated how valuable mouse models have been for the study of cortical development and malformations. However, in many cases, we observe discordances between the observed phenotypes in humans and mouse models. As illustrated, many knockout models do not show a clear phenotype,

while acute intervention, like RNA interference (RNAi), does. It has remained unclear why that is so.

Furthermore, rodents show obvious biological differences to humans. Humans have a much more complicated variety of progenitors, that reside in a proliferative zone that rodents do not have, the OSVZ (see section 1.1.2). The environment neurons have to migrate in is radically different from the one seen in mouse. Therefore, there is a need for models that reflect the situation in humans.

Induced pluripotent stem cells (iPSC) offer a way to access tissue specific human cells, derived from control individuals or patients. This technology has become more and more important for the study of human biology and human disease. However, most protocols for differentiating iPSC into specific cell types result in the generation of single cells in traditional monolayer culture systems. While these culture systems still are very valuable for the study of human specific biological processes, they exclude all effects that stem from the three-dimensional tissue context a cell is normally embedded in.

Organoids offer a way to partly overcome this problem. Organoids are three-dimensional structures derived from stem cells. Their value stems from the fact that they recapitulate structural properties of organs (Clevers 2016).

Organoids can be derived from adult stem cells, as has been demonstrated, for instance, for intestinal organoids, but a lot of protocols for the generation of organoids make use of embryonic stem cells. Using these methods, quite remarkable three-dimensional structures, such as eye-cups, can be formed (Eiraku et al. 2011). *Cerebral organoids* represent three-dimensional organoids of the developing CNS, being able to generate several regions of the brain (Lancaster et al. 2013). As it has been stressed that the biology of radial glia cells is crucially shaped by its tissue context and its spatial and physical properties, cerebral organoids offer an interesting way to look at the biology of human neural progenitor cells in a more natural context. Still it has to be kept in mind, however, that cerebral organoids are artificial in-vitro systems, retaining influences on the cells coming from tissue interactions, but also lacking many influences one would find in an embryo, and being equally susceptible to in-vitro artefacts as traditional cell culture systems are.

The goal of this work is to analyze the defects of human, patient derived cells with mutations in *FAT4* or *DCHS1* in neuronal migration. Specifically, the question is whether defects in patients can be explained by phenotypes in patient derived progenitors, neurons or both of these cell types. As the mouse model did not

yet clearly answer the question if neuronal migration would be intrinsically impaired, this work tries to access neurons in isolation, and look at their migration capabilities.

2 Results

2.1 Reprogramming patient fibroblasts into induced pluripotent stem cells

Van Maldergem Syndrome is a hereditary disease leading to a multitude of defects. Patients suffer, among other symptoms, from cystic kidney disease as well as hearing and breathing defects. One of the major clinical features they present with are cortical malformations (Mansour et al. 2012).

As disease causing genes, *FAT4* and *DCHS1* could be identified (Cappello et al. 2013). Patients usually have compound heterozygous or homozygous mutations in either *FAT4* or *DCHS1*. Most of these mutations are point mutations or single-base deletions, leading to missense mutations or truncations (Cappello et al. 2013) (Table 2.1).

Table 2.1: Description of fibroblast samples from *van Maldergem Syndrome* patients, including the mutation and the protein domain affected (Cappello et al. 2013)

<i>DCHS1</i>			
Individual	Mutation	Protein	Affected domain
D1	c.2503G>T	p.Gly842X	Cadherin Repeats
D2	c.2543delC	p.Thr848Asn30X	Cadherin Repeats, Truncation
D3	c.7109A>T	p.Asn2370Ile	Cadherin Repeats
<i>FAT4</i>			
Individual	Mutation	Protein	Affected domain
F1	c.12476G>T; c.13193G>A	p.Cys4159Phe;p.Cys4398Tyr	Juxtamembrane domain, missense mutation
F2	c.7123G>A; c.9841G>T	p.Glu2375Lys; p.Glu3161X	Cadherin Repeats
F3	c.14512_14513de	p.Ser4838Leufs*3	Intracellular domain

Fibroblasts from patients or control individuals can be reprogrammed into induced pluripotent stem cells (iPSC). iPSC, behaving much like embryonic stem cells, can be used to derive tissue specific cell types for analysis. For example, they can be used to derive neural tissue for analysis of phenotypes relevant for diseases of the CNS.

For this study, fibroblasts from individuals D1-3, F1 and F2 were available. To

generate neural cells from these cells, they were reprogrammed into iPSC (in collaboration with Dr. Micha Drukker, Helmholtz-Center Munich). Not all lines were successfully reprogrammed, and in the end, only line D2 and F1 were analyzed for further experiments (henceforth referred to as “DCHS1 mutant” and “FAT4 mutant”). The mutation in D2 is predicted to cause a truncation of the whole protein, only leaving a fragment of 7 cadherin repeats. The mutation in F1 is predicted to be a missense mutation in the juxtamembrane domain of the protein (Cappello et al. 2013).

In order to generate neural cells from these iPSC, two approaches were taken: the generation of neural progenitor cells (NPCs) on the one hand, and the generation of cerebral organoids on the other hand.

2.2 Generation of neural stem cells and human cerebral organoids from control and patient fibroblast derived iPSC

2.2.1 Neural progenitor cells derived from iPSC

A well established method for deriving neural progenitors from iPSC is to use monolayer cultures and specific inhibitors to promote neural fate (Chambers et al. 2009). These protocols usually provide a high yield of neurons, however, subculturing neural *progenitors* from these cells is difficult.

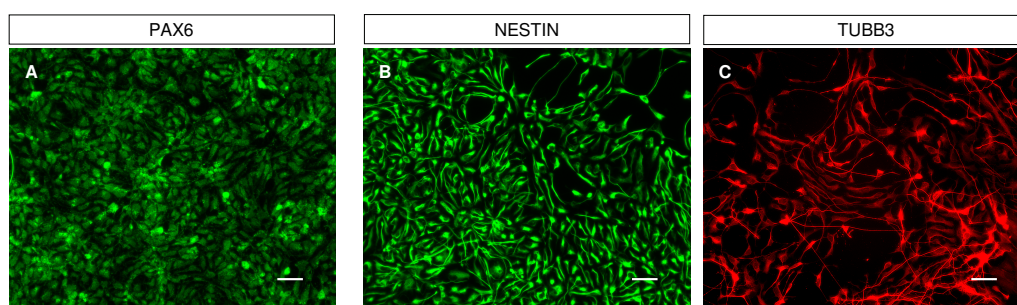


Figure 2.1: Marker expression of NPCs generated from iPSC by picking rosettes from embryoid bodies. (A-C) Progenitor markers PAX6, NESTIN, and neuronal marker TUBB3. Scalebar: 50 μ m

Another protocol makes use of the generation of embryoid bodies, which can be generated from iPSC by culturing them in suspension (Brennand et al. 2011; Topol et al. 2015). Embryoid bodies are cellular aggregates that contain cells from all three germ layers. Neuroectodermal tissue can be discerned after plating em-

bryoid bodies, because neuroepithelial cells form characteristic tubular structures, *neural rosettes*. Neural rosettes can be selected and picked under a microscope, dissociated and further cultured as NPCs.

Neural progenitors generated by this method express NESTIN and give rise to TUBB3+ neurons (Fig. 2.1, B,C). They also express PAX6 (Fig. 2.1, A). The number of TUBB3+ cells increases with further passaging, and it also increases when leaving out bFGF from the culture medium. More mature neurons can be derived by adding factors such as BDNF, GDNF, cAMP and Vitamin C (Topol et al. 2015).

2.2.2 Human cerebral organoids

Keeping embryoid bodies in suspension under appropriate conditions will allow rosettes to expand and to develop into neuroepithelial structures (Eiraku et al. 2008). In order to stabilize them, extracellular matrix proteins, as are provided by cell-culture additives like Matrigel, can be supplied in the culture medium (Kadoshima et al. 2013). Alternatively, the aggregates can be embedded in a droplet of Matrigel (Lancaster et al. 2013).

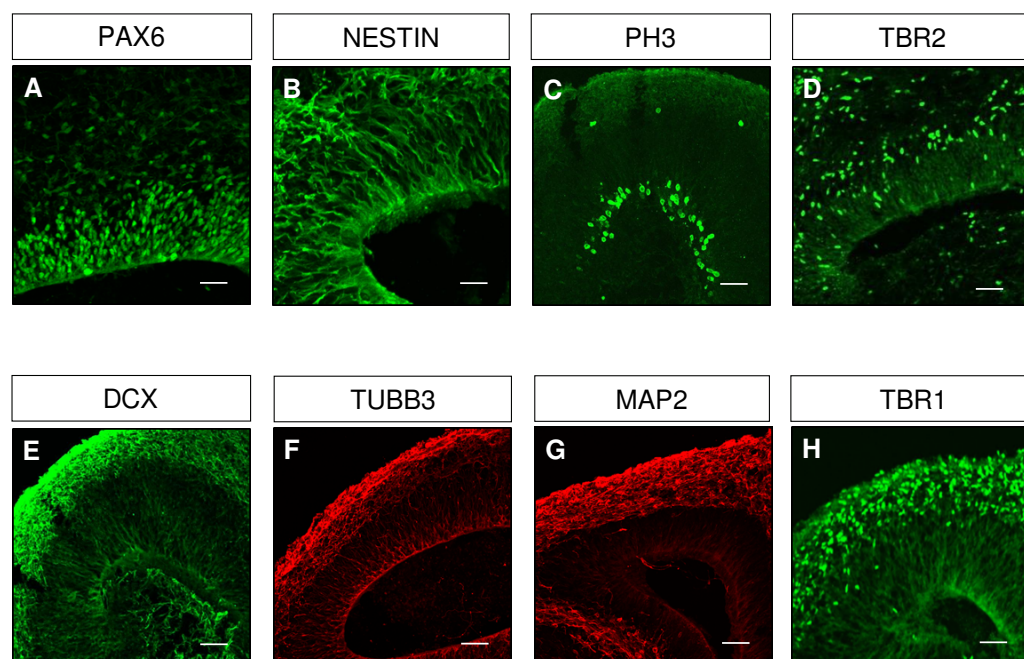


Figure 2.2: Expression of markers in cortical zones of control organoids, day 30 after plating. Organoids express progenitor markers PAX6 and NESTIN (A,B). Mitotic progenitors in the cortical zone (C). TBR2+ cells in an organoid (D). Expression of neuronal markers in organoids (E-H).

Allowing them grow further under constant agitation leads to the development of structures that very much resemble an early stage of the developing cerebral cortex: a zone of PAX6+ radial glia (Fig. 2.2, A) which proliferate (Fig. 2.2, C) and express other progenitor markers, such as NESTIN and PH3 (Fig. 2.2, A,B,C) are surrounded by a neuronal layer, labeled by different neuronal markers (Fig. 2.2. E-H). TBR2 positive intermediate progenitor cells can also be observed, spread across the whole structure, but accumulating in a band above the ventricular zone, reminiscent of the subventricular zone that is found in the developing cortex.

Cerebral organoids are quite variable and it turned out that not all of these markers can be reliably found. Especially markers indicative of dorsal forebrain identity, namely TBR1, SATB2 or CTIP2 were not always found, and the same is true for TBR2. The lack of controllability of regional identity is a central weakness of the protocol used.

However, the generation of neurogenic structures, *cortical zones*, with a clear separation of neurons from progenitors, remained very stable, and prompted the question whether mutations in *FAT4* or *DCHS1* would affect the organization of cortical zones and the position of neurons, which is aberrant in patients. First, it had to be checked whether *FAT4* and *DCHS1* are expressed in organoids.

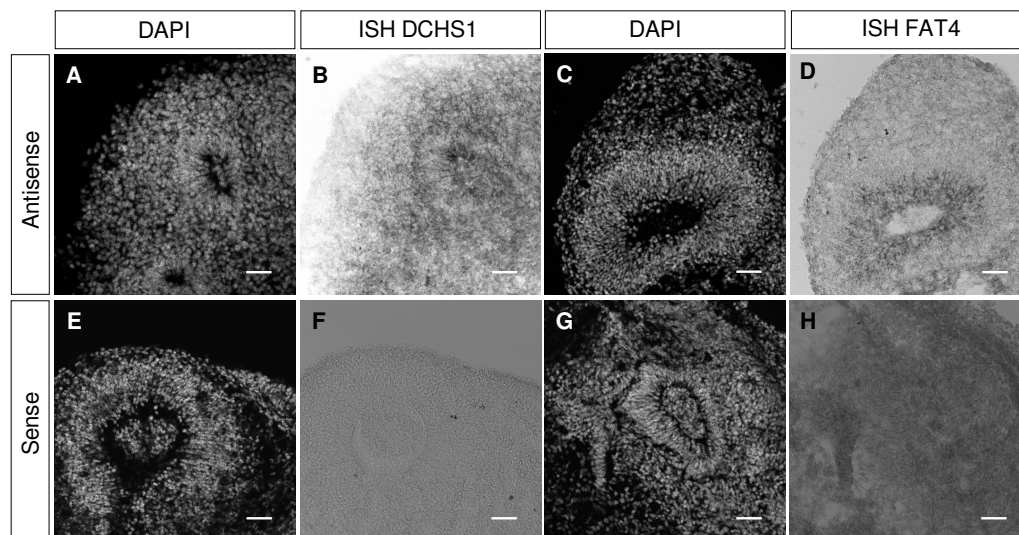


Figure 2.3: ISH using probes against *DCHS1* and *FAT4* mRNA in control organoids, day 70. Signal of *DCHS1* antisense probe (B) and antisense probe (F). Signal of *FAT4* sense (D) and antisense probe (H). Scalebar is 50 μ m

FAT4 and *DCHS1* are indeed expressed by developing organoids, as could be shown by *in situ hybridization* experiments using probes against *FAT4* or *DCHS1*

mRNA (Fig. 2.3) in control organoids. The probe against *FAT4* showed a strong signal around the ventricular lumen. There was also signal in more superficial layers, where one would expect neurons, albeit less strong (Fig. 2.3, C,D). Also the probe against *DCHS1* showed signal around the ventricular lumen that sometimes was more evenly distributed, also in the superficial layers (Fig. 2.3, A,B). This pattern is very similar to the expression pattern found in the human fetal cortex, where both *FAT4* and *DCHS1* mRNA can be detected in progenitors as well as in the cortical plate (Cappello et al. 2013). It also is confirmed by published single cell RNA sequencing data, which shows the expression of *FAT4* in both progenitors and neurons in organoids, as well as the expression of *DCHS1*, albeit the latter was found in fewer cells, with a slight overrepresentation in neurons (Camp et al. 2015).

2.2.3 Organisation of cortical zones and location of neurons in organoids from mutant cell lines

In order to see how *FAT4* and *DCHS1* would affect the organization of cortical zones in organoids, organoids derived from a control iPS cell line and the two mutant cell lines were generated (see Table 2.1). Both cell lines were able to form organoids that grew comparably to organoids from the control cell line (Fig. 2.4).

Tendentially, organoids from *FAT4* had a less regular shape and more easily formed cysts and outgrowths, but all organoids differed widely from batch to batch in this respect, and a clear pattern could not be found.

Neuronal heterotopia affects the localization of neurons. A way to see if the localization of neurons is also changed in organoids from patient cells is to perform immunohistochemistry for a neuronal marker. MAP2 is a microtubule associated protein specifically expressed in neuronal dendrites, and it can be used

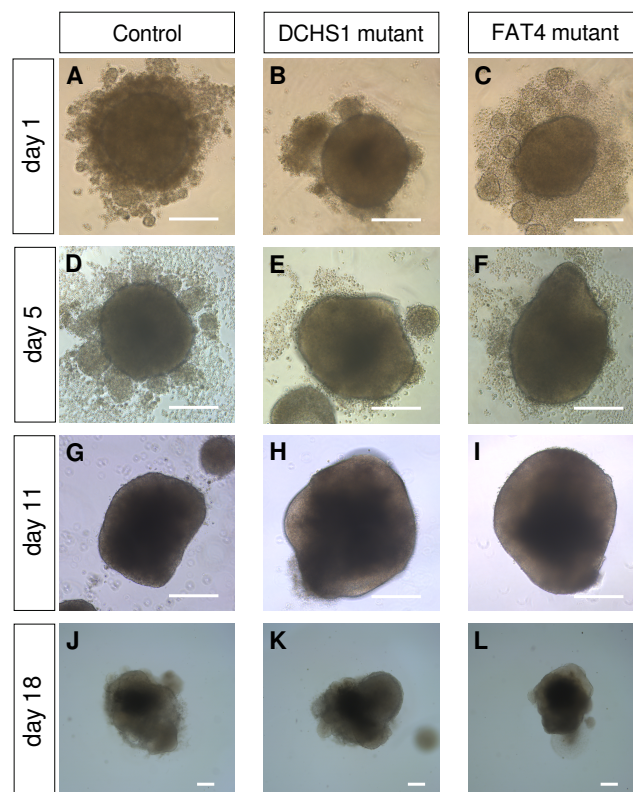


Figure 2.4: Organoids from control and mutant cell lines during their development, starting one day after plating. Day 1 and day 5 represents the initial plating step (A-F). Day 11 in neural induction medium (G-H). Day 18 shortly after embedding in matrigel (J-L). Scalebar: 200 μm in all panels.

as a general neuronal marker. To see if there are any changes in the localization of neurons, immunostaining for MAP2 was performed in organoid slices from organoids at age day 42 and day 70. As both time points did not show striking differences, they were pooled together for further analysis.

Indeed, most control organoids showed a clear separation of MAP2+ neurons from the progenitor zone (Fig. 2.5, A,B). However, in some cases, intruding fibres could be observed in the control (Fig. 2.6, B, white arrowheads). In many cases, *DCHS1* mutant organoids showed cortical zones organized similarly to control zones, but very often, the morphology of the neurites, labeled by MAP2, was clearly changed (Fig. 2.5, D, and Fig. 2.6, D). Compared to control, neurites were thicker and appeared in bundles, forming a trunk-like appearance. Between these thick fibres, patches devoid of MAP2 immunostaining could be seen, in contrast to control organoids, where fibers usually formed a dense network, leaving no empty spaces.

FAT4 mutant organoids, on the other hand, provided a different picture. The morphology of neurites seems comparable to the control, but the cortical zones seemed to be much less organized. Especially, the separation between neuronal layer and progenitor zone was much less clear (Fig. 2.5, C,D and Fig. 2.6, C,D), with many fibres intruding back. In some cases, the border between the neuronal layer and the progenitors could hardly be seen (Fig. 2.7, C,D), and massive intrusion of MAP2+ fibres into the progenitor zone could be observed in some cases (Fig. 2.7, A,B).

In addition, not only was the progenitor zone less discernible from the neuronal layer, but it also seemed to have a less coherent ventricular surface, which very often had a irregular and disrupted appearance (Fig. 2.5,D).

In patients with neuronal heterotopias, neurons very often form nodular clusters of heterotopic cells. Would this be reflected in mutant organoids? Indeed, there were cases where clusters of MAP2+ cells could be observed, being localized in the progenitor area (Fig. 2.8, A-C, approx. 45% in *DCHS1* mutant cortical zones and 25% of *FAT4* mutant cortical zones). This was much more clear in *DCHS1* organoids, where an otherwise well organized structure contained a clump of MAP2 immunostaining, but could also sometimes be seen in *FAT4* organoids.

In order to quantify the percentages of phenotypes seen in organoids, a simple scoring analysis was performed. Cerebral zones were judged to be either normal, disorganized – which comprises also the phenotype of neurites in *DCHS1* mutants – or whether they showed a cluster of MAP2 (“nodule”). The resulting

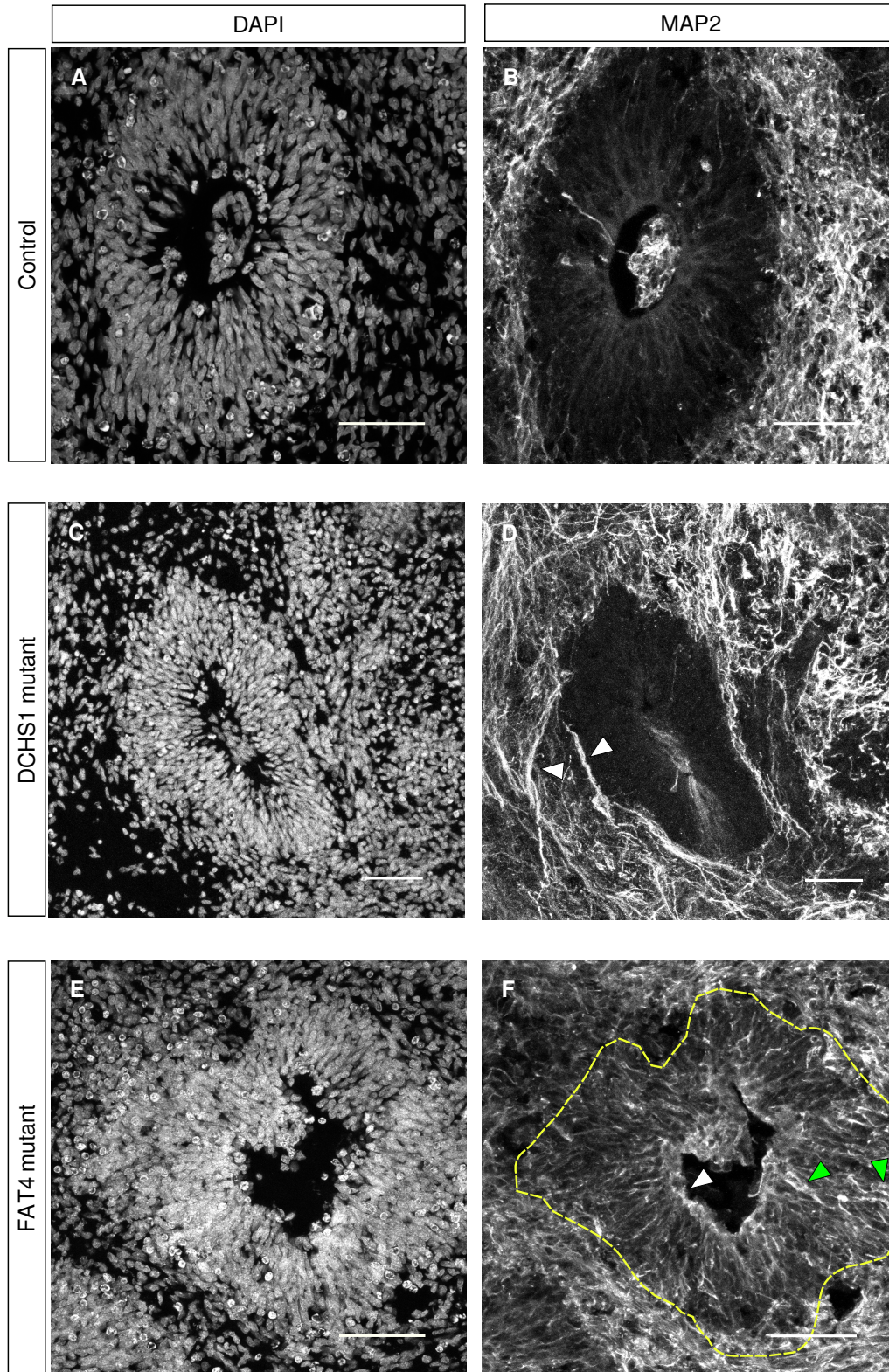


Figure 2.5: MAP2 immunostaining in organoids from control cells and mutant cells. Clear separation between neurons and the progenitor zone in control (B). Thickened neurite bundles in DCHS1 mutant organoid (D, white arrowheads). Unclear separation between neurons and progenitors in FAT4 mutant organoids (E, green arrowhead) and disturbed apical surface (E, white arrowhead). Scalebar: 50 μ m

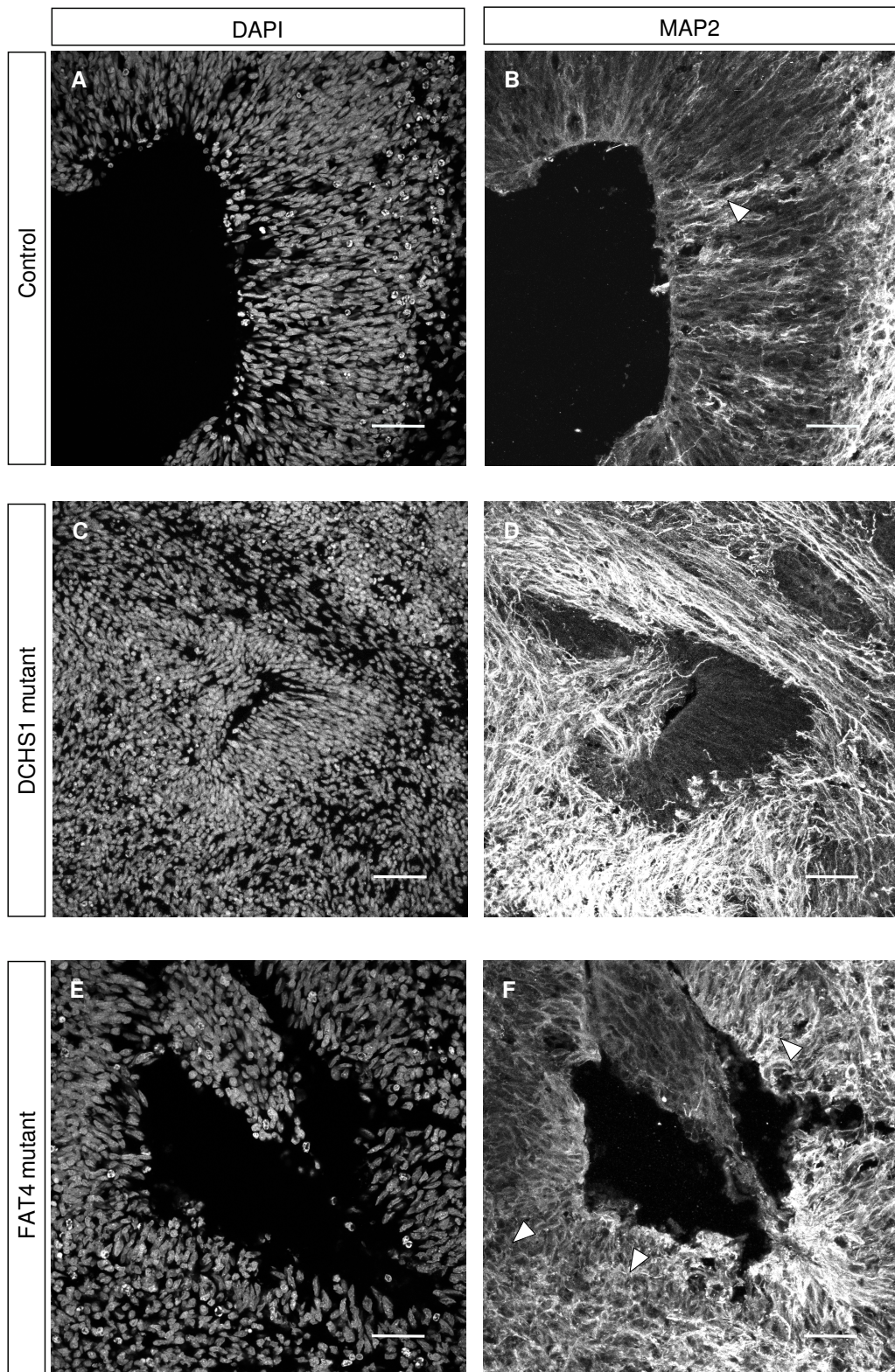


Figure 2.6: Additional examples of MAP2 immunostainings in mutant organoids. In this case, the control shows some intruding neuronal fibers (B, white arrowhead). Extreme deformed neurite bundles in DCHS1 mutant organoid (D). Neuronal intrusions in FAT4 mutant organoid (F, white arrowheads). Scalebar: 50 μm

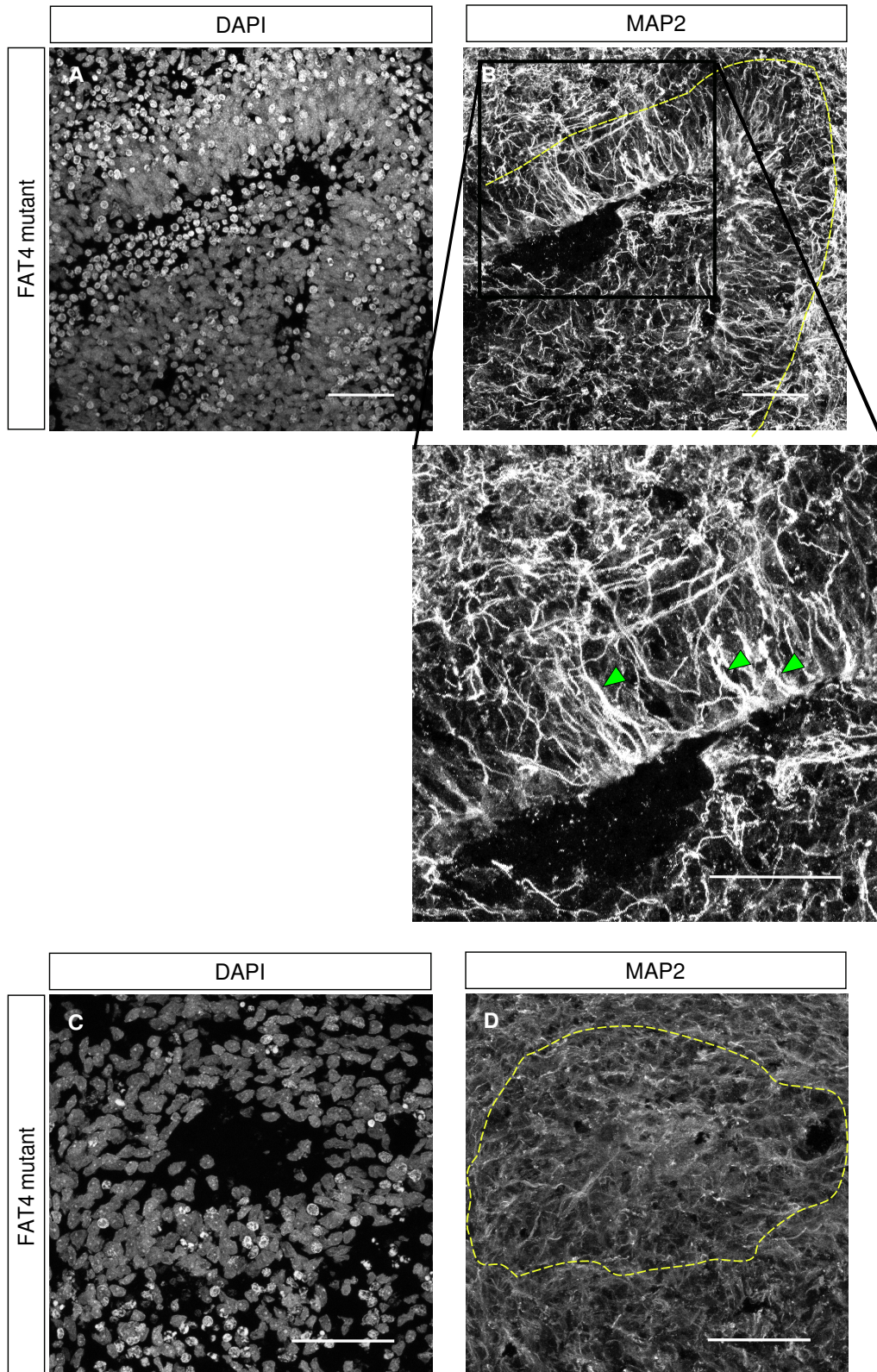


Figure 2.7: Example for massive intrusions of MAP2 fibres in progenitor zones of FAT4 mutant organoids. FAT4 mutant organoid with massive intrusions of neuronal processes. Cerebral zone is marked by yellow line (B). Another example of almost absent separation of the neuronal and the progenitor layer in FAT4 mutant organoid, progenitor zone marked by yellow line (D). Scalebar: 50 μm

quantification showed significantly more aberrations in mutant organoids (Fig. 2.8, D, Chi-squared test, $\chi^2(4) = 32.56$, $p < 0.0001$, both “aberrant” categories were put together as one category in this test).

These results demonstrate that there are indeed differences in the organization of cortical zones between control and mutant organoids. Especially in *FAT4* mutant organoids, zones showed poor organization, and both organoids showed the appearance of nodules in the progenitor zone that were positive for MAP2.

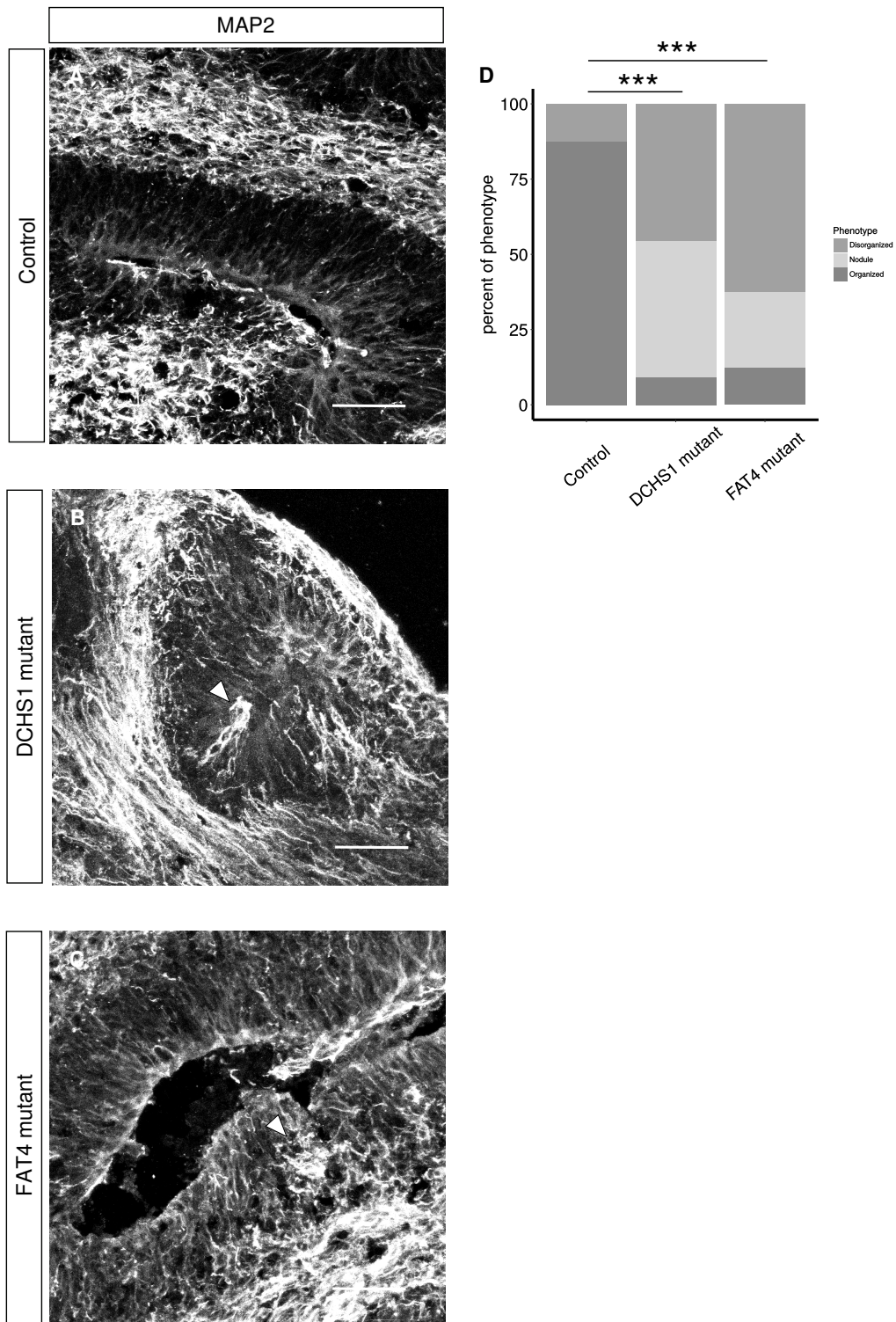


Figure 2.8: Examples for MAP2+ nodules in mutant organoids (A-C). Quantification of phenotypes in organoids (Ctrl: N = 24; DCHS1: N = 11; FAT4: N = 16 single germinal zones from 10 - 12 organoids, D). Scalebar: 50 μ m

2.2.4 Proliferation of progenitors in mutant organoids

Acute knockdown of *Fat4* and *Dchs1* in mouse leads to over-proliferation and delamination of progenitors (Cappello et al. 2013). Generally, mouse *Fat4* and *Dchs1* have been implied in proliferation, which is thought to be regulated via Hippo-signaling.

This data from mouse suggested that there might also be changes in proliferation in human cerebral organoids. To check this, immunohistochemistry for markers specifically expressed in cycling cells can be performed, especially markers that are expressed in mitotic cells, such as PH3.

However, no very specific change was found in either *DCHS1* or *FAT4* mutant organoids at both time points, 42 days or 70 days. In 70 days old organoids, *DCHS1* mutant organoids showed a tendential increase, while *FAT4* mutant organoids showed a tendential decrease, but this did not reach statistical sig-

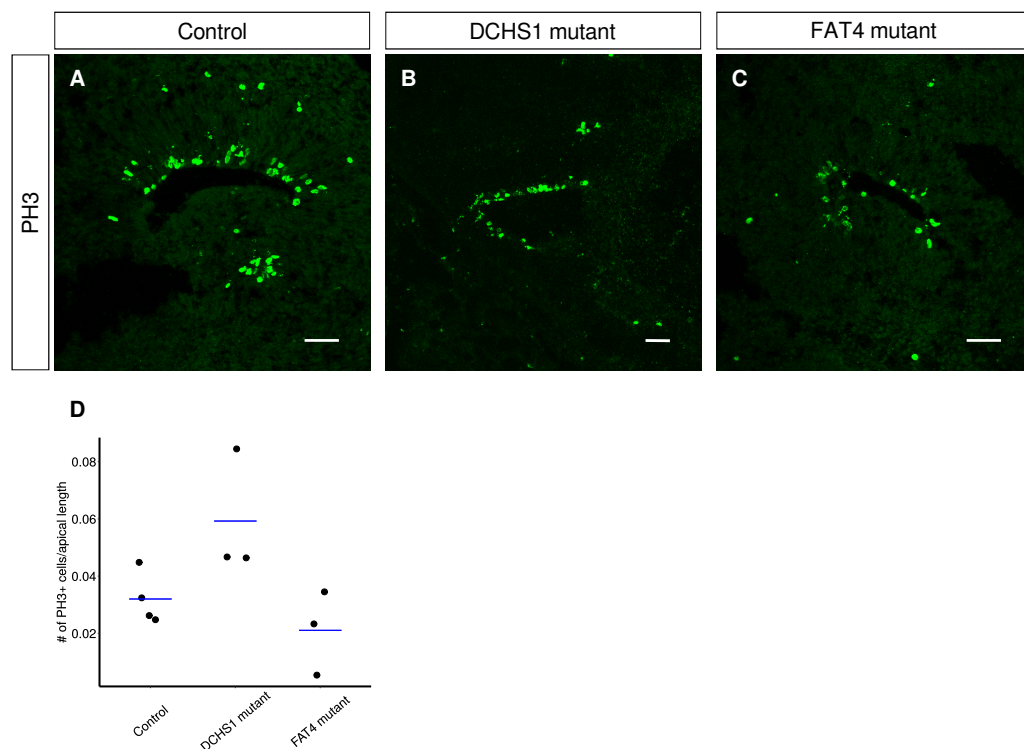


Figure 2.9: Quantification of PH3 immunostaining in organoids. (A-C) Staining for PH3 in control and mutant organoids, 70 d. (D) Quantification of the number of apically located cells that are PH3 positive, divided by the length of the apical surface that was considered (data from 70 days old organoids, N = 3 - 4 organoids per condition). Scalebar: 50 μ m

nificance (Fig. 2.9, D, Wilcoxon test). As however in a dataset for 42 days the variation was already found to be very high (data not shown), this analysis was not further continued.

2.2.5 Polarity of radial glia in progenitor zones from mutant organoids

In the developing mouse cortex, Fat4 and Dchs1 localize underneath the adherent junctions, forming a heterophilic complex (Ishiuchi et al. 2009). Depleting Fat4 or Dchs1 leads to changes in the organization of the apical membrane, reducing the apposing areas of two neighbouring cells (Ishiuchi et al. 2009). Furthermore, Fat4 localizes with Pals1, a polarity protein. It may be hypothesized that in the human ventricular zone, FAT4 and DCHS1 are implied in regulating apico-basal polarity of cells.

The analysis of apico-basal polarity was done by performing immunohistochemistry for proteins localized at adherent junctions. Proteins of adherent junctions, such as β -CATENIN, are localized apically, and adherent junctions also play a role in regulating apico-basal polarity (see section 1.1.1). As in mouse, Pals1 has been shown to be localizing together with Fat4 at the apical surface (Ishiuchi et al. 2009), it was also checked whether the localization of PALS1 is changed in FAT4 and DCHS1 mutant organoids. This analysis was done in both organoids from day 42 and day 70, which were again pooled for analysis.

In control progenitor zones, β -CATENIN and PALS1 are localized at the ventricular surface, forming a dense line delineating the ventricle (Fig. 2.10, A,B). Also *FAT4* and *DCHS1* mutant organoids form progenitor zones with correct localization of these two markers (Fig. 2.10, B-D). Despite of their mutation, they can form properly polarized neuroepithelial tissue, and there do not seem to be major defects that would lead to complete mislocalization of the two markers analysed (Fig. 2.10, C-E).

In *FAT4* mutant organoids, the ventricular surface has a more disrupted morphology. In many cases, the area of localization of β -CATENIN or PALS1 seems broader than in controls, and often, en-face views of the surface are exposed (Fig. 2.10, C, white arrowheads, another example is given in Fig. 2.11). In this example, the control shows some degree of interruption and en-face view of the surface, however, in the *FAT4* mutant, the degree of disorganization is much stronger.

These results show that the mutations in *FAT4* and *DCHS1* do not disturb apico-basal polarity in a fundamental way. Mutant organoids still contain progenitor

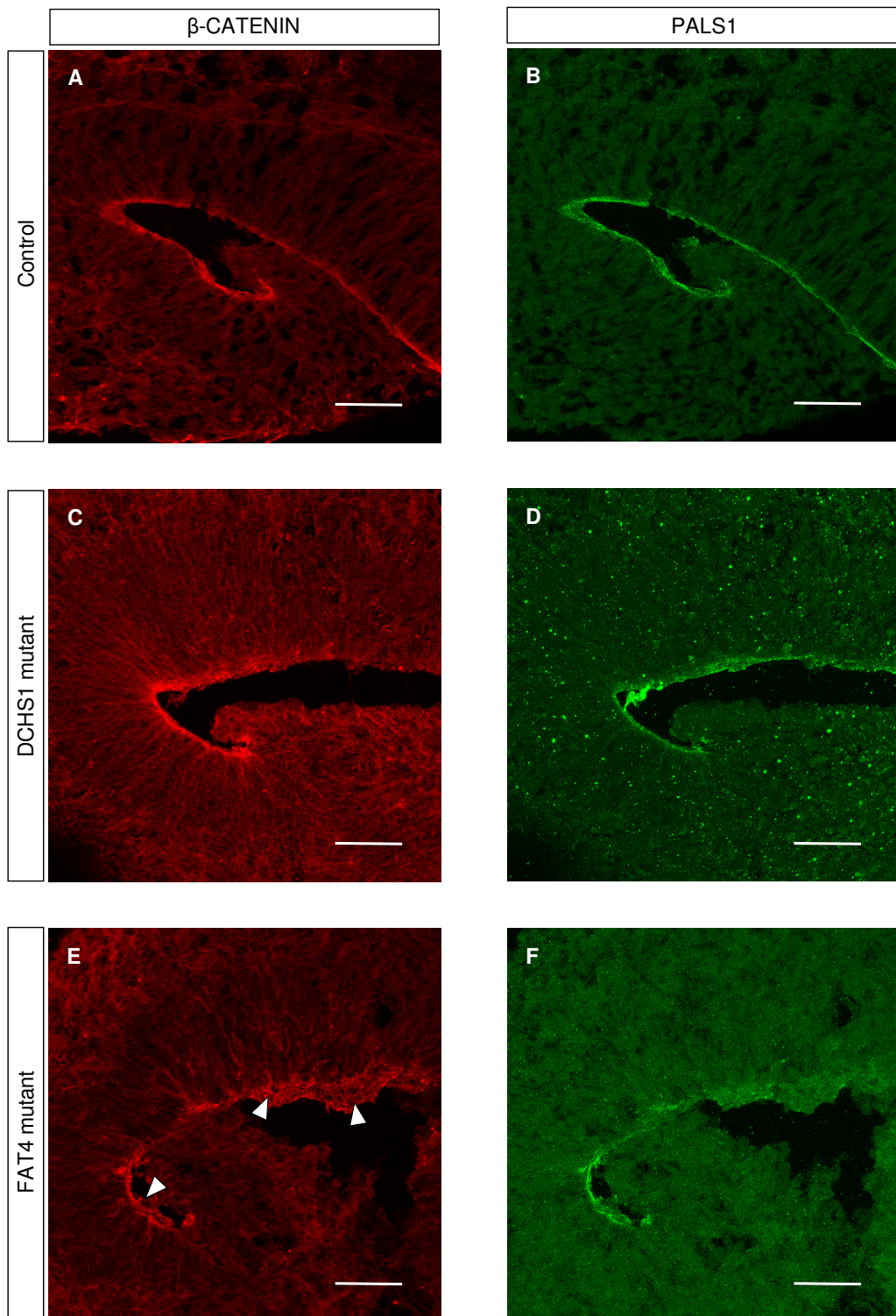


Figure 2.10: Polarity markers β -CATENIN and PALS1 in organoids. Shown are representative immunostainings for β -CATENIN and PALS1 in cortical zones of control and mutant organoids. Proper localization at the apical surface can be seen in all conditions (A-F). Note the higher degree of disruption in the FAT4 mutant (E, white arrowheads). Scale bar: 50 μ m

zones that show proper polarization with respect to the markers tested. However, it is important to note that *FAT4* mutant organoids show a higher degree of disruptions at their apical surface: it could mean that the stability of apical coherence is reduced, allowing for more disruptions to occur, and playing a role in the less organized appearance of *FAT4* mutant progenitor zones.

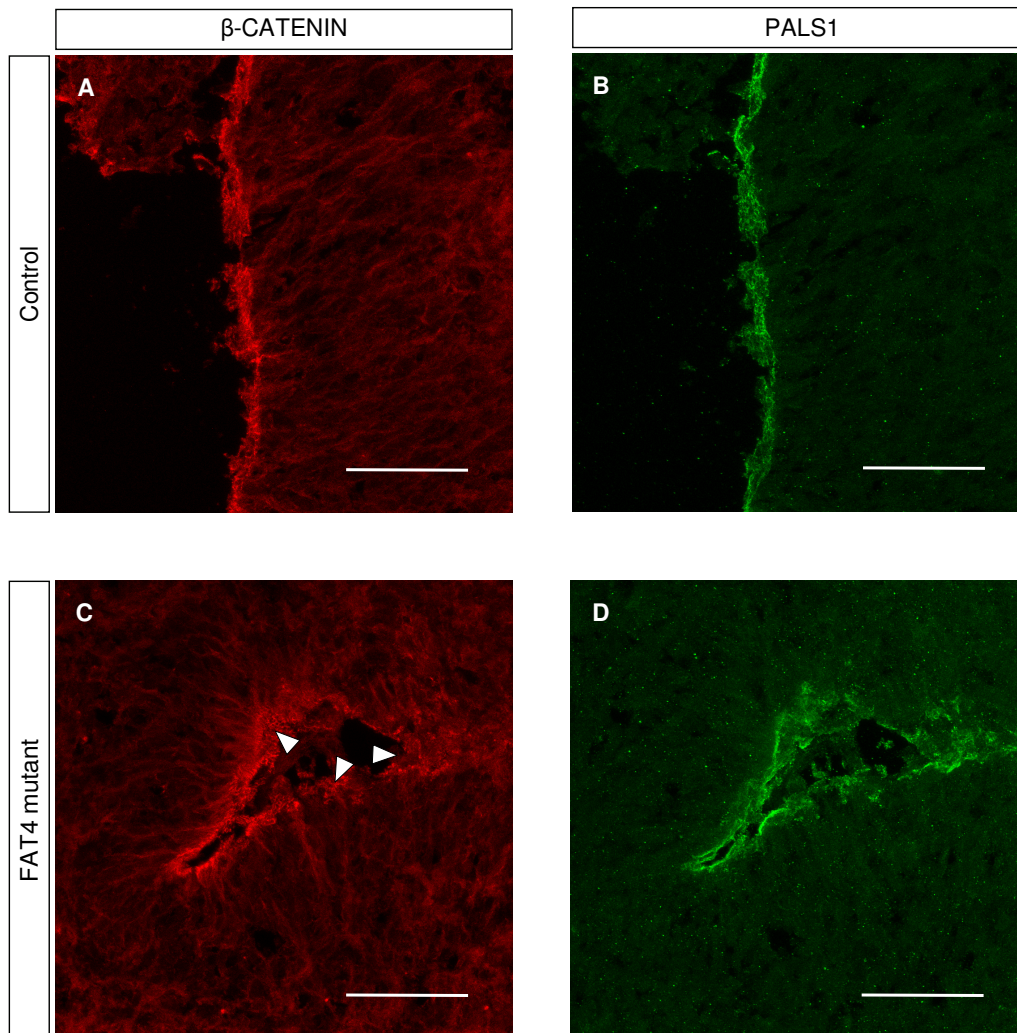


Figure 2.11: Additional example of disrupted apical surface in *FAT4* organoids compared to control. In this example, also the control shows a slightly more disrupted, but still well organized morphology (A,B), while in the *FAT4* mutant, immunostaining is sometimes patchy, spread and very often, en-face views of the surface can be seen (C,D,white arrowheads). Scale bar: 50 μm

2.2.6 Morphology of radial glia in mutant organoids

The integrity of radial glia is important for the correct migration of neurons in the developing cortex (see section 1.1.3). Disrupting their morphology leads to the appearance of malformations in mouse models. Knockout of *RhoA*, for example, leads to delamination and the formation of rosettes in the cortex of the mouse (Cappello et al. 2012). It is therefore of interest to see whether mutations in *FAT4* or *DCHS1* affect the structure and stability of radial glia in organoids.

Complete disruption of the radial glia scaffold would probably lead to complete disintegration of the progenitor zone in organoids, as stabilizing structures, such as a skull or meninges, are missing. This makes it difficult to observe extreme phenotypes of radial glia disintegration. However, while mutant organoids do form progenitor zones which are properly polarized (see above), milder disruptions are indicated especially in the *FAT4* mutant, which shows a disrupted apical morphology. It is therefore possible to observe milder defects that can be meaningfully related to the morphology of progenitor cells. To analyze the morphology of radial glia in organoids, frozen sections of organoids from day 42 and day 70 were analyzed by immunohistochemistry for NESTIN, an intermediate filament which delineates the morphology of radial glia, especially allowing for visualization their processes.

In control progenitor zones, radial glia processes are well organized and oriented in a radial fashion (Fig. 2.12, A, B). This is also true for *DCHS1* mutant organoids, which, judged by NESTIN immunostaining, did not show gross disturbances in their morphology (Fig. 2.12, B,C). However, in *FAT4* mutant organoids, very often a disrupted morphology of NESTIN+ fibers was observed, showing “whirly” pattern with non-parallel, truncated processes that did not reach up straight to the neuronal layer (Fig. 2.12, D, white arrowheads, and Fig. 2.13, D, white arrowheads).

These disruptions indicate that there are indeed changes in the morphology of progenitors in *FAT4* mutant organoids, being a possible explanation for the less coherent organization of *FAT4* cortical zones. In order to corroborate these findings, single progenitor cells in control and mutant organoids were labeled by electroporation of organoids with a Gap43-GFP-expressing plasmid (Cappello et al. 2006). Gap43-GFP localizes to the cell membrane and visualizes the morphology of cells, especially their processes. 50 day old organoids from control and mutant backgrounds were electroporated and analyzed two days after electroporation (Fig. 2.14).

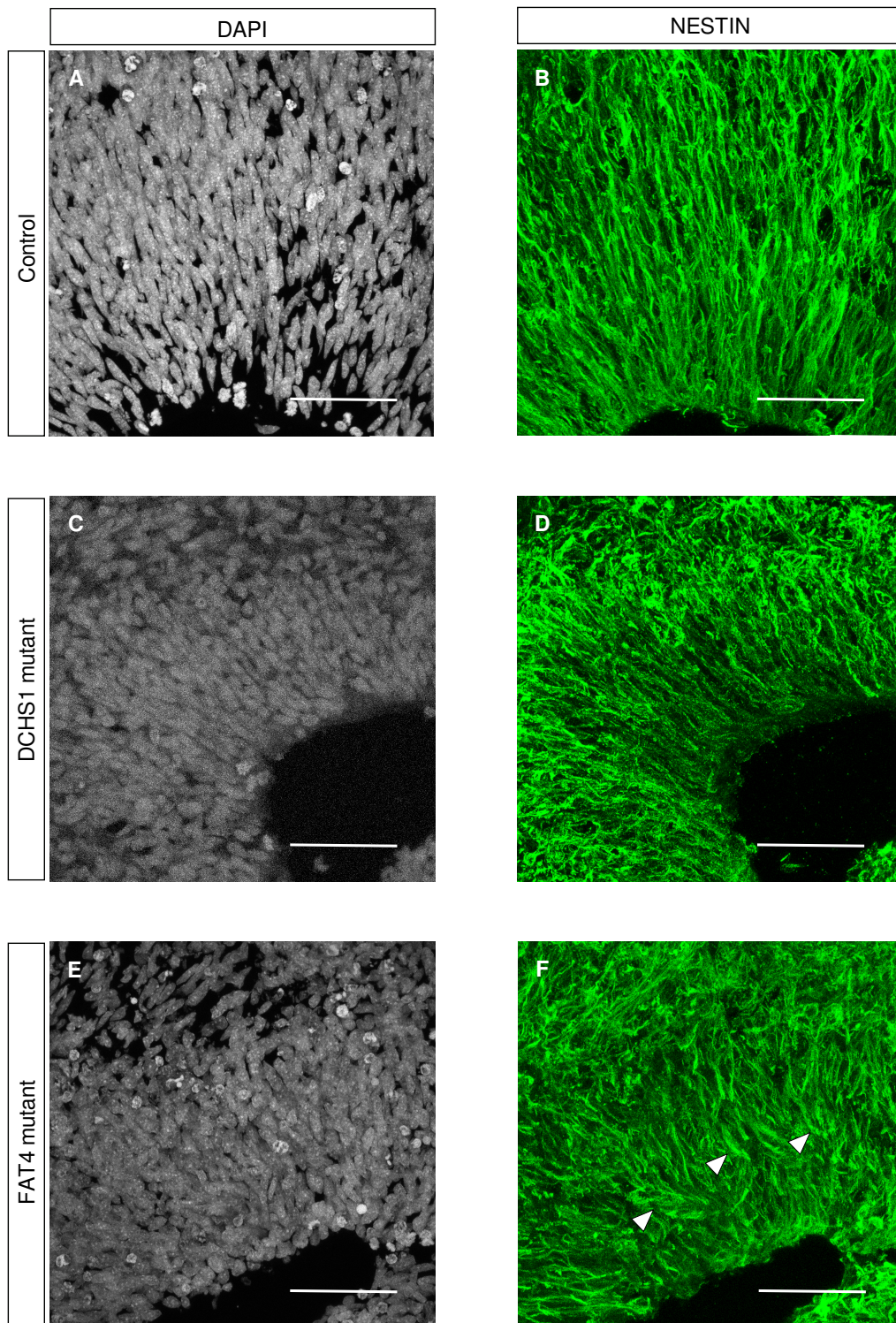


Figure 2.12: *NESTIN* immunohistochemistry to label radial glia processes in organoids derived in control organoids (B) and *DCHS1* mutant as well as *FAT4* mutant organoids (D,F). Processes appear straight in the control (B), and also in the *DCHS1* mutant (D), but twisted and broken in the *FAT4* mutant (E, white arrowheads).

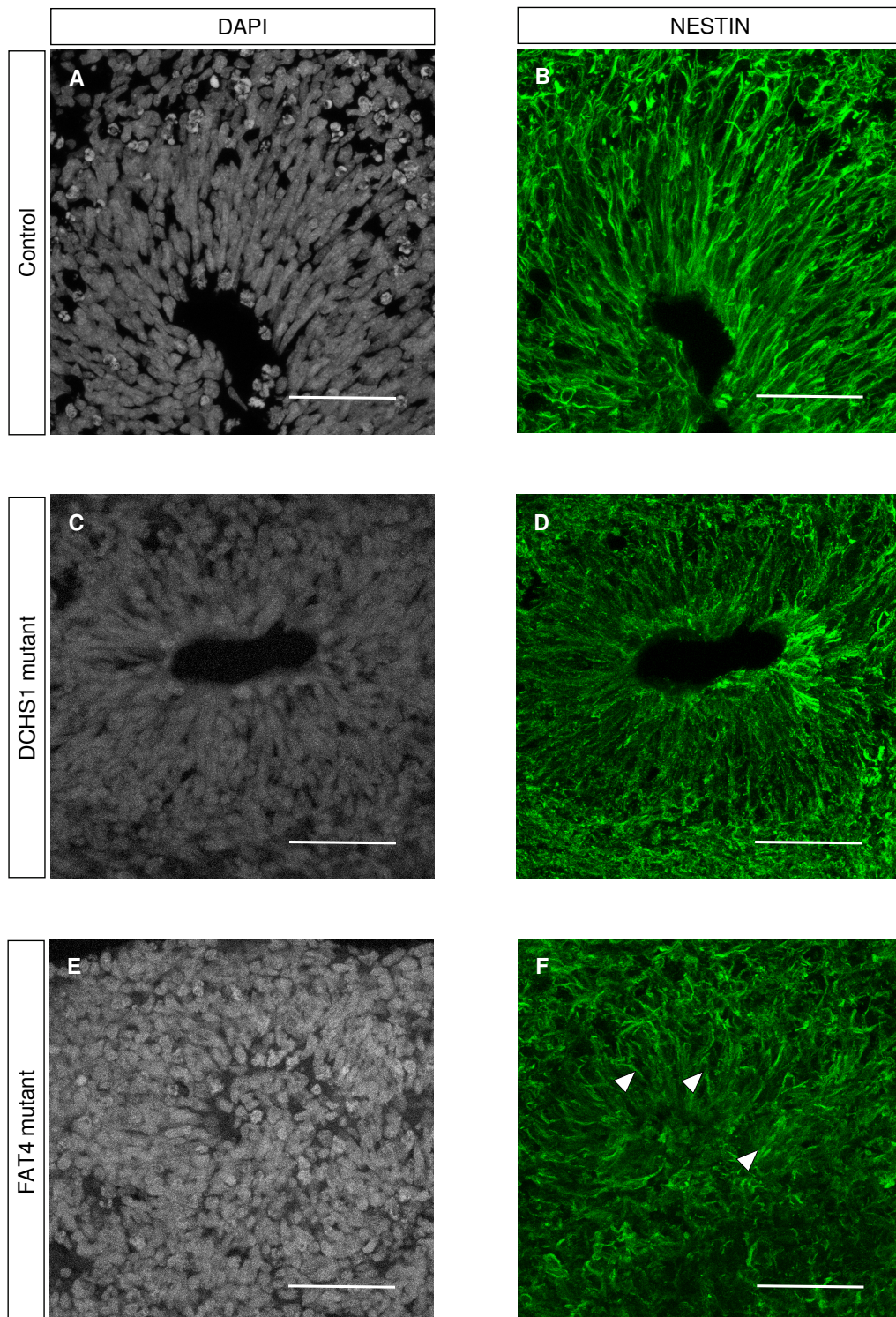


Figure 2.13: Additional example of NESTIN immunostaining in organoids, showing again the difference between control (B), DCHS1 mutant (D) and FAT4 mutant radial glia in organoids, again with a disrupted appearance in FAT4 mutants (F, white arrowheads). Scalebar: 50 μm .

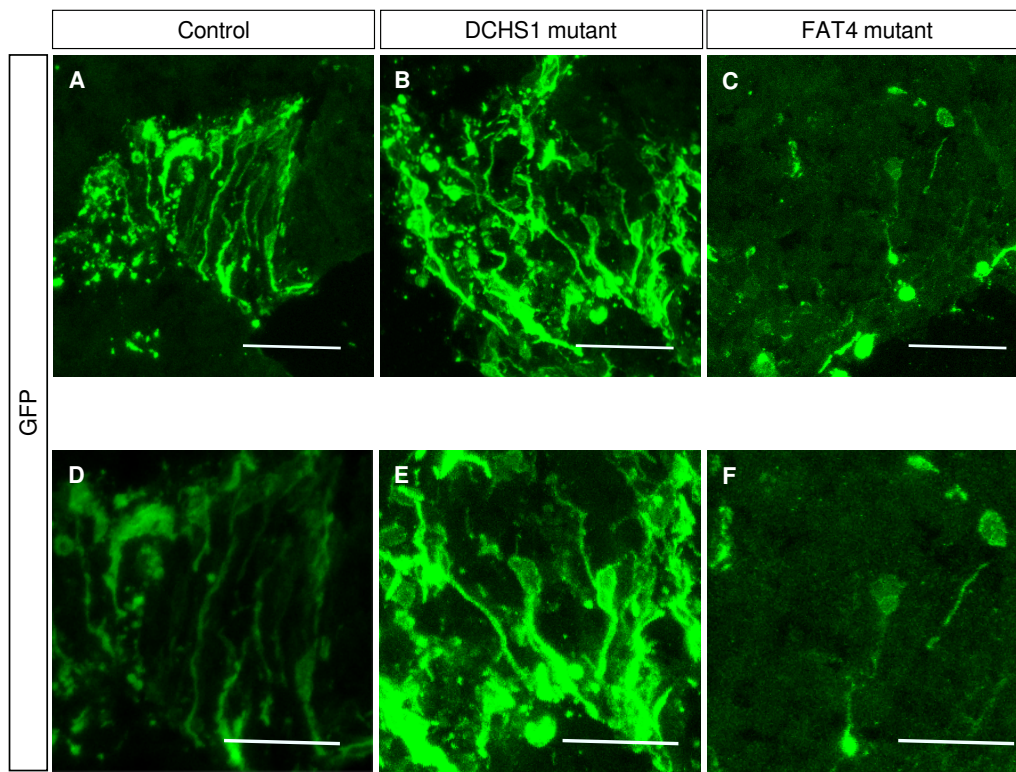


Figure 2.14: Electroporation of *Gap43-GFP* in organoids at around day 50 ($N = 3 - 6$ organoids per condition). Organoids were fixed two days after electroporation. Immunohistochemistry for GFP was performed. Cell processes labeled in control organoids (A). More disrupted morphology in *DCHS1* organoids (B), but strong disruptions in *FAT4* organoids (C). Scalebar: $50 \mu\text{m}$ in the upper row, $25 \mu\text{m}$ in the lower row.

In progenitor zones from control organoids, cells with long, straight processes could be labeled (Fig. 2.14, A, B). In *DCHS1* mutant organoids, the morphology of labeled processes was quite straight too, but interestingly, they often showed disruptions, like being bent, and some cells had no process (Fig. 2.14, B,E). In *FAT4* mutant organoids, however, it was very difficult to label progenitor cells in progenitor zones, as many cells seemed to be delaminated. Some cells could be found located in progenitor zones, and they usually were delaminated and showed truncated processes (Fig. 2.14, C,F). These findings indicate that progenitors with mutations in *FAT4* indeed tend to delaminate, and show disruptions in their processes, as well as a less organized apical belt. Of note, in these examples, also progenitors with mutations in *DCHS1* showed disruptions, but still showed more elongated processes than *FAT4* mutant cells, indicating that this phenotype is still milder in *DCHS1* mutated organoids.

The question remained whether this would be a phenotype depending on the specific mutations, or also occur after knockdown of *FAT4* or *DCHS1* in control

organoids. To check whether the phenotype could be reproduced with another method, miRNAs against *FAT4* and *DCHS1* were generated. The different miRNA constructs were nucleofected into SH-SY5Y cells and mRNA levels of *FAT4* and *DCHS1* were measured using qPCR. The two constructs with the strongest knockdown efficiency were selected for further experiments (*DCHS1* approx. $70\% \pm 28\%$ (SD) knockdown eff., *FAT4* approx. $44\% \pm 31\%$ (SD) knockdown eff., 3 independent exp.). Knockdown constructs were electroporated in organoids around day 50. The electroporated organoids were analyzed three days after electroporation.

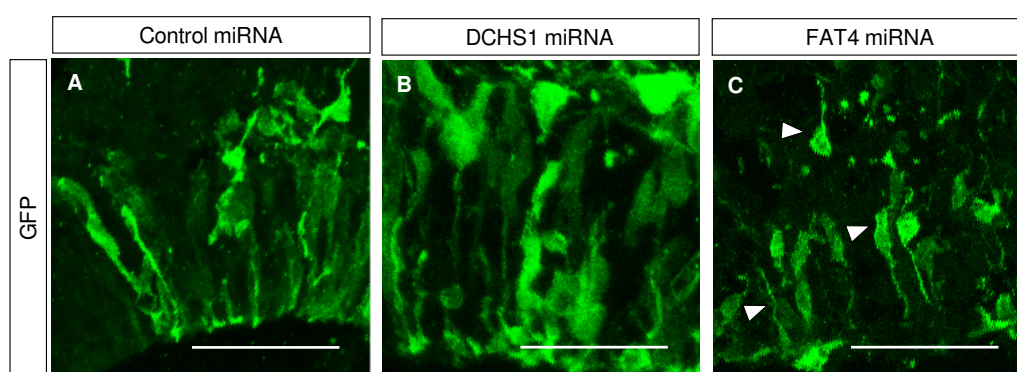


Figure 2.15: Electroporation of miRNAs against *FAT4* or *DCHS1* in organoids ($N = 3 - 6$ organoids per condition). 50 day old organoids were electroporated with the respective miRNA and fixed and analyzed three days after electroporation. Cell morphology of control electroporated cells (A). Morphology of cells electroporated with miRNA against *DCHS1* (B) and *FAT4*, the latter one showing disrupted morphology and delamination (C, white arrowheads). Scalebar: $50 \mu\text{m}$

Indeed, cells electroporated with control miRNA still showed long, straight processes (Fig. 2.15, A). Electroporation of *DCHS1* miRNA also had no striking effects on progenitor cells (Fig. 2.15, B), however, knockdown of *FAT4* lead to the appearance of many delaminated cells and cells with shortened and truncated processes (Fig. 2.15, C, white arrowheads).

These data suggest that downregulation or dysfunction of *FAT4* has effects on progenitor cells. First, they seem do delaminate more easily, which goes in line with the observed changes in apical organization, and might also explain why it was more difficult to label progenitor cells anchored in progenitor zones in *FAT4* mutant organoids. Second, they more often display truncated and shortened processes, indicating that progenitor cells have not only problems in their apical organization, but with their basal portions as well. Interestingly, these effects

are not so pronounced in *DCHS1* mutant organoids, although some degree of disturbance could also be observed in mutant organoids labeled with Gap43-GFP.

2.3 Defects in migration of neurons with mutations in *FAT4* and *DCHS1*

Disruptions in radial glia are very likely involved in many pathogenetic mechanisms of cortical malformations (see section 1.1.6). However, intrinsic defects in neuronal migration might also be important. In this respect, it is important to understand whether mutations in *FAT4* or *DCHS1* also change the behavior of neurons.

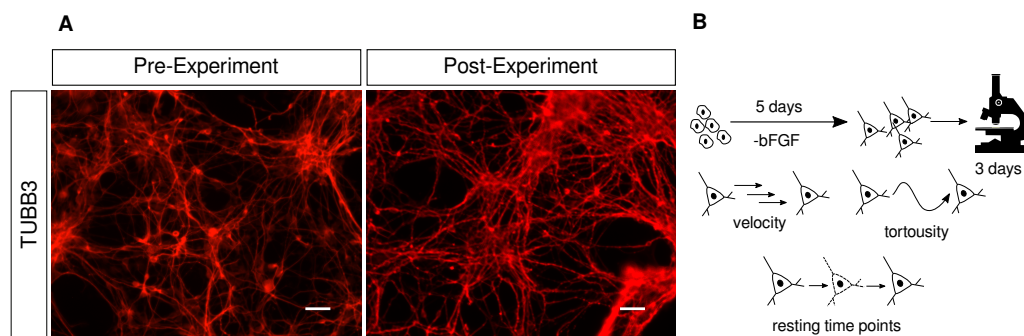


Figure 2.16: Scheme of time lapse experiment. Pre- and post-imaging pictures showing TUBB3+ neurons in the culture (A). Scheme of experiment and parameters analyzed (B). Scalebar: 50 μ m

One simple way of assessing the migration of cells is to track their movements in a two-dimensional culture in vitro. To generate neurons for this purpose, monolayer cultures of neural progenitors can be used. The differentiation of these cells to neurons can be induced by leaving out bFGF from their culture medium.

The cells were let to differentiate for approximately five days before the imaging experiments were started. In order to observe the migration of neurons, cells were imaged for three days, an image being taken every 5 minutes. The movement of the cells was tracked until the end of the movie, or until the cell disappeared from the frame. Neurons were recognized by morphology (c.f. Fig. 2.17, A), but their identity was confirmed by post-experiment immunostaining for TUBB3 (Fig. 2.16, A).

For analysis of the migration dynamics of the cells, three parameters were calcu-

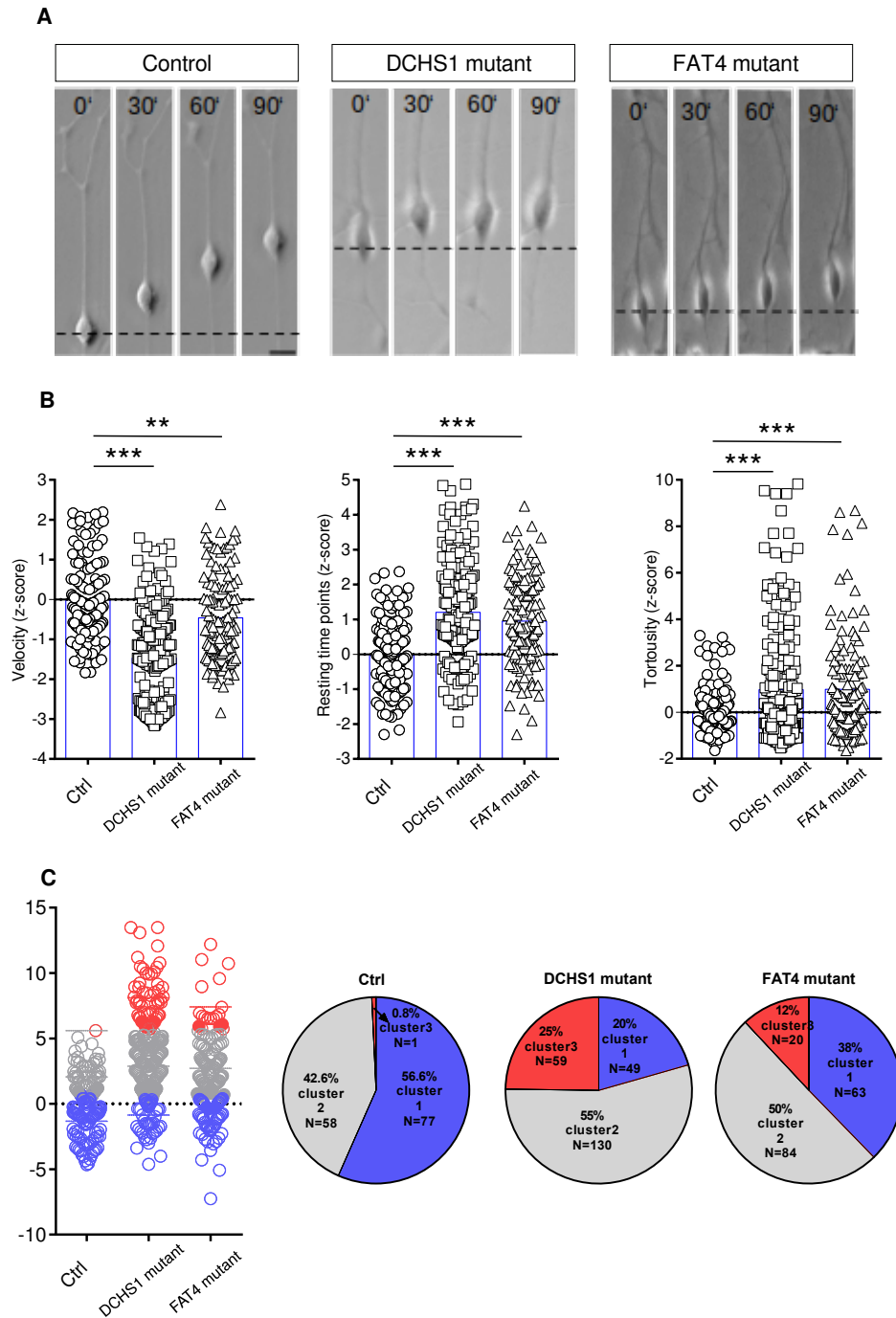


Figure 2.17: Results of time lapse imaging experiment. Exemplary images of cells in the control and the two mutant conditions, movement during 90 minutes (A). The average velocity, number of resting time points and tortuosity, displayed as z-scores (Ctrl: N = 158 cells, DCHS1: N = 251 cells, FAT4: N = 139 cells from 4 independent experiments) (B). Clustering analysis of migration dynamics across the whole cell population (C).

lated from the tracking data (Fig. 2.16, B). The first parameter was the average velocity. The second parameter was the tortousity, which is calculated by dividing the length of the path taken by the cell by its net displacement throughout the movie. The less direct the cell moves to its final destination, the greater the tortousity is, as the cell moves less straight. The third parameter calculated was the number of time points the cell did not move at all, i.e. the number of time points the velocity of the cell was zero. This number of *resting time points* was then divided by the number of time points the cell could be followed to account for differences in the number of resting time point that were due to differences in track length.

Mutant cells show changes in all three parameters (Fig. 2.17, B, MANOVA, $F(6, 956) = 33.07$, $p < 0.001$). Namely, the average velocity was decreased (Ctrl: $0.11 \mu\text{m/s}$, *DCHS1*: $0.08 \mu\text{m/s}$, $p < 0.001$; *FAT4*: $0.09 \mu\text{m/s}$, $p < 0.01$; ANOVA/Tukey). The tortousity, on the other hand, was clearly increased (Ctrl: 1.0 ; *DCHS1*: 1.55 , $p < 0.001$; *FAT4*: 1.46 , $p < 0.001$, ANOVA/Tukey), indicating that the cells also move less straight. Thirdly, the number of resting time points was increased significantly (Ctrl: 0.31 ; *DCHS1*: 0.44 , $p < 0.001$; *FAT4*: 0.41 , $p < 0.001$, ANOVA/Tukey).

These data are indicative of a profound change in the migration dynamics of neurons with mutations in *FAT4* or *DCHS1*, suggesting a slower, less directed and more saltatory movement. However, not all the cells are affected to the same degree, opening up the possibility that it is different populations that are affected differently.

In order to look into this in more detail, all three parameters were combined to create a measure of the overall migration behavior of each cell, and patterns of movement behaviors were identified in the whole cell population. Indeed, three different patterns could be identified, named *cluster one*, *cluster two* and *cluster three*.

In in the case of control cells, only one cell could be assigned to cluster three, while approximately half the population was assigned to cluster two, the other half to cluster one (Fig. 2.17, C). But the mutations changed this picture in an interesting way: cluster two remained unchanged, still comprising around half the population. Cluster three, however was increased at the expense of cluster one.

This indicates that the population analyzed was heterogeneous regarding its migration behavior, falling into two main populations in the control. It is possible that these differences reflect different subclasses of neurons, displaying distinct

migration mechanisms that are differentially affected by the mutations or that a third subtype of neuron, showing yet another migration mechanism, increases in number in the patient lines.

It is important to note that the appearance of cluster three for mutant cells is at the expense of cluster one. If cluster three represented just the appearance of another cell type, which, for some reason, would be more abundant in populations of mutant cells, one would expect a symmetric decrease in the number of cells belonging to the other two clusters. As this seems not to be the case, it is more likely that this phenomenon is based on the fact that one population of cells is specifically affected by the mutations in *FAT4* and *DCHS1*, while the other one is not.

2.4 The cytoskeleton and cytoskeletal genes are changed in mutant cells

2.4.1 Changes in the cytoskeleton of mutant cells

The cytoskeleton plays an important role in the pathogenesis of neural migration disorders (see section 1.1.3). The cytoskeleton consists of microtubules and actin fibers, both of which are involved in processes like neuronal migration.

In order to function properly in cells, the stability of the cytoskeleton has to be tightly regulated. In the case of the microtubule skeleton, there is a balance between the turnover and stabilization of microtubules. As the stability of microtubules might be changed in cells with mutations in *FAT4* and *DCHS1*, this was investigated by analyzing post-translational modifications of microtubules. These modifications are indicative of microtubule dynamics, acetylation usually labeling stabilized microtubules, while tyrosination representing newly formed microtubules and therefore being indicative of microtubule turnover (Schulze 1987).

In order to compare the expression of acetylated tubulin compared to tyrosinated tubulin, NPCs from monolayer cultures were used for immunoblotting and quantification (Fig. 2.18, A-C). Indeed, in *FAT4* samples, acetylated tubulin was downregulated compared to control, while *DCHS1* mutant cells did not show a change. In contrast, tyrosinated tubulin was not clearly changed in either of two samples (Fig. 2.18, D, one sample t-test, $p < 0.05$ for acetylated tubulin in *FAT4* mutant cells).

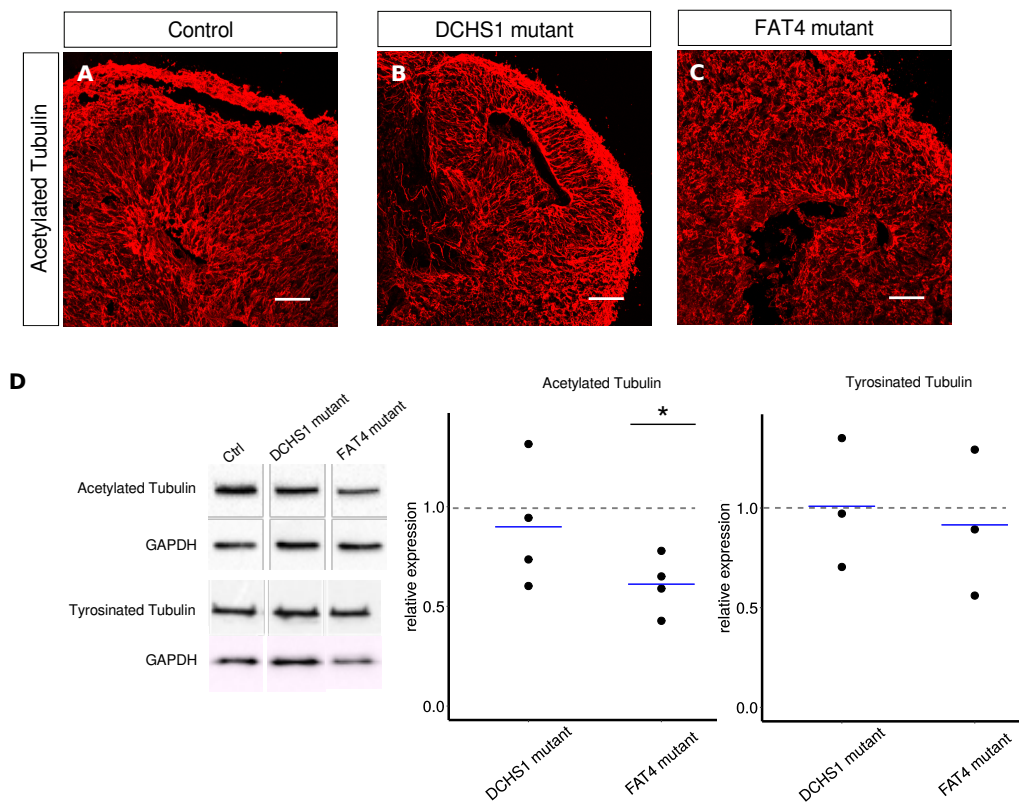


Figure 2.18: Changes in the expression of acetylated tubulin (A-E). Staining for acetylated tubulin in 30 day old organoids (A-C). Quantification of the expression of acetylated tubulin and tyrosinated tubulin of NPCs (N = 4 independent samples for acet. tubulin and 3 independent samples for tyr. tubulin, E). Scalebar: 50 μ m in all panels.

This results points to a change in the balance of stable and newly created microtubules, with stable microtubules being reduced in *FAT4* mutants. This indicates an overall destabilization, which could account for radial glia process instability.

Besides microtubules, the cytoskeleton is also composed of actin fibers, which have very distinct function in many processes (see section 1.1.3), such as neuronal migration. To analyze this, polymerized F-Actin was labeled by using fluorescent Phalloidin, a toxin which specifically binds to F-Actin fibers, in organoids and NPCs. In control organoids, F-Actin accumulates at the ventricular surface, as expected (Fig. 2.19, A). In mutant organoids, this is true as well, again indicating no gross disturbance of apico-basal polarity (Fig. 2.19, B,C). In *FAT4* mutants, the distribution of F-Actin is fine as well, however, the structure again seems to be less coherent (Fig. 2.19, C). In NPCs, mutant cells show a different morphology of their actin cytoskeleton (Fig. 2.19, D-F). While in the control, F-Actin forms elongated fibrils, in mutant cells, F-Actin structure has lost its fibril structure, and

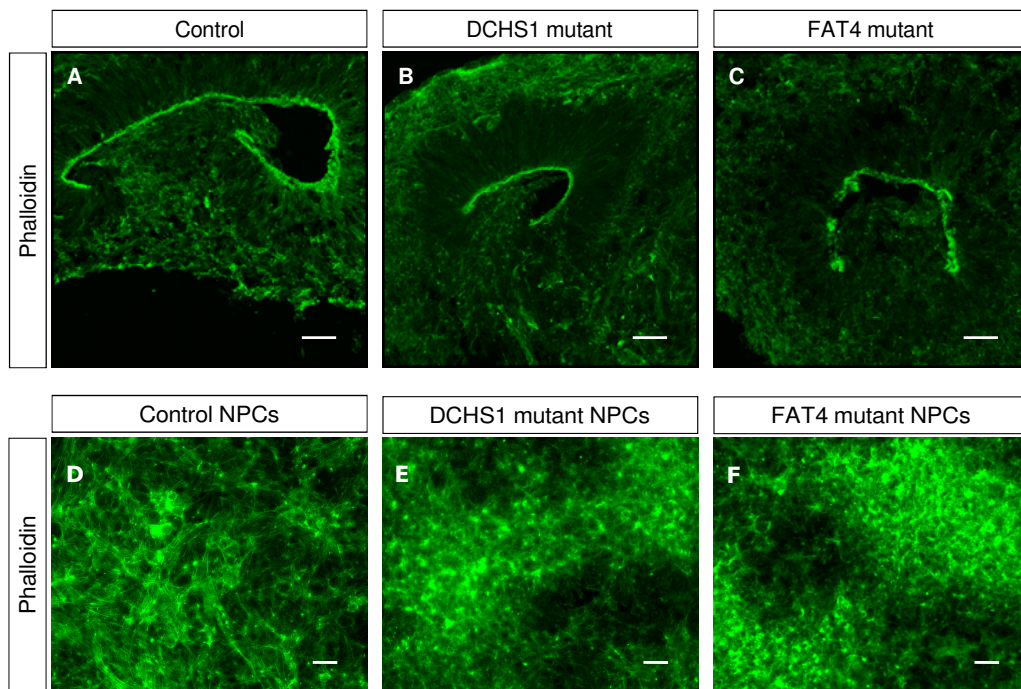


Figure 2.19: *F-Actin labeling in organoids with Phalloidin (A-C). In both control (A) and mutant organoids (B,C), F-Actin accumulates at the ventricular surface. Note however the more disrupted appearance in the case of FAT4 mutants (C). F-Actin labeling in NPCs (D-F). Note the more nodular, less fibrillous appearance of F-Actin in mutant NPCS (E,F). Scalebar: 50 μ m in all panels.*

shows a more disorganized, condensed pattern. Both these findings point to the fact that the actin cytoskeleton might also be disturbed in cells with mutations in *FAT4* or *DCHS1*.

2.4.2 Single cell RNA sequencing of microdissected cortical zones

The possibility of analyzing single cells from cortical zones of organoids that have been microdissected offer new insights into transcriptional properties of cells found in organoids (Camp et al. 2015). It allows to assess transcriptional changes by at the same time preserving the information about the identity of cells, as the latter can be deduced from the expression of transcriptional markers. Therefore, using single cell RNA sequencing techniques, the advantages of organoids – the differentiation of cells in properly organized tissue context – can be combined with the advantage of using isolated cells, such as the easier separation of cell types.

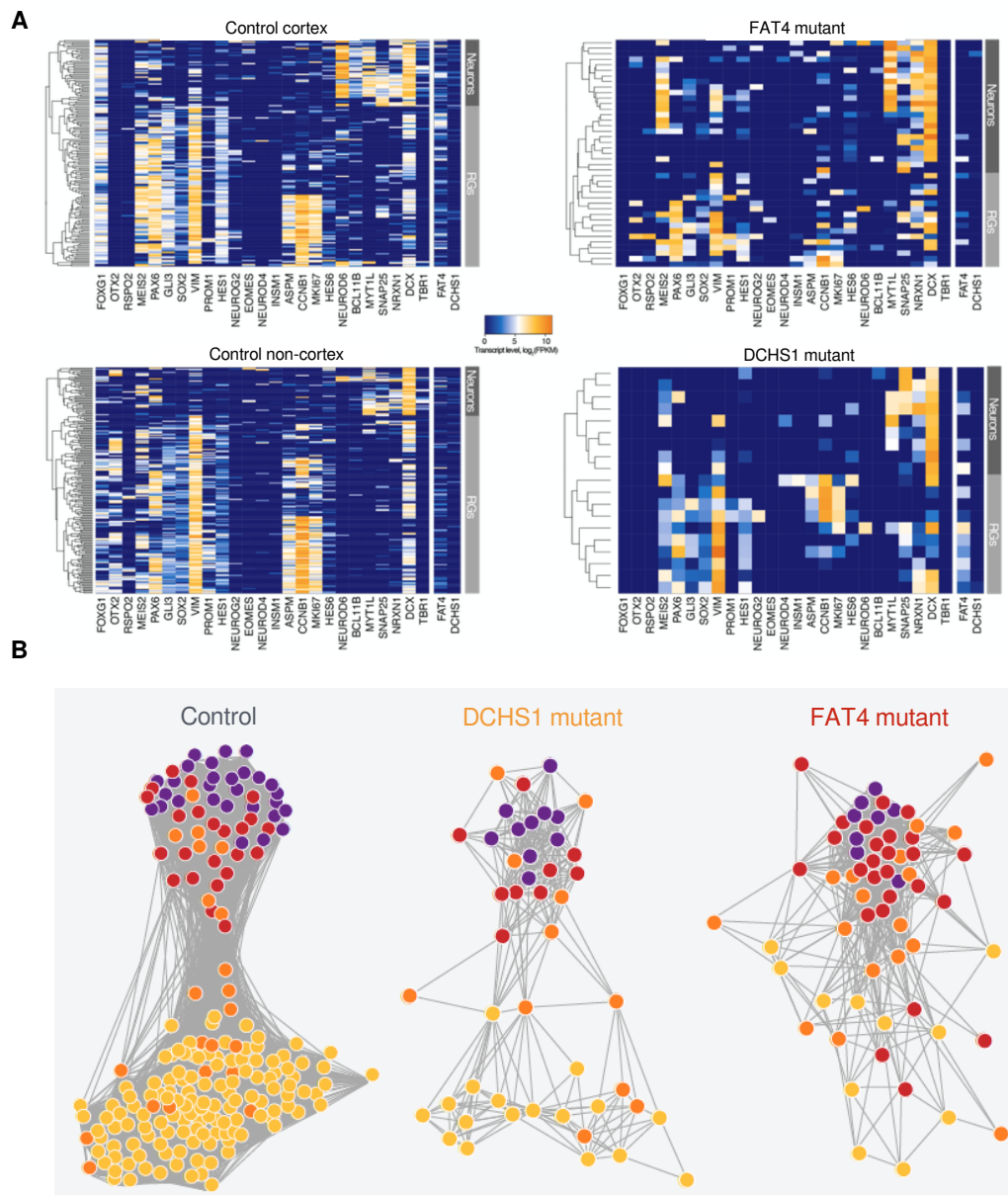


Figure 2.20: Single cell RNA sequencing of cells from microdissected cortical zones. Heatmaps showing the expression of markers (A). Intercellular correlation network, identifying progenitors (orange) and neurons (purple) (B).

The data described above show that *FAT4* and *DCHS1* mutant cells show aberrations both in progenitor cells as well as neurons. As at the time of finishing this thesis not all the experiments were analyzed yet and it was not yet possible to separate neuronal and progenitor populations completely, both cell types are taken together in the analysis shown below. The next step was to try to get more insight on the molecular level.

For this analysis, 50 days old organoids from control and mutant backgrounds were used for microdissection and single cell RNA sequencing (in collaboration with Dr. Barbara Treutlein and Sabina Kanton, Max-Planck-Institute of Evolutionary Anthropology, Leipzig). First, the expression of markers known to be important to assess cell type identity in the developing cortex was analyzed (Fig. 2.20, A). Control cells could be split into two populations: dorsal forebrain and non-dorsal forebrain cells by marker expression, such as *FOXP1* and *OTX2*. However, in mutant organoids, a clear assignment to dorsal forebrain identity was not possible. For example, expression of *FOXP1* was completely lacking. For the further analysis, *FAT4* and *DCHS1* mutant cells were compared to control cells of all types of regional identity.

Clustering the cells using intercellular correlation showed that, in control organoids, cells could clearly be clustered according to their position in the differentiation trajectory, i.e. progenitors separated very well from neurons (Fig. 2.20, B). The same could also be done for *DCHS1* mutant cells.

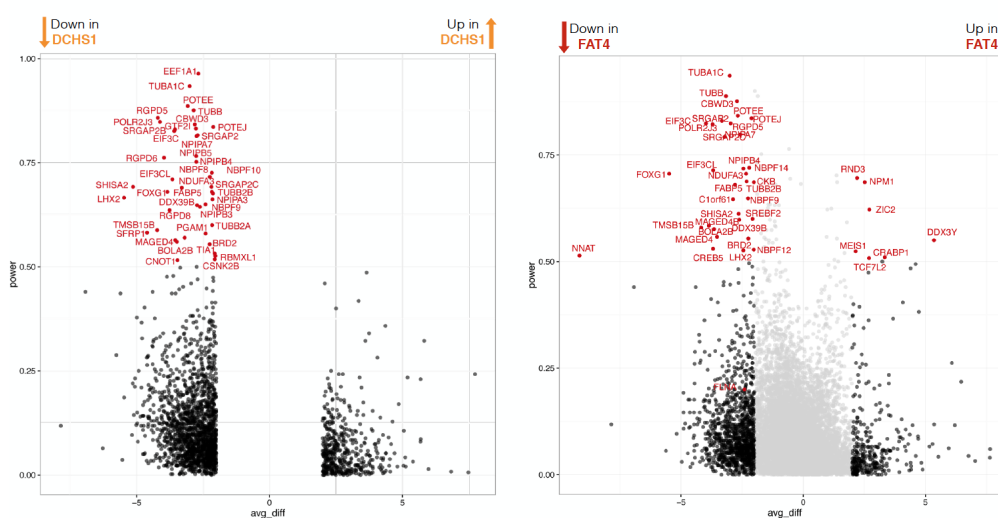


Figure 2.21: Volcano plot plotting the average degree of regulation against the power in *DCHS1* (left panel) and *FAT4* (right panel) mutant cells.

Based on the sequencing data, the genes that show the clearest differences between control and mutant cell populations were determined. To do this, a ROC test was performed, which essentially tests how well a gene of interest performs in separating two cell populations, and the *classification power* was calculated. The classification power indicates how well a gene separates control cells from mutant cell populations, a value of one indicating perfect separation, while a value of zero indicates no separation at all. This measure allows to assess which genes are differentially expressed between cell populations, taking both expression differences as well as the number of cells that show differences in that gene into account (see appendix A.1).

Strikingly, doing this analysis, the cytoskeleton showed up as being strongly regulated. Regulated were GO terms like *microtubule process* or *structural constituent of the cytoskeleton* (genes with class. power > 0.4, see appendix A.2). The genes behind these GO terms were foremost tubulins, such as *TUBA1C* (class. power \approx 0.9), *TUBB* (class. power \approx 0.8) or *TUBB2B* (class. power \approx 0.7).

In addition, genes involved in the regulation of RHO GTPases were also deregulated in this dataset. For example, regulators of RAC1 were changed, such as *SRGAP2* (class. power \approx 0.8). Furthermore, in the *FAT4*-dataset, *RND3*, a regulator of RHOA, was downregulated (class. power \approx 0.7).

These results were constant across batches, and the classification power was always similarly strong for these genes. This indicates that indeed, cytoskeletal components are deregulated in both mutant datasets, indicating that mutations in *FAT4* and *DCHS1* might lead to profound changes in the regulation of the cytoskeleton.

What role do these genes play in neural development? To get a hint to the answer to this question, the genes deregulated in the mutant datasets were compared to genes that are known to accumulate de novo mutations in cohorts of patients with developmental diseases of the CNS, such as autism spectrum disorder (ASD), intellectual disability (ID) or schizophrenia (SCZ) (in collaboration with Dr. Adam O'Neill, Institute of Stem Cell Research, Helmholtz-Center, Munich). To do this, for all genes in the dataset of deregulated genes in mutant organoids with a class. power greater than 0.4, the theoretical number of expected de novo mutations was determined (Table 2.2 and Table 2.3, 3rd column) and compared to the actual number of de novo mutations observed in a patient cohort (Table 2.2 and Table 2.3, 4th column). Indeed, especially in the *FAT4* dataset, deregulated genes were significantly more prone to harbor de novo mutations in patients with autism

spectrum disorder (ASD) and other diseases, indicating that the deregulated pathways are developmentally important and implied in these diseases. For the *DCHS1* dataset, the same relationship could be found for ASD.

Table 2.2: Analysis of genes mutated in patients with developmental diseases for the *FAT4* dataset. EE = epileptic encephalopathy, ASD = autism spectrum disorder, ID = intellectual disability, SCZ = schizophrenia

Gene set	Nr. of cases	FAT4 (n = 163)		
		Total Expected	Total observed	P-value
EE	264	0.924	4	0.01449
ASD	945	3.308	18	1.39×10^{-8}
ID	145	0.508	3	0.01476
SCZ	680	2.380	7	0.01097

Table 2.3: Analysis of genes mutated in patients with developmental diseases for the *DCHS1* dataset. EE = epileptic encephalopathy, ASD = autism spectrum disorder, ID = intellectual disability, SCZ = schizophrenia

Gene set	Nr. of cases	DCHS1 (n = 69)		
		Total Expected	Total observed	P-value
EE	264	0.451	0	1
ASD	945	1.613	8	2.73×10^{-4}
ID	145	0.248	0	1
SCZ	680	1.161	0	1

2.5 Summary

This work demonstrates the relevance of human cerebral organoids for studying human disease. Cells with mutations in *FAT4* or *DCHS1* are able to generate organoids with progenitor zones. While these progenitor zones show no gross defect in polarity, they do show defects in their organization which are meaningful for understanding the disease pathomechanisms.

Cerebral zones in *FAT4* mutant organoids are less well organized, with intruding neurons and a disrupted ventricular surface. *DCHS1* mutant organoids are usually more clearly defined, but show aberrations in the morphology of neurites of neurons. Furthermore, radial glia morphology is disturbed especially in *FAT4*

mutant organoids, although *DCHS1* mutant organoids seem to show some degree of aberrations as well.

Looking at the question whether not only progenitors, but also neurons show defects when carrying mutations in either *FAT4* or *DCHS1*, time lapse experiments using neurons in a two-dimensional culture revealed striking differences in migration behavior. Interestingly, changes in migration behavior seem to affect one distinct population, leaving the other one virtually unchanged.

It could be shown that the cytoskeleton seems to be affected by specific changes in *FAT4* or *DCHS1* mutant cells. Stabilized microtubules are reduced, F-Actin fibers show a change in morphology, and scRNA sequencing experiments revealed differential regulation of cytoskeletal genes. All in all, this suggests the possibility that a misregulation of the cytoskeleton underlies the phenotypes seen in progenitor cells as well as neurons with mutations or dysfunctions in *FAT4* and *DCHS1*.

3 Discussion

3.1 iPSC based models of neurodevelopmental disease

Induced pluripotent stem cells have proven their usefulness for modeling neurological diseases. For example, many studies have tried to find phenotypes related to neurodegenerative diseases using iPSC-derived neurons. Despite the fact that iPSC-derived neurons are supposedly more fetal in nature, while neurodegeneration usually becomes apparent at high age, interesting phenotypes could be found (Srikanth and Young-Pearse 2014).

In addition to neurodegenerative diseases, neurodevelopmental diseases have also been investigated using iPSC. For examples, aspects of schizophrenia, a psychiatric disorder now more and more recognized to have a neurodevelopmental component, have been modeled using iPSC-derived neurons (Brennand et al. 2011). Mostly, the focus lies on the examination of more or less mature neurons derived from iPSC to analyze their morphological, transcriptional or electrophysiological properties. Few studies pay much attention to neural progenitor cells *per se*. Some studies could indeed show phenotypes in NPCs derived from schizophrenia patients (Brennand et al. 2014; Yoon et al. 2014). One study found differences in the localization of apical junction proteins in neural rosettes derived from schizophrenia patient iPSC (Yoon et al. 2014).

Neuronal migration disorders have not been extensively modeled using iPSC based models. There is one study showing differences in the expression of *CHCHD2*, but the relevance is not clear and migration behavior was not tested (Shimojima et al. 2015). As two-dimensional cultures of NPCs or neurons do not allow for more elaborate analysis of tissue structure, cerebral organoids have been viewed as a promising tool for analyzing neurodevelopmental disorders.

3.2 Modeling neuronal migration disorders using organoids

Although mouse models are a valuable tool for understanding neuronal migration disorders, they not always faithfully recapitulate all aspects of the diseases, and it is important to have access to more sophisticated models that make use of stem cell-derived human cells.

Human cerebral organoids represent a promising possibility to make more effective use of patient specific stem cells for modeling developmental diseases such as neuronal migration disorders, as they offer the potential to reflect phenotypes that are dependent on a three-dimensional tissue context. There are already some studies that demonstrate the value of organoids in representing developmental processes and to uncover defects that can be meaningfully related to the disease in question (Lancaster et al. 2013; Mariani et al. 2015; Bershteyn et al. 2017). For example, changes in the proliferative behavior of progenitor cells could be accurately reflected in organoids derived from microcephaly patients (Lancaster et al. 2013). Also aspects of lissencephaly, studied in cells from patients with Miller-Dieker-Syndrome, which is caused by a deletion comprising *LIS1*, could be modeled in organoids (Bershteyn et al. 2017). In this study, interesting differences to the mouse model could be found, as knockdown of *Lis1* leads to changes in interkinetic nuclear migration in mouse apical progenitors, while apical progenitors in human cerebral organoids show normal interkinetic nuclear migration. In contrast, specific defects could be found in outer radial glia (Bershteyn et al. 2017). Other studies examined the pathomechanism of microcephaly observed in newborns after their mothers have been infected by Zika virus. There, organoids revealed changes in progenitor proliferation after exposure to Zika virus (Qian et al. 2016). Also first studies trying to look at neuropsychiatric illness found specific changes in the generation of inhibitory neurons at the expense of excitatory neurons in cerebral organoids derived from autism spectrum patients (Mariani et al. 2015).

Still, it is not easy to estimate where the potentials and the limitations of organoids lie. Obviously, structures found in organoids bear remarkable similarities to the developing CNS of the fetus, but similarity alone does not mean that all aspects are accurately reflected, nor does it imply that the *processes* that generate these structures are the same as in the embryo. In fact, while organoids show the same basic developmental program as fetal tissue on the transcriptional level, they also show striking differences (Camp et al. 2015). For instance, the ratio of basal to apical progenitors is different, with basal progenitors playing less of a role in human cerebral organoids (Camp et al. 2015).

Before turning to the discussion of modeling FAT4 and DCHS1 mediated defects in cerebral organoids, I quickly want to turn to fundamental aspects to keep in mind when considering organoids as an experimental system.

3.2.1 Organoids as a model for development

Organoids represent a remarkable example of the ability of biological systems to self-assemble and self-organize. What organoids show us is that stem-cell-derived cellular aggregates are able to activate developmental programs and coordinate them solely based on local cell-cell interactions, resulting in the formation of complex three-dimensional structures.

One must assume that in a developing embryo, similar processes take place and are underlying the genesis of tissues and organs. But the development of an embryo is evidently not solely based on local cell-cell interactions that induce the unfolding of genetic and cellular programs of development. It also relies on external cues and long-range control by morphogen gradients that help establishing directional information which is the basis for body axis determination and sets up developmental constraints for tissues to form. These framing constraints are largely missing in the case of organoids that develop *in vitro*.

Local interactions establish cellular structures in organoids without the help of external influences, but they lack the orchestration of all these events that lead to the formation of a healthy fetus. For example, although the formation of coherent floor plate tissue can be observed in organoids (Turner et al. 2015), in contrast to the embryo, more than one patch of floor plate can be specified, and their position and orientation in relation to other structures will be random (Turner et al. 2015). In contrast, in the embryo, floor plate tissue formation is regulated by influence from the notochord, which lies underneath the neural tube. Because of this extrinsic signal, only one floor plate is specified at the right position, allowing for the generation of motorneurons at just the right place.

There are other limitations to organoids that should be mentioned, such as the suboptimal nutrient and oxygen supply that becomes worse with increasing organoid size, and the stochasticity of developmental fate choices, which also lead to the formation of non-neural tissues that can exert unpredictable influence on the tissue type in consideration.

For this reason, the interpretation of organoids is not trivial, and should not be based on the assumption that organoids simply represent an artificially generated fetal structure. Instead, they should be treated as an assay system of their own, including a yet to be established framework of interpretation. Keeping this in mind, organoids can surely model many aspects of development, especially when it comes to the behavior of subcellular structures or cells, for example regarding polarity, INM or mitotic behavior, things that are influenced by the

three-dimensional embedding of cells in an tissue context, which is represented in organoids.

This thesis draws conclusion about the behavior of human neural progenitor cells and neurons based on organoids. Organoids reveal, for example, that neural progenitor cells with mutations in *FAT4* or *DCHS1* can still form neuroepithelial tissue that is properly polarized, but shows characteristic changes in process morphology and stability. In many cases, the mutations might also lead to complete delamination of progenitor cells, but in this case, no germinal zone would have been detected in the first place, making this kind of drastic structural phenotype difficult to analyze in this system.

3.2.2 Defects in organoids derived from *FAT4* and *DCHS1* mutated cells

In order to gain insight into the pathomechanism of neuronal migration defects in patients with mutations in *FAT4* and *DCHS1*, in this study organoids derived from patient-derived iPSC cells were generated and compared to control cell-derived organoids.

One might assume neuronal mislocalization to be one of the striking phenotypes to observe, as this is what is seen in patients. Indeed, organoids showed mislocalized neurons appearing in nodules in the progenitor zone of the ventricular structures of organoids.

However, overall, there was no drastic and generalized mislocalization of neurons, but mostly, neurons were localized outside of the progenitor zone. A really drastic phenotype of neuron mislocalization, leading to the complete intermingling of progenitors and neurons, potentially might not be spotted in organoids, as it would probably lead to dismantling of the whole germinal zone, making it unrecognizable.

It should additionally be noted that it is not yet clear which mechanism neurons use in organoids for migration. This question could be resolved, for example, by time-lapse imaging in organoid slices. It is well possible that neurons in organoids undergo radial glia guided migration, but given the fact that germinal zones in organoids are not very large, they might as well undergo somatic translocation, or even some other way of migration.

Furthermore, it is important to consider that in patients, the migration defect is not absolute and does not affect all neurons, which is one of the puzzling

facts about many neuronal migration defects that still remains to be solved. For instance, in subcortical band heterotopia, clearly, a part of the neurons manages to migrate to the cortical plate, and only a fraction remains at the heterotopic cortex. The same is true for periventricular heterotopia, where many neurons still migrate properly to form a cortex, and only some remain as heterotopic neurons at the ventricle.

In light of this, one might not expect a total loss of migration in cerebral organoids, but only a partial defect, as can be seen in cerebral organoids from *FAT4* or *DCHS1* mutants. As this is the first attempt to model neuronal migration defects in cerebral organoids, it was not clear what to expect. It is therefore of importance to see how organoids reflect the defects seen in patients.

3.2.3 Morphology of germinal zones in organoids

More than a simple mislocalization of neurons, mutant organoids are characterized by a much lower degree of organization in germinal zones. Especially germinal zones in *FAT4*-mutant organoids showed a much less clear border between the neuronal layer and the progenitor layer, and often massive intrusions of neuronal fibers back to the “ventricle”.

Interestingly, germinal zones of both backgrounds showed no striking defect in polarization. β -CATENIN as well as PALS1 were localized properly at the apical surface of the germinal zone. This is interesting because, as *FAT4* and *DCHS1* localize to the ventricular surface in the mouse developing cortex, and are implied in adhesion (Ishiuchi et al. 2009), one might assume defects in polarization when the function of *FAT4* and *DCHS1* is impaired. This is further suggested by the fact that *FAT4* has been shown to bind polarity proteins, such as *PARD3* (Badouel et al. 2015). On the other hand, however, knockout mice of *Fat4* and *Dchs1*, do not always show polarity defects in the neural epithelium (Badouel et al. 2015).

One might conclude from this data, that there is no *fundamental* defect in apico-basal polarity. It should be kept in mind, however, that there might well be more subtle defects, which reveal themselves on the level of radial glia morphology, which is defective in *FAT4* mutant organoids. It might still be that the localization of yet to be identified proteins is disturbed and negatively affects the ability of radial glia to uphold structural features necessary for neuronal migration.

Additionally, the ventricular surface of germinal zones of *FAT4* mutant organoids is disturbed and has a disrupted, discontinuous appearance. While not being

enough to destroy the whole structural integrity, this may point to a defect in adherent junctions stabilization, leading to a mechanical weakness of the ventricular surface.

Not only at the ventricular surface, but also with regard to the separation of the neuronal layer from the progenitor zone, mutant germinal zones had a less organized appearance, and this is again stronger in *FAT4* mutants than in *DCHS1* mutants. This probably reflects a general inability to form and uphold structure and retain clear separation.

3.2.4 Radial glia in mutant organoids

In order to analyze the morphology of radial glia in control and mutant organoids, immunohistochemistry for NESTIN was performed on frozen sections, as NESTIN is a marker commonly used to visualize the morphology of radial glia. Additionally, radial glia in mutant organoids were labeled by electroporating a Gap43-GFP expressing plasmid, and control organoids were electroporated with miRNAs against *FAT4* and *DCHS1* in order to look at the effects of knockdown on radial glia morphology.

It was shown that radial glia in mutant organoids differed from cells in control organoids. Especially in *FAT4* mutants, radial glia had a bent and twisted morphology, often with truncated or shortened processes. *DCHS1* mutants also did show a mild phenotype, especially after electroporation of the miRNA, but radial glia still had a much more elongated and intact appearance.

In addition, radial glia also seemed to delaminate more often in *FAT4* mutants and upon knockdown of *FAT4*, as cells were more often seen in basal locations under these conditions. These goes in line with the supposed weakness in stabilizing apical cohesion and fits the data from mouse, where acute knockdown of *FAT4* (as well as *DCHS1*) leads to delaminated progenitors, that then proliferate at ectopic positions (Cappello et al. 2013).

Why *DCHS1*-mutants do not show the same phenotype is not clear, especially as in mouse models, the phenotypes seen after knockout of *Fat4* and knockout of *Dchs1* commonly are very similar, indicating that they function together (Mao et al. 2011). One reason might be other combinations of interactions between FAT and DCHS proteins in the developing human brain, like for instance the interaction of *FAT4* with *DCHS2*, whereby compensating the loss of *DCHS1*. Alternatively, it could be that the phenotype is not at all related to the interaction

of FAT4 with DCHS proteins, but relies on an independent function of FAT4 in this context.

A defect in radial glia is a very plausible explanation for the structural aberrations seen in organoids, as progenitor zones in organoids should be structurally defined by radial glia cells. Furthermore, many mouse models show disruptions of the radial glia scaffold as causative for neuronal migration defects (Cappello et al. 2012; Kielar et al. 2014).

3.3 Defects in neuronal migration

Analysis of organoids has revealed structural deficits in mutant organoids, which could be related to defects in the stability of radial glia. However, the mutations might not only affect radial glia, but also intrinsically impair the ability of neurons to migrate, as even in the context of a completely intact radial glia scaffold, neurons might have lost their capability to polarize, to sense guiding signals, to move or to attach to radial glia fibers. In this situation, neurons show an autonomous migration defect, that can be revealed by transplantation experiments, putting neurons with a specific defect in a healthy background, where defective neurons fail to migrate despite the intact radial glia scaffold. Using iPSC-derived neurons, simply tracking their movement in a two-dimensional culture in a dish can reveal very basic defects of their ability to move and to migrate, independent of radial glia.

For this study, neurons derived from mutant cells were plated and followed by live imaging over three days. From their movements, three basic parameters were calculated, namely the average velocity, the number of resting time points and the tortuosity. Indeed, mutant cells display changes in all three parameters, a decrease in average velocity, increase in tortuosity and increase in the number of resting time points.

From this data, it becomes clear that mutations in *FAT4* and *DCHS1* not only affect radial glia but neurons as well. Neurons with mutations move slower, less directed, and they pause more. However, not all neurons in this experiment are affected to the same degree. In order to analyze if different groups could be found in the cell population analyzed, hierarchical clustering was performed on all cells based on their migration behavior which is characterized by all three parameters combined. And indeed, different subpopulations could be found.

Starting from two different groups in the control, only one of them was affected by the mutation. Again, this was not affecting all cells of this group, but only a fraction of them.

It is not possible to conclusively say something about the biological reason behind this. Basically, these different populations could represent different neuronal subtypes, such as excitatory vs. inhibitory neurons, employing different migration mechanisms that are affected by the mutations to a different degree. The fact that one group is again only partially affected can also be viewed in light of the fact that in patients, not all neurons show migration defects, but many still migrate properly, only a subpopulation of them forming heterotopic neuronal tissue.

It should be mentioned in this context that the cells in these experiments only had sparse contact with each other and in many cases were isolated. This poses a problem if one assumes that FAT4 and DCHS1 need to interact in order to be biologically active, either with each other or with different, yet unknown, interactors. If this is the case, how then, one might ask, should one explain a phenotype in cells with no apparent interactions?

It is well possible that both proteins do not need interactions for all of their functions, but they might also have a constitutive activity regardless of intercellular binding, which is lacking in mutant cells. In this context, it is of interest that in *Drosophila* it has been shown that the intracellular domain of Fat can have some independent function regardless of binding (Matakatsu and Blair 2006).

3.4 Mechanism behind the effects of FAT4 and DCHS1 defects on cerebral development

3.4.1 Role of the canonical functions of FAT4 and DCHS1

Mainly, mouse Fat4 and Dchs1 have been described to function in the regulation of PCP as well as in the regulation of proliferation via Hippo signaling. They are most known, as are their orthologs in *Drosophila*, for the regulation of PCP, which is important for a variety of developmental processes. For instance, the coordinated movement of cells in the development of the sternum, a process called *convergent extension*, which defines length and size of the sternum, crucially depends on Fat4 and Dchs1 mediated PCP (Mao et al. 2016). Also in the kidney, the oriented division of cells, which controls the direction of growth of tissue layers, has been shown to depend on Fat4 and Dchs1 (Saburi et al. 2008).

Generally, PCP is defined as directional information along the tangential plane of a sheet of cells. Processes that depend on this kind of directional information, such as directed tissue extension, the directed movement of cilia or the orientation of stereocilia crucially depend on it. But what about neuronal migration?

Indeed, the migration of facial-branchiomotor neurons in the rhombencephalon depends on Fat4 and Dchs1 mediated PCP (Zakaria et al. 2014). Facial-branchiomotor neurons are generated in rhombomere four in the rhombencephalon and migrate caudally as well as laterally, before commencing radial migration up to the pial surface in order to form a nucleus that innervates facial muscles. The caudal as well as the lateral movement is a form of tangential migration. Knock-out of Fat4 or Dchs1 still allows neurons to initiate the caudal movement, while abrogating the lateral movement (Zakaria et al. 2014). In contrast, interfering with the canonical, Fz-dependent, PCP signaling pathway inhibits the caudal movement (Zakaria et al. 2014). This indicates that both PCP pathways, the Fat4-Dchs1 mediated one and the Fz-mediated one, function on orthogonal tissue planes. Interestingly, radial migration is at least partially intact in Fat4 and Dchs1 knockout animals, which suggests that radial migration per se is not dependent on PCP signaling.

In fact, it is not easy to imagine how PCP would influence radial migration. As has been said, PCP is defined tangentially along a tissue plane, and becomes apparent when looking at a whole population of cells. Apico-basal polarity, in contrast, is defined radially, and is much more apparent within single cells. As radial migration involves movement in the radial direction, less along tangential paths, it is not clear what role PCP could play in this process.

In this study, PCP was not extensively addressed, partly due to technical reasons, as in organoids, which lack a clear tissue axis, PCP is not easily analyzed. It can not be excluded that PCP is disturbed in the mutant cells. But for the reasons given, the effects this would have on *radial* migration remains unclear.

3.4.2 Proliferation and Hippo signaling

The second putative function of Fat4 and Dchs1 is the regulation of proliferation via Hippo-signaling. Mechanistically, Dchs1 is thought to act as ligand to Fat4, which then interacts with Hippo signaling components to inhibit the activity of Yap, a transcription factor which activates pro-proliferative genes. As such, Fat4 mediated activation of Hippo functions to restrict proliferation. Indeed,

Fat4 has been described to be a tumor suppressor (Hou et al. 2016), and in many systems, control of proliferation, and specifically, the control of the balance between progenitors and differentiated cells, has been described as an important function of Fat4 signaling (Bagherie-Lachidan et al. 2015; Badouel et al. 2015).

However, the connection to Hippo signaling is not at all clear. First, the knockout mouse for Fat4 and Dchs1 does not show an overgrowth phenotype typically seen in Hippo defective mutants (Mao et al. 2011; Bossuyt et al. 2013). Especially, a liver-specific knockout of Fat4 does not show a phenotype that one would expect from disturbances in Hippo signaling (Bossuyt et al. 2013). Furthermore, in vertebrae, proliferation is *decreased* upon Fat4 deactivation, and this has been shown to be independent of Yap (Kuta et al. 2016).

Knockout of Fat1, and Fat1 together with Fat4 in the neural epithelium leads to overproliferation of progenitors, as does knockdown of Fat1 by in-utero electroporation in the cortex (Badouel et al. 2015). The authors of this study report that this is not accompanied by an apparent change in Yap localization to the nucleus or a change in the ratio of inactive P-Yap to active Yap (Badouel et al. 2015), although it seems they did not investigate this in detail. However, the over-proliferation of progenitor cells after knockdown of Fat4 or Dchs1 by in-utero electroporation in the cortex can be rescued by concomitant downregulation of Yap (Cappello et al. 2013).

Of note, a more recent study finds indeed a possibility of the regulation of Yap activity by Fat4 in the mouse myocardium beyond a direct interaction with Hippo signaling components. Specifically, Fat4 was shown to sequester Amotl1, an interactor of Yap, to regulate its activity (Ragni et al. 2017).

In this context, it is interesting that in organoids derived from *FAT4* or *DCHS1* mutant cells, there is no clear change in proliferation, as measured by PH3 positive cells per apical length. Additionally, no GO term associated with proliferation was detected to be deregulated in the scRNA sequencing data. But looking at the contradictory data from the literature, and given that in this case one is looking at a constitutive mutation, not an acute knockdown intervention, this apparent contradiction might be explicable. It could be, for example, that FAT1 is able to compensate for the loss of FAT4 in mutant organoids, while acute knockdown prevents this compensation. This is supported by the fact that in the knockout mouse for Fat4 and Dchs1, no strong phenotype was reported in the CNS, though one might suspect to see one if proliferation of progenitors is changed drastically upon loss of Fat4.

3.4.3 Hints towards a molecular mechanism

This study did not address the question of the molecular mechanism behind the action of *FAT4* and *DCHS1* extensively. However, in order to see what is happening on a transcriptional level in cell with mutations in *FAT4* and *DCHS1*, single cell RNA sequencing was performed using microdissected germinal zones from human cerebral organoids.

Looking at the transcripts that are differentially regulated between mutant and control organoids, it becomes apparent that many cytoskeletal genes are changed. The GO terms with the strongest changes are for instance *structural constituent of the cytoskeleton*, *microtubules* and *microtubule-based process*.

Many of the genes behind these GO terms are tubulins themselves. Indeed, in both *FAT4* and *DCHS1* mutant organoids, a list of different tubulin isoforms is downregulated. In both mutants, *TUBA1C*, for example, is strongly and reproducibly downregulated, and strongly separates the mutant cell populations from the control population. The microtubule cytoskeleton is known to play a fundamental role in many aspects of cerebral development. It is striking in this context that many of the tubulins that are deregulated in the mutant samples, are tubulins that often bear mutations in patients with cerebral malformations (Bahi-Buisson et al. 2014). These mutations very often are point mutations, leading to a broad variety of defects, such as corpus callosum agenesis, malformations of the basal ganglia, but also defects in gyrification, such as polymicrogyria or lissencephaly. However, neuronal heterotopia has also been described for mutations of some tubulins, namely *TUBB2B* and *TUBA1A* (Cushion et al. 2013).

Another class of cytoskeleton-related genes are Rho GTPases and their regulators. Rho GTPases are implicated in many developmental processes, including neuronal migration (Govek et al. 2011). The *FAT4*-dataset, for instance, shows differential expression of regulators of *RAC1*, such as *SRGAP2*, *SRGAP2B* or *SRGAP2* as well as *RAC1* itself. In mouse, *Rac1* has been implicated in the radial migration of neurons (Kawauchi 2003), although loss of *Rac1* does not seem to completely inhibit migration (Chen et al. 2007). Furthermore, *RHOA* was found to be changed, and *RhoA* has been implied in regulating radial glia scaffold stability (Cappello et al. 2012).

How this transcriptional regulation comes about cannot be told from the data at hand. While *FAT4* and *DCHS1* might be able to act on transcription, for example by modulating Hippo signaling or via still unknown factors, many of

the changes seen might also reflect secondary effects due to changes in identity or cell behavior, and they may reflect compensatory mechanisms.

Still, the fact that many of the genes changed are connected to cerebral malformations is indicative of their relevance for neural development, a fact which is further underlined by comparing the list of genes that are changed in mutant organoids with genes which show high rates of de novo mutations in patient cohorts with neural developmental disorders, such as autism or intellectual disability. Here, especially *FAT4* mutant cells stick out as many of the genes deregulated in those cells are found to be mutated in patients with developmental neural diseases.

The notion that the cytoskeleton is affected by mutations in *FAT4* and *DCHS1* is further underlined by the fact that the expression of acetylated tubulin, but not tyrosinated tubulin, is changed in *FAT4* mutant NPCs. As acetylated tubulin is an indicator of stabilized microtubules (Schulze 1987), while tyrosinated tubulin expression is indicative of microtubule turnover, this points to a change in microtubule stability in *FAT4* mutant cells. Furthermore, the actin cytoskeleton also seems to be changed, as staining for F-Actin, using Phalloidin, shows structural changes in both mutant NPCs.

The molecular link between *FAT4*, *DCHS1* and the cytoskeleton is unclear, and not much has been described in the literature so far. Some hints come from a study in zebrafish, which shows that *DCHS1* orthologs, *Dachsous1b* and *Dachsous2*, are important during zebrafish development and regulate microtubules as well as the actin cytoskeleton (Li-Villarreal et al. 2015). Furthermore, it was shown that in mouse, *Fat4* (as well as its homolog, *Fat1*) can bind actin-regulating proteins (Badouel et al. 2015).

3.5 Conclusion

The question of this study at the outset was whether iPSC-derived cells would reflect phenotypes related to the defect seen in patients, and whether the defects could be related to the migration of neurons or to defects in progenitors.

The data indeed shows defects both in progenitors as well as in neurons. Therefore, it first shows that defects can be modeled in iPSC-derived cells, and especially in human cerebral organoids. Second, it means that the defects seen in

patients are indeed related to both neurons and progenitors, and it supports the hypothesis that both cell types are contributing to the disease.

The exact molecular mechanism of the action of FAT4 and DCHS1 in human cells could not be elucidated in this work. However, the data acquired from scRNA sequencing and from western blot strongly suggests changes in the cytoskeleton in mutant cells, which are very promising in explaining the defects at hand.

4 Materials and Methods

4.1 Cell culture

For all cell culture materials, refer to table 4.1.

Table 4.1: Cell culture reagents used for in-vitro experiments in this study.

Reagent	Vendor
mTesR1 stem cell medium	StemCell Technologies, Vancouver, Canada
DMEM F12 with HEPES and Glutamin (NPC culture)	Thermo Fisher, Waltham, USA
DMEM F12 with Glutamax (Organoid culture)	Thermo Fisher, Waltham, USA
Neurobasal medium (Organoid culture)	Thermo Fisher, Waltham, USA
Non-essential amino acids	Thermo Fisher, Waltham, USA
B27 supplement with Vitamin A	Thermo Fisher, Waltham, USA
B27 supplement without Vitamin A	Thermo Fisher, Waltham, USA
N2 supplement	Thermo Fisher, Waltham, USA
Knockout Serum Replacement (KSR)	Thermo Fisher, Waltham, USA
ES grade Fetal Bovine Serum	Thermo Fisher, Waltham, USA
β -Mercaptoethanole (50 mM)	Thermo Fisher, Waltham, USA
Accutase	StemCell Technologies, Vancouver, Canada
Collagenase IV (1 mg/ml solution)	StemCell Technologies, Vancouver, Canada
Matrigel Growth Factor Reduced	Corning, New York, USA
Matrigel non-growth factor reduced	Corning, New York, USA
Geltrex coating solution	Thermo Fisher, Waltham, USA
Polyornithine powder	Sigma Aldrich, St. Louis, MO, USA
Laminine from murine sarcoma (1-2 mg/ml solution)	Sigma-Aldrich, St. Louis, USA
bFGF	Thermo Fisher, Waltham, USA
Y-27632 (Rock inhibitor)	StemCell Technologies, Vancouver, Canada
Heparin sodium salt from procine mucosa, cell culture grade	Sigma-Aldrich, St. Louis, MO, USA
Insulin solution human for cell culture	Sigma-Aldrich, St. Louis, MO, USA
Trypsin-EDTA 0.25%	Thermo Fisher, Waltham, USA
Antibiotic-Antimycotic	Thermo Fisher, Waltham, USA

4.1.1 Culture of human fibroblasts

Human fibroblasts were cultured in DMEM with Glutamax and 10% FBS. Cells were kept in an incubation chamber with 5% carbon dioxide and ambient oxygen levels at 37°C. The cells were split at confluency, roughly every 4-5 days. To split them, the cells were washed with sterile PBS and incubated with 0.25% trypsin for approximately 5 minutes. After this, the cells were washed off with DMEM F12 with 10% FBS, collected in a 15 ml collection tube, and spun down at 1200 rpm for 5 minutes. The supernatant was removed and the cells were resuspended in culture medium and distributed in a ratio appropriate for the desired downstream use.

4.1.2 Reprogramming of fibroblasts into induced pluripotent stem cells

Reprogramming of fibroblasts into iPSC was performed by Ejona Rusha, ISF, Helmholtz-Center Munich.

For reprogramming, a mRNA transfection based method was used. First, NuFF3-RQ feeder fibroblasts (GlobalStem, Gaithersburg, MD, USA) were seeded on a six-well dish in advanced MEM with 5% HyClone FBS (GE Healthcare, Buckinghamshire, GB), 1% non-essential amino acid and GlutaMax. Fibroblasts were dissociated using 0.25% Trypsin-EDTA, counted and seeded on the feeders at a density of 2×10^4 or 4×10^4 per well. One day later, the medium was changed to Pluriton Reprogramming medium (Stemgent, Cambridge, MA, USA). From day 3 to day 18, modified mRNAs of the reprogramming factors *OCT4*, *SOX2*, *KLF4*, *LIN28* and *C-MYC* (provided by the RNA core facility, Houston Methodist Hospital, Houston, TX, USA) were transfected at a ratio of 3:1:1:1:1 in Opti-MEM I Reduced Serum Medium (Thermo Fisher, Waltham, MA, USA) using Lipofectamine RNAiMAX transfection reagent (Thermo Fisher, Waltham, MA, USA). Transfection was done every day.

On day 16, medium was changed to StemPro hESC SFM (Thermo Fisher, Waltham, MA, USA) for five days. The iPSC colonies were harvested using 2 mg/ml collagenase IV in DMEM/F12. The iPSC were plated on γ -irradiated mouse fibroblasts and grown in StemPro medium for 10 passages. Afterwards, iPSC were adapted to a feeder free culture on Matrigel in mTeSR1 medium.

The control cell line was derived from BJ fibroblasts (ATCC CRL-2522, ATCC, Manassas, VA, USA) which were reprogrammed using the same method.

4.1.3 Culture of iPSC

iPSC were cultured in a 6-well dish coated with Geltrex. In order to coat the dish, Geltrex solution was diluted 1:200 in DMEM/F12 and spread evenly across the growth area. The plate with the coating solution was then incubated in the incubator at 37°C for at least 30 minutes.

iPSC were cultured in mTeSR1 culture medium at 5% carbon dioxide and ambient oxygen level at 37°C. Medium was replenished every day. The cultures were subjected to maintenance measures when needed: when appropriate, the culture was cleaned from differentiating colonies using a stereological microscope and a 1000 µl pipette tip. Differentiating colonies were localized based on morphology, scratched off using the tip and then washed away by medium change.

In the case of more widespread differentiation, colonies of high quality were manually picked under a stereological microscope. For this, a 200 µl pipette tip was used to scrape the colony off the plate, disrupting it into 2-3 pieces. The pieces were immediately sucked in and plated on a fresh Geltrex-coated 6-well plate.

Splitting of iPSC cells

For splitting, medium was removed from the iPSC and substituted by 1 ml of collagenase IV solution. Cells were incubated for about 10 to 15 minutes in collagenase in the incubator at 37°C. After this, the collagenase was carefully removed and new culture medium was added. The colonies were disrupted by scratching twice through the whole well. Afterwards, they were scraped off using a cell lifter. After this the suspension was taken off the plate and distributed according to the desired split ratio. Usually, cells were split in a ratio between 1:3 to 1:6, approximately 1 to 2 times a week.

4.2 Generation of neural progenitor cells

4.2.1 Coating of culture dishes

For experiments with NPCs, cells were cultured on polyornithine/laminin coated dishes. Dishes were first incubated with a solution of 10 µg/ml polyornithine in water over night in the incubator at 37°C. The next day, the polyornithine

solution was removed and the growth area was covered with 5 µg/ml laminin solution in PBS for at least 2 hours at 37°C. On glass coverslips, the concentration of polyornithin used for coating was 100 µg/ml and the concentration of laminin was 20 µg/ml.

4.2.2 Differentiation of iPSC into NPCs

In order to derive neural tissue from iPSC, the procedure described in Topol et al. 2015 was followed. At confluency, medium was changed to neural induction medium for EBs (DMEM F12 with HEPES and Glutamine, N2 1:100, B27 without Vitamin A 1:50), and colonies were made smaller by scratching through the whole growth area once. After this, colonies were lifted off the plate using a cell lifter. The suspension was when plated on a new plate and kept on a shaker in the incubator in order to prevent the colonies to settle again on the plate. Kept in suspension, colonies started to form spherical embryoid bodies that were kept in neural induction medium for 7 days. Medium was replenished every second day or as needed.

After 7 days, the embryoid bodies were plated on a dish coated with polyornithin and laminin. The embryoid bodies were then kept in neural induction medium for EBs for another 7 days, the medium being replenished every second day. After 7 days, emerging rosettes were picked using a stereological microscope and a 1000 µl pipette tip. Rosettes were discerned by their characteristic tubular morphology and lifted off using the pipette tip. After all rosettes have been lifted off the plate, the medium was collected and plated on a fresh polyornithin/laminin coated plate. After one day, rosettes usually settled down as chunks. The rosettes were cultured for another 3-4 days. Subsequently, they were picked again, this additional purification step avoiding contamination with too many non-neural cells. At this picking step, the rosettes were dissociated by trituration, and plated on a fresh polyornithin/laminin coated plate in neural progenitor medium (DMEM F12 with HEPES and Glutamine, N2 1:100, B27 without Vitamin A 1:50, bFGF 10 ng/µl).

4.2.3 Culture of NPCs

Once dissociated, the neural progenitor cells were further cultured on polyornithin/laminin coated dishes in neural progenitor medium. At confluency, cells

were split 1:3. For splitting, the medium was removed and cells were incubated with Accutase for five minutes. Once cells were dissociated, they were spun down at 1200 rpm for five minutes. Subsequently, they were resuspended in culture medium and distributed on a fresh polyornithin/laminin coated plate.

4.2.4 Time lapse imaging of neurons

For time lapse imaging, NPCs were plated on a polyornithin/laminin coated 24-well plate and left in neural progenitor medium (DMEM F12 with HEPES and Glutamine, N2 1:100, B27 without Vitamin A 1:50) without bFGF for 5 days. After this, cells were imaged using a Zeiss Fluorescent Microscope for three days in a incubation chamber, maintaining 37°C and 5% carbon dioxide concentration. The cells were imaged every 5 minutes, several positions being taken per well.

From the time lapse movies, movement data was derived by manual tracking the cells using the Manual Tracking plugin for ImageJ (Schindelin et al. 2012). No centering correction was applied.

From the tracking data, parameters were calculated using the R software package (R Development Core Team 2008). The average velocity was directly calculated from the measured velocities, the number of resting time points was calculated by counting the number of time points with a velocity of 0, and dividing this number by the length of the whole dataset for each cell. The tortousity was calculated as

$$\frac{\sum_{i=1}^{i=n} \sqrt{(X_{i+1} - X_i)^2 + (Y_{i+1} - Y_i)^2}}{\sqrt{(X_n - X_1)^2 + (Y_n - Y_1)^2}}$$

for a track of a cell of length n , X and Y being the X and Y coordinates of the cell at a certain time point. The numerator calculates the path the cell actually traveled, including all diversions, while the denominator calculates the net displacement of the cell from the beginning to the end of the movie.

The subsequent steps of analysis were done with the help of Mariana Schröder, MPI of Psychiatry, Munich. Z-Scores were calculated by subtraction of the mean of the control from the raw data points and subsequent division by the standard deviation of the control within each experiment. Combined migration behavior scores were calculated by computing the sum of the values of the three parameters

for each cell. For this calculation, the sign of the the z-scores for the velocity were inverted to equalize the direction of z-score change for the three parameters in mutants with respect to control. For the clustering analysis, the combined z-score was subjected to a 2-step hierarchical clustering algorithm.

All these analysis were done using GraphPad PRISM (GraphPad Software, La Jolla, CA, USA) and SPSS (IBM Corp., Armonk, NY, USA).

4.3 Generation of cerebral organoids

The generation of cerebral organoids followed the protocol by Madeline Lancaster (Lancaster and Knoblich 2014). When ready for splitting, iPSC cells were harvested by incubating them for 3 minutes in Accutase and washing them off with an equal amount of mTeSR1. The cell suspension was then collected in a 15 ml collection tube and spun down for 4 minutes at 300 g. The cells were then resuspended in 0.5 mL of *low bFGF hES medium* (DMEM F12 with Glutamax, 20% Knockout Serum Replacement, 3% ES grade FBS, 1% Non-essential amino acids) that was supplemented 4 ng/ml bFGF and contained Y-27632 at a concentration of 50 μ M. The cells were then counted in a Neubauer counting chamber and diluted to reach a concentration of 60 000 cells/ml with low bFGF human ES medium, supplemented as stated above. For plating, 150 μ l, i.e. 9000 cells, of this suspension were given into each well of a 96-well round-bottom low adhesion plate (Corning, New York, USA, Cat.No 7007).

After plating, the cells were incubated in a incubator at 37°C and 5% carbon dioxide and ambient oxygen. Medium was changed every second day with low bFGF human ES medium with bFGF and Y-27632 until day 4. From day 4 on, bFGF and Y-27632 supplements were left out.

The forming EBs were monitored for their size and morphology. Once they started to brighten at the outside and reached a size of approx. 400 μ m, typically after 5 days, they were transfered to a 24 well low adhesion plate (Corning, New York, USA, Cat. No 3473). To do this, the medium was changed to neural induction medium (DMEM F12 with Glutamax, N2 1:100, 1% non-essential amino acids, 5 μ g/ml Heparin). Using a cut 200 μ l pipette tip, the embryoid bodies were ransfered from the 96-well plate to the 24 well plates, containing 500 μ l neural induction medium, usually putting 2-3 embryoid bodies into one well.

The embryoid bodies were further cultured in neural induction medium for 6

to 7 days with medium changes every second day. Once they showed a bright, clear rim at the outside, indicating the induction of neuroepithelial tissue, they were transferred into droplets of Matrigel (non-growth factor reduced). To do this, a sheet of parafilm was put over a Terasaki plate and pushed into the wells, so wells would form in the sheet of parafilm. The embryoid bodies were taken out of the 24 well plate using a cut 200 μ l pipette tip and each put into one well of the parafilm sheet. Residual medium was removed, and a drop of Matrigel was put onto the embryoid body. Once every embryoid body had been covered by Matrigel, the parafilm was put into a 10 cm dish and incubated in the incubator at 37 °C for approx. 30 minutes. After this, the embryoid bodies were washed off the parafilm with neural differentiation medium without Vitamin A (DMEM F12 with Glutamax and Neurobasal 1:1, N2 1:200, B27 without Vitamin A 1:100, Insulin 2.5 μ g/ml, Antibiotic-Antimycotic 1:100) and kept in this medium for another 3-4 days in the incubator.

Once radial outgrowths were emerging on the organoids, the medium was changed to neural differentiation medium with Vitamin A (same as above, with B27 without Vitamin A substituted by B25 with Vitamin A), and the plate with organoids was put on a shaker in the incubator. Medium was changed every 3-4 days. The organoids were kept in this condition until analyzed.

4.3.1 Electroporation of organoids

For the electroporation of organoids, plasmid DNA was diluted to a concentration of 1 μ g/ μ l in sterile PBS. The organoid was put into a electroporation chamber (Harvard Apparatus, Holliston, MA, USA) with Neural Differentiation Medium without antibiotics. Using a manually pulled glass capillary, the plasmid solution, mixed with 0.1% FastGreen stain, was injected at random positions into the organoid, in total injection around 5 μ l. After injection, 5 pulses at 80 V with a 50 ms duration were applied with a 1 s interval using the ECM830 electroporation device (Harvard Apparatus, Holliston, MA, USA).

4.3.2 Analysis of cerebral organoids

For immunohistochemistry, cerebral organoids at the desired time point were fixed in 4% formaldehyde for 2 hours at 4°C. They were then left in a 30% sucrose

solution over night at 4°C. After this, they were embedded in embedding molds with OCT (VWR, Radnor, PA, USA) and kept at -20°C until further processing.

Frozen organoid samples were cut at a cryotome, preparing 16 µm sections. Usually, 3-4 organoids were embedded together.

4.4 Immunohistochemistry

For immunohistochemistry on frozen sections, the sections were first incubated in PBS for 5 minutes. After this, the sections were permeabilized with a solution of 0.1% Triton X in PBS for 5 minutes. Following permeabilization, sections were incubated for one hour in 0.1% Tween in PBS with 10% Normal Goat Serum for approximately 1 hour for blocking. After blocking, the primary antibody (see Table 4.2) was immediately put onto the sections in a solution of 0.1% Tween in PBS with 10% NGS. The primary antibody was incubated on the sections overnight at 4°C. The secondary antibody was diluted in a solution of 0.1% Tween in PBS with 10% NGS and incubated on the section for 90 minutes. Nuclei were stained for using DAPI (0.02 mg/ml in H₂O). Secondary antibodies were diluted 1:1000. All secondary antibodies were bought from Thermo Fisher, Waltham, MA, USA.

Images of the stainings were taken using a confocal laser scanning microscope (Olympus, Leica).

4.5 Quantification of PH3

For quantification of PH3⁺ cells in sections of cerebral organoids, maximum projections of the slices were used. PH3 cells were quantified that were located at the apical surface, and the length of the surface measured was quantified using ImageJ. Number of PH3⁺ cells was divided by this length to get the number of PH3⁺ cells per apical surface length.

Table 4.2: List of antibodies used and their dilutions on sections.

Marker	Vendor	Catalog Nr.	Dilution
Pax6	Biologend	PRB-278p	1:500
Map2	Sigma Aldrich	M4403	1:500
Tbr1	Abcam	ab31940	1:500
Tbr2	Millipore	ab31940	1:500
Tubb3	Sigma Aldrich	T8660	1:500
Nestin	Millipore	MAB5326	1:200
Tyrosinate Tubulin	Merck Millipore	ABT171	Western Blot: 1:1000
Actetilated Tubulin	Sigma Aldrich	T7451	Western Blot: 1:6000
Pals1	Sigma Aldrich	07-708	1:500
Beta-Catenin	BD Biosciences	610154	1:500
PH3	Millipore	06-570	1:500
GAPDH	Millipore	CB1001	Western Blot: 1:6000
GFP	Aves Lab	GFP-1020	1:1000
Alexa Flour 584 Phalloidin (Actin)	Thermo Fisher	A12381	1:40

4.6 In-situ hybridization

In-situ hybridization was performed by Timucin Oeztuerk, MPI of Psychiatriy, Munich. The probes were provided by Stephen Robertson, University of Otago, Dunedin, New Zealand. Probe sequences for both *DCHS1* and *FAT4* were cloned in the pGEM-T vector backbone.

For the generation of probes, plasmids were digested with SpeI for the sense and SacII for the antisense probe. (NEB, Ipswich, MA, USA). CDNA was synthesized from the linearized plasmid using T7 polymerase. DNA was extracted by using phenol-chloroform-isoamyl alcohol extraction and precipitation using ammonium acetate. After centrifugation, the precipitated pellet was resuspended in RNase free water. In-vitro transcription of the probes was done using the DIG RNA labeling mix (Roche, Basel, Switzerland) according to the manufacturers protocol. Probes were extracted using phenol-chloroform-isoamyl alcohol, pelleted using ammonium acetate and resuspended in RNase free water.

For detection of mRNA transcripts, 16 μ m frozen sections were pre-hybridized in 2 mL of hybridization buffer (formamide 50%, SSC buffer (20x stock: 3M sodium chloride, 300 mM trisodium citrate, adjusted to pH 7.0 with HCl) 1x, SDS 2%, Yeast tRNA 50 μ g/mL (Roche, Basel, Switzerland), Blocking Reagent (Roche, Basel, Switzerland) 2%, heparin (Sigma) 50 μ g /mL) for 1 h at 65 °C. After this, the buffer was replaced by 1350 μ l hybridization buffer containing the probe of interest in a 1:100 dilution. The hybridization was performed at 65 °C overnight.

The next day, hybridization buffer was replaced by washing buffer (formamide 50 %, SSC 1x, Tween20 0.1%, H₂O) and the sections were washed at 65 °C for 1h. This step was repeated 3 times. Subsequently, the washing buffer was replaced by MABT (5x stock: maleic acid 100 mM, sodium chloride 150 mM, Tween20 0.1%, H₂O, pH adjusted to 7.5 with sodium hydroxide). Sections were incubated in MABT twice for 30 minutes at room temperature. Subsequently, sections were blocked using ISH blocking buffer (MABT 1x, Blocking Reagent (Roche, Basel, Switzerland) 2%, FCS 2%, H₂O) for 1 hour at room temperature. Anti-Digoxigenin Fab Fragments (Roche, Basel, Switzerland) were then diluted 1:2500 in ISH blocking buffer and incubated on the sections at 4 °C overnight.

The next day, sections were washed with MABT 5x stock solution for 20 minutes. Afterwards, sections were incubated two times for 15 minutes in AP staining solution (Tris 100 mM, pH 9.5, magnesium chloride 50 mM, sodium chloride 200 mM, Tween20 0.1%, H₂O). The AP staining solution was then replaced by AP staining solution containing NBT and BCIP (both Roche, Basel, Switzerland) in a 0.35% concentration. The color reaction was allowed to proceed over night at 4°C and stopped by washing the sections with PBS. Sections were then stained with DAPI (0.02 mg/ml in H₂O) to visualize nuclei.

4.7 Generation of miRNAs

MiRNAs were generated with the help of Yang Lu using the BockIT system from Invitrogen (Thermo Fisher, Waltham, MA, USA). MiRNA sequences were generated using Invitrogens RNAi design tool ¹ with the cDNA sequences of *FAT4* and *DCHS1* as seed sequence. Three miRNA sequences were chosen and ordered as oligonucleotide from Sigma.

DCHS1 and *FAT4* miRNA oligonucleotides were ligated into an pENTR entry vector (Thermo Fisher, Waltham, MA, USA). To do this, a ligation reaction was performed using T4 DNA Ligase (Thermo Fisher, Waltham USA) according to the manufacturers protocol. Subsequently, the miRNA sequences were then cloned into the pCAGGS destination vector using the Gateway system (Thermo Fisher, Waltham, MA, USA) according to the manufacturers protocol.

¹<https://rnaidesigner.thermofisher.com/rnaiexpress/setOption.do?designOption=mirna&pid=1961720787891316464>, accessed on March 20th, 2017

Table 4.3: Sequences of miRNAs used against FAT4 and DCHS1

Gene	Sequence
DCHS1 top	TGCTGTACACTGTCAGGTTGATCTCCGTTTTGGCCAC TGACTGACGGAGATCACTGACAGTGTA
DCHS1 bottom	CCTGTACACTGTCAGTGATCTCCGTCAGTCAGTGGC CAAAACGGAGATCAACCTGACAGTGTA
FAT4 top	GCTGATCAGTTGCAGTAACAGAGGAGTTTTGGCCAC TGACTGACTCCTCTGTCTGCAACTGAT
FAT4 bottom	CCTGATCAGTTGCAGACAGAGGAGTCAGTCAGTGG CCAAAACCTCCTCTGTTACTGCAACTGATC

4.8 Plasmid preparation

4.8.1 Small scale plasmid preparation

Plasmid DNA was transformed into the DH5 α strain of competent bacteria. For transformation, bacteria were incubated with the plasmid DNA for 15 minutes, and subsequently treated with a heat shock of 42°C for 45 seconds. After this, the bacteria were shortly put back on ice, and then incubated for 30 minutes in LB-Media warmed to 37°C. Subsequently, bacteria were streaked out on a Agar plate with the respective antibiotic.

Colonies were inoculated into 5 mL of LB-Medium containing the respective antibiotic. The tube was incubated overnight at 37°C. After this, plasmid DNA was extracted using the Qiagen Plasmid Mini Kit (Qiagen, Venlo, Netherlands).

4.8.2 Large scale plasmid preparation

For large scale plasmid preparation, plasmid DNA was transformed as described above. Colonies were inoculated into 250 ml of LB medium and incubated at 37°C overnight with the respective antibiotic. Plasmid was then extracted using the Qiagen Plasmid Maxi Kit (Qiagen, Venlo, Netherlands).

4.9 qPCR

For validation of miRNA knockdown efficiency, the SH-SY5Y cell line was used. MiRNA constructs were electroporated using the Nucleofector 2B system from Lonza (Lonza, Basel, Switzerland). 1×10^6 cells were used per reaction. Cells were mixed with 100 μ l nucleofection solution that included 18 μ l nucleofection supplement (Nucleofection Kit VCA-1003, Lonza, Basel, Switzerland) and 1 μ g of the respective plasmid DNA. Subsequently, pulse sequence A-023 (preprogrammed by the manufacturer) was applied. Cells were immediately taken up in pre-warmed culture medium (DMEM F12 with Glutamax, 10% FBS) and plated on one well of a 6-well plate.

After three days, cells were washed with ice-cold PBS and scraped in ice-cold PBS on ice. Cells were spun down at 1200 rpm at 4 °C for 5 minutes. RNA was extracted from the pellet using miRNeasy Mini Kit (Qiagen, Venlo, Netherlands).

From the isolated RNA, cDNA synthesis was performed using SuperScript III reverse transcriptase (Thermo Fisher, Waltham, MA, USA) according to the manufacturers protocol using random primers. 2 μ g of RNA were used for this reaction. Subsequently, qPCR was performed on a Roche LightCycler (Roche, Basel, Switzerland) using the following reaction mix for each reaction:

Forward Primer	1 μ l
Reverse Primer	1 μ l
LightCycler 480 SYBR Green I Master (Roche)	5 μ l
H ₂ O	2 μ l

The following primer sequences were used:

FAT4

Forward	5'-CTTCCAAATGGACCCTGAGA-3'
Reverse	5'-CGGTGCCCACTTGAGCATTC-3'

DCHS1

Forward	5'-TGCACCTGAAGACACGGTAT-3'
Reverse	5'-CAGAGGCCTCATAAGCCGTA-3'

For each reaction, 1 μ l of cDNA was used. The reaction was run after a preincubation step at 95°C for 10 minutes with 45 cycles of 95°C for 10 seconds, followed by 60°C for 10 seconds and 72°C for 10 seconds. At the end of the qPCR, melting

curves were measured for the PCR products. C_p values were determined using the second derivative maximum of the amplification curve. Fold expression was calculated using this formula:

$$E = 2^{-\Delta\Delta C_p}$$

$\Delta\Delta C_p$ representing the difference of the difference of the C_p value of the gene of interest and the C_p value of the housekeeper for control and treatment, respectively.

4.10 Western Blot

For western blot, cell lysates were prepared by scraping the cells on ice, spinning them down in ice-cold PBS, and freezing the pellet for later use at -80°C . For analysis, the pellet was lysed using lysis buffer (62.5 mM Tris-HCl, pH 6.8, 2% SDS, 10% saccharose in water with proteinase and phosphatase inhibitors (Roche, Basel, Switzerland)) by pipetting up and down and incubation on ice for 15 minutes.

The protein concentration was measured using a standard BCA assay and a standard dilution series based on BSA (Kit from Thermo Fisher, Waltham, MA, USA). The desired amount of protein was mixed with Laemmli buffer (4% SDS, 20% glycerol, 10% β -mercaptoethanol, 0.004% bromphenol blue and 0.125 M Tris HCl, pH 6.8) and heated for 3 minutes at 95°C . The sample was when loaded on a 12% SDS gel. Electrophoresis was performed at 180 V. Usually, 10 or 20 μg of protein were loaded on the gel.

After the completion of electrophoresis, proteins were blotted on a nitrocellulose membran using the tank method. To do this, three whatman paper, followed by the nitrocellulose membrane, the gel and again three whatman paper and a sponge (order from anode to cathode) were put into a blotting frame. This blotting frame was then put into a tank filled with blotting buffer (129 mM Glycine, 25 mM Tris-base, methanol 20%). Blotting was performed for 90 minutes at 100 V.

After blotting, the membrane was incubated for 1 h with a solution of milk in TBST 5%. The primary antibody was then incubated on the membrane overnight

at 4°C in TBST (137 mM NaCl, 2.7 mM KCl, 19 mM Tris base, 0.01% Tween). The antibody against acetylated tubulin was diluted 1:6000, the antibody against tyrosinated tubulin 1:1000, the antibody against GAPDH 1:6000. After incubation with the primary antibody, the membrane was washed 3 times with TBST and then incubated with the secondary antibody in TBST with 2.5% milk for 1 hour. The secondary antibodies were diluted 1:10000.

For protein detection, membranes were incubated with ECL detection reagent (Millipore, Billerica, MA, USA) and visualized using the ChemiDoc system (Biorad, Hercules, CA, USA). Band intensities were quantified using ImageJ.

4.11 Single cell RNA sequencing

Single Cell RNA sequencing was performed by Sabina Kanton and Barbara Treutlein, MPI of Evolutionary Anthropology, Leipzig. The method used for single cell RNA sequencing of organoid cortical zones is described in Camp et al. 2015. For all experiments, single cortical zones were microdissected from organoids. To do this, organoids were embedded in 4% low melting agarose (Sigma), dissolved in Dulbecco's PBS (Thermo Fisher, Waltham, MA, USA) and cut at a vibratome in 150 µm sections. Individual regions were identified under a stereomicroscope, microdissected and dissociated using Accutase (StemCell Technologies, Vancouver, Canada).

Single cells were captured on a Fluidigm C1 chip for mRNA-seq (Fluidigm, San Francisco, CA, USA). cDNA was prepared using the SMARTer Ultra Low RNA Kit for Illumina (Clontech, Mountain View, CA, USA). Quality control was done by adding external Spike-In RNA (RNA Controls Consortium RNA Spike-In Mix, Ambion, Thermo Fisher, Waltham, MA, USA). Sequencing libraries were generated in 96-well plates using Illumina Nextera XT DNA Sample Preparation Kit (Fluidigm, San Francisco, CA, USA). Sequencing was done using Illumina HiSeq. The data was processed using various packages for R and custom scripts as described in Camp et al. 2015.

A Tables for single cell RNA sequencing data

A.1 List of differentially expressed genes with a power greater than 0.4

myAUC: Area under the curve (the farther this value is from 0.5, the better the separation between control and mutant cell populations); avg diff: average difference of expression; power: a measure of the ability of a gene to separate control and mutant cell populations (derived from myAUC), the closer to 1, the better the ability to separate

<i>DCHS1</i>				<i>FAT4</i>			
gene	myAUC	avg diff	power	gene	myAUC	avg diff	power
EEF1A1	0.018	-2.6762774493	0.964	TUBA1C	0.032	-3.0068318662	0.936
TUBA1C	0.033	-3.0030145998	0.934	H3F3A	0.05	-1.9786313502	0.9
POTEE	0.057	-3.0738039334	0.886	EEF1A1	0.056	-1.8586279215	0.888
TUBB	0.062	-2.8546421448	0.876	TUBB	0.056	-3.1564812447	0.888
RGPD5	0.071	-4.2019324415	0.858	CBWD3	0.062	-2.7071608284	0.876
POLR2J3	0.076	-4.1199210356	0.848	POTEE	0.079	-2.6745412785	0.842
CBWD3	0.079	-2.8107727459	0.842	POTEJ	0.082	-2.1149669337	0.836
POTEJ	0.082	-2.1149669337	0.836	SRGAP2	0.085	-3.3290618726	0.83
GTF2I	0.084	-2.7694061567	0.832	EIF3C	0.088	-3.9744798388	0.824
SRGAP2B	0.085	-3.5532563309	0.83	RGPD5	0.088	-2.9669719031	0.824
EIF3C	0.087	-3.5852397411	0.826	POLR2J3	0.089	-3.7070170309	0.822
SRGAP2	0.092	-2.7033403158	0.816	NPIPA7	0.101	-2.5759919008	0.798
NPIPA7	0.093	-2.746357309	0.814	SRGAP2C	0.104	-3.2255683268	0.792
NPIPB5	0.117	-2.7613128143	0.766	CBWD7	0.118	-0.5820845613	0.764
RGPD6	0.119	-3.9696500375	0.762	SRGAP2B	0.124	-1.7114994616	0.752
NPIPB4	0.124	-2.7552638729	0.752	CBWD5	0.134	-1.8946914445	0.732
NBPF8	0.137	-2.1689691958	0.726	NBPF14	0.14	-2.2065029278	0.72
NDUFA3	0.142	-2.2422498216	0.716	NPIPB4	0.141	-2.4485009109	0.718
EIF3CL	0.145	-3.6518286294	0.71	RGPD6	0.141	-1.8174529366	0.718
NBPF10	0.154	-2.183805536	0.692	EIF3CL	0.143	-3.6793825034	0.714
SHISA2	0.154	-5.1334414516	0.692	FOXG1	0.147	-5.4789896598	0.706
FABP5	0.155	-3.3010896122	0.69	NDUFA3	0.147	-2.3349521112	0.706
FOXG1	0.16	-3.8388162779	0.68	SRP14	0.851	1.3605761931	0.702

Tables for single cell RNA sequencing data

<i>DCHS1</i>				<i>FAT4</i>			
gene	myAUC	avg diff	power	gene	myAUC	avg diff	power
SRGAP2C	0.16	-2.1674840064	0.68	RND3	0.848	2.2068621057	0.696
TUBB2B	0.162	-2.1255996474	0.676	HNRNPA1L2	0.153	-0.5308783553	0.694
LHX2	0.167	-5.4729441861	0.666	POTEI	0.155	-1.5762832841	0.69
NPIPA3	0.169	-2.1452797512	0.662	TUBB2B	0.156	-2.3130059544	0.688
NBPF9	0.175	-2.4066143612	0.65	CKB	0.157	-2.0161874863	0.686
DDX39B	0.176	-2.7284243804	0.648	FTL	0.843	1.3862336986	0.686
NPIP3	0.178	-2.6148036493	0.644	NPM1	0.843	2.5214805724	0.686
RGPD8	0.182	-3.7596333549	0.636	GTF2I	0.159	-0.0944317021	0.682
TUBB2A	0.2	-2.1583371195	0.6	FABP5	0.16	-2.7863416124	0.68
TMSB15B	0.206	-4.227160752	0.588	NPIPA8	0.16	-1.1224081006	0.68
SFRP1	0.209	-4.6073679863	0.582	NPIP5	0.166	-1.5029200081	0.668
PGAM1	0.21	-2.4039253541	0.58	NBPF10	0.171	-1.8765922104	0.658
MAGED4B	0.215	-3.1920793771	0.57	NBPF9	0.176	-2.2531274624	0.648
MAGED4	0.218	-3.5425116009	0.564	C1orf61	0.177	-2.8672893631	0.646
BOLA2B	0.22	-3.4849333347	0.56	EEF1G	0.183	-1.3509075927	0.634
BRD2	0.223	-2.2473027958	0.554	NBPF8	0.183	-1.4260645502	0.634
TIA1	0.234	-2.0578000929	0.532	BCAS4	0.184	-0.9921497034	0.632
RBMXL1	0.237	-2.0371150566	0.526	POLR2J2	0.184	-1.1604676287	0.632
CSNK2B	0.241	-2.0576357706	0.518	HNRNPA1	0.187	-1.4361624997	0.626
CNOT1	0.242	-3.4631152827	0.516	CAPZA1	0.812	1.1490990543	0.624
PGAM4	0.25	-2.7436535241	0.5	TRA2A	0.811	0.9853696994	0.622
CREB5	0.251	-3.3584149166	0.498	ZIC2	0.811	2.7063554457	0.622
HOXA3	0.743	3.6524899665	0.486	NDUFA6	0.194	-1.5942023975	0.612
PSMC1	0.261	-3.6198209953	0.478	SHISA2	0.194	-2.6399475829	0.612
PHLDA1	0.262	-3.858466791	0.476	SREBF2	0.2	-2.0713933761	0.6
EFNB2	0.263	-2.1197981205	0.474	DDX39B	0.201	-2.6117071457	0.598
CCNT2	0.265	-2.7087331658	0.47	TMSB4X	0.201	-1.3600385984	0.598
EIF4E	0.267	-2.1073419944	0.466	SERF1A	0.203	-1.164745896	0.594
TLE1	0.27	-2.9502159919	0.46	ZFH3	0.796	1.7873216975	0.592
EDARADD	0.73	2.0797410797	0.46	EIF1AX	0.208	-1.1603342021	0.584
C21orf33	0.274	-3.2491999581	0.452	MAGED4B	0.208	-3.8597814449	0.584
PJA1	0.276	-2.3670669484	0.448	SMN1	0.209	-1.1211916714	0.582
SMIM11	0.277	-3.3972182595	0.446	TMSB15B	0.21	-4.1746256601	0.58
RAP1B	0.279	-2.1331423287	0.442	BOLA2B	0.212	-3.6453287899	0.576
PIGY	0.28	-6.9250273744	0.44	CBWD1	0.213	-1.2918756267	0.574

Tables for single cell RNA sequencing data

<i>DCHS1</i>				<i>FAT4</i>			
gene	myAUC	avg diff	power	gene	myAUC	avg diff	power
TFAP2C	0.28	-4.3967993823	0.44	NPIPA3	0.213	-1.5006334357	0.574
DGCR8	0.282	-3.6743930113	0.436	SFRP1	0.217	-1.7224395068	0.566
IFI44L	0.282	-5.6104924048	0.436	MAGED4	0.221	-3.5232855529	0.558
RASA4	0.282	-3.5314974035	0.436	YWHAZ	0.779	0.9587178187	0.558
CRABP1	0.709	3.3527994967	0.418	NACA2	0.222	-1.588821532	0.556
GTF2H2C	0.293	-2.0390465023	0.414	BRD2	0.223	-2.2437663139	0.554
PIK3C2B	0.293	-2.1684202436	0.414	SON	0.777	1.3760073807	0.554
DHCR24	0.299	-4.7012667079	0.402	ARL17A	0.224	-1.0977421945	0.552
QARS	0.299	-2.1260583323	0.402	NPIPA1	0.224	-1.5260008533	0.552
U2AF1	0.299	-2.3717315781	0.402	SERF1B	0.225	-1.3997013407	0.55
WWTR1	0.3	2.5016326597	0.4	DDX3Y	0.775	5.3510923523	0.55
				NPIP3	0.228	-1.2478350818	0.544
				SMN2	0.228	-1.4047759237	0.544
				RGPD8	0.233	-1.5848553677	0.534
				CREB5	0.235	-3.6839020829	0.53
				NBPF12	0.236	-2.0212407607	0.528
				LHX2	0.237	-2.4499389774	0.526
				MEIS1	0.762	2.1459445277	0.524
				TMSB10	0.76	1.6883073619	0.52
				NNAT	0.243	-9.1509121485	0.514
				CRABP1	0.755	3.3365116332	0.51
				TCF7L2	0.754	2.6937325194	0.508
				SAR1A	0.752	1.2768472526	0.504
				SMS	0.25	-1.6309752338	0.5
				RUNX1T1	0.75	1.4334734794	0.5
				USP9Y	0.75	3.2352361745	0.5
				ARL17B	0.251	-0.9690497885	0.498
				EFNB2	0.252	-2.2168941991	0.496
				ZIC1	0.747	4.5986445575	0.494
				COX7A2	0.746	1.0375902354	0.492
				CSNK2B	0.256	-2.0855656706	0.488
				SERF2	0.743	1.299165902	0.486
				WNK1	0.258	-1.6145683544	0.484
				TES	0.742	4.3945769387	0.484
				NFIA	0.259	-1.8548973599	0.482

Tables for single cell RNA sequencing data

<i>DCHS1</i>				<i>FAT4</i>			
gene	myAUC	avg diff	power	gene	myAUC	avg diff	power
				PDZD8	0.259	-2.6559517446	0.482
				ANKRD36C	0.26	-1.0960307839	0.48
				LRP6	0.26	-1.5367225687	0.48
				PPIA	0.26	-0.7246524353	0.48
				TUBGCP4	0.26	-1.5421861495	0.48
				NAIP	0.262	-0.8458325868	0.476
				ANKRD36	0.263	-0.9325343728	0.474
				PRR4	0.263	-1.5670039133	0.474
				NEFL	0.737	2.6694177322	0.474
				TPI1	0.265	-1.1145570383	0.47
				USP11	0.266	-1.3709494955	0.468
				LSM12	0.268	-0.9311061477	0.464
				ARPC4	0.732	1.1039565026	0.464
				NBPF11	0.269	-1.4346041942	0.462
				UBBP4	0.269	-2.053527092	0.462
				PTGES3	0.271	-1.4262362559	0.458
				HMGB1	0.272	-1.4714708235	0.456
				PTOV1	0.272	-0.6364394924	0.456
				RBBP7	0.272	-1.4538202093	0.456
				ATP5O	0.728	1.672635376	0.456
				TUBB2A	0.273	-1.371859354	0.454
				C21orf33	0.274	-3.2491999581	0.452
				HSPE1	0.726	1.5249692533	0.452
				HDAC9	0.275	-2.6419583628	0.45
				PHLDA1	0.277	-2.9880194015	0.446
				SPCS2	0.277	-2.0744502448	0.446
				HEY1	0.278	-3.263356263	0.444
				UBL5	0.722	1.3624653822	0.444
				HSPA8	0.721	0.8973965012	0.442
				PIGY	0.28	-6.9250273744	0.44
				TFAP2C	0.28	-4.3967993823	0.44
				ATP5I	0.72	1.7380357173	0.44
				HSP90AA1	0.717	0.7523680642	0.434
				SOX4	0.717	0.8593681016	0.434
				NBPF15	0.284	-0.7845443495	0.432

Tables for single cell RNA sequencing data

<i>DCHS1</i>				<i>FAT4</i>			
gene	myAUC	avg diff	power	gene	myAUC	avg diff	power
				PTGFRN	0.285	-1.9517292287	0.43
				ALG13	0.286	-1.6711637641	0.428
				FDFT1	0.286	-0.7101986342	0.428
				PGAM1	0.287	-2.1427948594	0.426
				H3F3B	0.713	0.7458852162	0.426
				ACLY	0.288	-1.85045338	0.424
				SNURF	0.288	-0.9854655926	0.424
				CCDC14	0.289	-0.5893155637	0.422
				MLLT4	0.289	-0.9131012385	0.422
				TUBA1B	0.289	-1.187328794	0.422
				CCND2	0.29	-1.1220011177	0.42
				EZR	0.29	-0.9442670613	0.42
				SMIM11	0.29	-2.4379778208	0.42
				STAG2	0.29	-0.6676812981	0.42
				C1orf56	0.71	1.710784093	0.42
				CHCHD3	0.291	-0.7238735503	0.418
				STMN2	0.709	1.0667316014	0.418
				NEFM	0.708	1.9594594528	0.416
				GSTM1	0.294	-3.7665971795	0.412
				OFD1	0.294	-1.0023717475	0.412
				DYNLL1	0.706	1.0552903353	0.412
				PGAM4	0.295	-1.8735313683	0.41
				PTPRS	0.704	0.7376208584	0.408
				SLIT2	0.704	0.6149093774	0.408
				MED14	0.297	-1.5938021949	0.406
				NBPF1	0.297	-1.0105349718	0.406
				NFIB	0.297	-1.5073228511	0.406
				HSP90AB1	0.703	0.6027570925	0.406
				CPSF6	0.298	-1.1751757261	0.404
				RASA4	0.298	-3.4947515086	0.404
				TMEM47	0.298	-2.165500402	0.404
				ZIC4	0.702	4.0747335487	0.404
				EIF4G3	0.299	-1.1873205698	0.402
				MAP4K5	0.299	-1.9472322141	0.402
				IGDCC4	0.7	2.0524401123	0.4

A.2 GO terms related to the cytoskeleton (based on genes with a power greater than 0.4)

GO term	Genes
	<i>FAT4 mutant</i>
structural constituent of cytoskeleton	TUBGCP4, TUBB, TUBB2B, TUBB2A, ARPC4, NEFL, TUBA1B, NEFM, TUBA1C
microtubule-based process	TUBB, TUBB2B, DYNLL1, TUBB2A, TUBA1B, TUBA1C
cytoskeleton organization	PDZD8, TUBB2B, TUBB2A, TUBA1C
GTPase activity	RND3, EEF1A1, TUBB, TUBB2B, TUBB2A, TUBA1B, TUBA1C
microtubule	TUBGCP4, TUBB, TUBB2B, DYNLL1, TUBB2A, TUBA1B, TUBA1C
	<i>DCHS1 mutant</i>
microtubule-based process	TUBB, TUBB2B, TUBB2A, TUBA1C
GTPase activity	EEF1A1, TUBB, TUBB2B, TUBB2A, RAP1B, TUBA1C
GTP binding	EEF1A1, TUBB, TUBB2B, TUBB2A, IFI44L, RAP1B, TUBA1C
structural constituent of cytoskeleton	TUBB, TUBB2B, TUBB2A, TUBA1C
microtubule	TUBB, TUBB2B, TUBB2A, TUBA1C
cytoskeleton organization	TUBB2B, TUBB2A, TUBA1C

Bibliography

- Aaku-Saraste, Eeva, Andrea Hellwig, and Wieland B. Huttner (1996). "Loss of Occludin and Functional Tight Junctions, but Not ZO-1, during Neural Tube Closure—Remodeling of the Neuroepithelium Prior to Neurogenesis". In: *Developmental Biology* 180.2, pp. 664–679. ISSN: 0012-1606. DOI: 10.1006/dbio.1996.0336. URL: <http://dx.doi.org/10.1006/dbio.1996.0336>.
- Anderson, S.A. et al. (2001). "Distinct cortical migrations from the medial and lateral ganglionic eminences". In: *Development* 128.3, pp. 353–363. ISSN: 0950-1991. eprint: <http://dev.biologists.org/content/128/3/353.full.pdf>. URL: <http://dev.biologists.org/content/128/3/353>.
- Ayala, Ramsés, Tianzhi Shu, and Li-Huei Tsai (2007). "Treking across the Brain: The Journey of Neuronal Migration". In: *Cell* 128.1, pp. 29–43. ISSN: 0092-8674. DOI: 10.1016/j.cell.2006.12.021. URL: <http://dx.doi.org/10.1016/j.cell.2006.12.021>.
- Badouel, Caroline et al. (2015). "Fat1 interacts with Fat4 to regulate neural tube closure, neural progenitor proliferation and apical constriction during mouse brain development." In: *Development (Cambridge, England)* 142 (16), pp. 2781–2791. ISSN: 1477-9129. DOI: 10.1242/dev.123539.
- Bagherie-Lachidan, Mazdak et al. (2015). "Stromal Fat4 acts non-autonomously with Dchs1/2 to restrict the nephron progenitor pool." In: *Development (Cambridge, England)* 142 (15), pp. 2564–2573. ISSN: 1477-9129. DOI: 10.1242/dev.122648.
- Bahi-Buisson, N. et al. (2014). "The wide spectrum of tubulinopathies: what are the key features for the diagnosis?" In: *Brain* 137.6, pp. 1676–1700. ISSN: 1460-2156. DOI: 10.1093/brain/awu082. URL: <http://dx.doi.org/10.1093/brain/awu082>.
- Barnes, Anthony P. and Franck Polleux (2009). "Establishment of Axon-Dendrite Polarity in Developing Neurons". In: *Annual Review of Neuroscience* 32.1, pp. 347–381. ISSN: 1545-4126. DOI: 10.1146/annurev.neuro.31.060407.125536. URL: <http://dx.doi.org/10.1146/annurev.neuro.31.060407.125536>.
- Bershteyn, Marina et al. (2017). "Human iPSC-Derived Cerebral Organoids Model Cellular Features of Lissencephaly and Reveal Prolonged Mitosis of Outer Radial Glia". In: *Cell Stem Cell*. ISSN: 1934-5909. DOI: 10.1016/j.stem.

- 2016.12.007. URL: <http://dx.doi.org/10.1016/j.stem.2016.12.007>.
- Betizeau, Marion et al. (2013). "Precursor Diversity and Complexity of Lineage Relationships in the Outer Subventricular Zone of the Primate". In: *Neuron* 80.2, pp. 442–457. ISSN: 0896-6273. DOI: 10.1016/j.neuron.2013.09.032. URL: <http://dx.doi.org/10.1016/j.neuron.2013.09.032>.
- Bossuyt, W et al. (2013). "An evolutionary shift in the regulation of the Hippo pathway between mice and flies". In: *Oncogene* 33.10, pp. 1218–1228. ISSN: 1476-5594. DOI: 10.1038/onc.2013.82. URL: <http://dx.doi.org/10.1038/onc.2013.82>.
- Brennand, Kristen J. et al. (2011). "Modelling schizophrenia using human induced pluripotent stem cells". In: *Nature* 473.7346, pp. 221–225. ISSN: 1476-4687. DOI: 10.1038/nature09915. URL: <http://dx.doi.org/10.1038/nature09915>.
- Brennand, K et al. (2014). "Phenotypic differences in hiPSC NPCs derived from patients with schizophrenia". In: *Molecular Psychiatry* 20.3, pp. 361–368. ISSN: 1476-5578. URL: <http://www.ncbi.nlm.nih.gov/pmc/articles/PMC4182344/>.
- Bultje, Ronald S. et al. (2009). "Mammalian Par3 Regulates Progenitor Cell Asymmetric Division via Notch Signaling in the Developing Neocortex". In: *Neuron* 63.2, pp. 189–202. ISSN: 0896-6273. DOI: 10.1016/j.neuron.2009.07.004. URL: <http://dx.doi.org/10.1016/j.neuron.2009.07.004>.
- Camp, J Gray et al. (2015). "Human cerebral organoids recapitulate gene expression programs of fetal neocortex development." eng. In: *Proc Natl Acad Sci U S A* 112.51, pp. 15672–15677. DOI: 10.1073/pnas.1520760112. URL: <http://dx.doi.org/10.1073/pnas.1520760112>.
- Cappello, Silvia et al. (2006). "The Rho-GTPase cdc42 regulates neural progenitor fate at the apical surface." In: *Nature neuroscience* 9 (9), pp. 1099–1107. ISSN: 1097-6256. DOI: 10.1038/nn1744.
- Cappello, Silvia et al. (2012). "A radial glia-specific role of RhoA in double cortex formation." eng. In: *Neuron* 73.5, pp. 911–924. DOI: 10.1016/j.neuron.2011.12.030. URL: <http://dx.doi.org/10.1016/j.neuron.2011.12.030>.
- Cappello, Silvia et al. (2013). "Mutations in genes encoding the cadherin receptor-ligand pair DCHS1 and FAT4 disrupt cerebral cortical development." eng. In: *Nat Genet* 45.11, pp. 1300–1308. DOI: 10.1038/ng.2765. URL: <http://dx.doi.org/10.1038/ng.2765>.

- Carabalona, A. et al. (2011). "A glial origin for periventricular nodular heterotopia caused by impaired expression of Filamin-A". In: *Human Molecular Genetics* 21.5, pp. 1004–1017. ISSN: 1460-2083. DOI: 10.1093/hmg/ddr531. URL: <http://dx.doi.org/10.1093/hmg/ddr531>.
- Chambers, Stuart M et al. (2009). "Highly efficient neural conversion of human ES and iPS cells by dual inhibition of SMAD signaling". In: *Nature Biotechnology* 27.3, pp. 275–280. ISSN: 1087-0156. DOI: 10.1038/nbt.1529. URL: <http://dx.doi.org/10.1038/nbt.1529>.
- Chen, L. et al. (2007). "Rac1 Controls the Formation of Midline Commissures and the Competency of Tangential Migration in Ventral Telencephalic Neurons". In: *Journal of Neuroscience* 27.14, pp. 3884–3893. ISSN: 1529-2401. DOI: 10.1523/jneurosci.3509-06.2007. URL: <http://dx.doi.org/10.1523/JNEUROSCI.3509-06.2007>.
- Choi, Ben H. and Lowell W. Lapham (1978). "Radial glia in the human fetal cerebrum: A combined golgi, immunofluorescent and electron microscopic study". In: *Brain Research* 148.2, pp. 295–311. ISSN: 0006-8993. DOI: 10.1016/0006-8993(78)90721-7. URL: [http://dx.doi.org/10.1016/0006-8993\(78\)90721-7](http://dx.doi.org/10.1016/0006-8993(78)90721-7).
- Clevers, Hans (2016). "Modeling Development and Disease with Organoids". In: *Cell* 165.7, pp. 1586–1597. ISSN: 0092-8674. DOI: 10.1016/j.cell.2016.05.082. URL: <http://dx.doi.org/10.1016/j.cell.2016.05.082>.
- Costa, M. R. et al. (2007). "Par-complex proteins promote proliferative progenitor divisions in the developing mouse cerebral cortex". In: *Development* 135.1, pp. 11–22. ISSN: 1477-9129. DOI: 10.1242/dev.009951. URL: <http://dx.doi.org/10.1242/dev.009951>.
- Cunningham, C. et al. (1992). "Actin-binding protein requirement for cortical stability and efficient locomotion". In: *Science* 255.5042, pp. 325–327. ISSN: 1095-9203. DOI: 10.1126/science.1549777. URL: <http://dx.doi.org/10.1126/science.1549777>.
- Cushion, T. D. et al. (2013). "Overlapping cortical malformations and mutations in TUBB2B and TUBA1A". In: *Brain* 136.2, pp. 536–548. ISSN: 1460-2156. DOI: 10.1093/brain/aws338. URL: <http://dx.doi.org/10.1093/brain/aws338>.
- Del Bene, Filippo et al. (2008). "Regulation of Neurogenesis by Interkinetic Nuclear Migration through an Apical-Basal Notch Gradient". In: *Cell* 134.6, pp. 1055–1065. ISSN: 0092-8674. DOI: 10.1016/j.cell.2008.07.017. URL: <http://dx.doi.org/10.1016/j.cell.2008.07.017>.

- Doetsch, Fiona (2003). "The glial identity of neural stem cells". In: *Nature Neuroscience* 6.11, pp. 1127–1134. ISSN: 1097-6256. DOI: 10.1038/nn1144. URL: <http://dx.doi.org/10.1038/nn1144>.
- Eiraku, Mototsugu et al. (2008). "Self-organized formation of polarized cortical tissues from ESCs and its active manipulation by extrinsic signals." eng. In: *Cell Stem Cell* 3.5, pp. 519–532. DOI: 10.1016/j.stem.2008.09.002. URL: <http://dx.doi.org/10.1016/j.stem.2008.09.002>.
- Eiraku, Mototsugu et al. (2011). "Self-organizing optic-cup morphogenesis in three-dimensional culture." eng. In: *Nature* 472.7341, pp. 51–56. DOI: 10.1038/nature09941. URL: <http://dx.doi.org/10.1038/nature09941>.
- Englund, C. (2005). "Pax6, Tbr2, and Tbr1 Are Expressed Sequentially by Radial Glia, Intermediate Progenitor Cells, and Postmitotic Neurons in Developing Neocortex". In: *Journal of Neuroscience* 25.1, pp. 247–251. ISSN: 1529-2401. DOI: 10.1523/jneurosci.2899-04.2005. URL: <http://dx.doi.org/10.1523/JNEUROSCI.2899-04.2005>.
- Evsyukova, Irina, Charlotte Plestant, and E.S. Anton (2013). "Integrative Mechanisms of Oriented Neuronal Migration in the Developing Brain". In: *Annual Review of Cell and Developmental Biology* 29.1, pp. 299–353. ISSN: 1530-8995. DOI: 10.1146/annurev-cellbio-101512-122400. URL: <http://dx.doi.org/10.1146/annurev-cellbio-101512-122400>.
- Faheem, Muhammad et al. (2015). "Molecular genetics of human primary microcephaly: an overview". In: *BMC Medical Genomics* 8.S1. ISSN: 1755-8794. DOI: 10.1186/1755-8794-8-s1-s4. URL: <http://dx.doi.org/10.1186/1755-8794-8-s1-s4>.
- Farkas, Lilla M. et al. (2008). "Insulinoma-Associated 1 Has a Panneurogenic Role and Promotes the Generation and Expansion of Basal Progenitors in the Developing Mouse Neocortex". In: *Neuron* 60.1, pp. 40–55. ISSN: 0896-6273. DOI: 10.1016/j.neuron.2008.09.020. URL: <http://dx.doi.org/10.1016/j.neuron.2008.09.020>.
- Feng, Yuanyi and Christopher A. Walsh (2004). "The many faces of filamin: A versatile molecular scaffold for cell motility and signalling". In: *Nature Cell Biology* 6.11, pp. 1034–1038. ISSN: 1476-4679. DOI: 10.1038/ncb1104-1034. URL: <http://dx.doi.org/10.1038/ncb1104-1034>.
- Ferland, R. J. et al. (2008). "Disruption of neural progenitors along the ventricular and subventricular zones in periventricular heterotopia". In: *Human Molecular Genetics* 18.3, pp. 497–516. ISSN: 1460-2083. DOI: 10.1093/hmg/ddn377. URL: <http://dx.doi.org/10.1093/hmg/ddn377>.

- Fietz, Simone A et al. (2010). "OSVZ progenitors of human and ferret neocortex are epithelial-like and expand by integrin signaling". In: *Nature Neuroscience* 13.6, pp. 690–699. ISSN: 1546-1726. DOI: 10.1038/nn.2553. URL: <http://dx.doi.org/10.1038/nn.2553>.
- Fish, J. L. et al. (2008). "Making bigger brains-the evolution of neural-progenitor-cell division". In: *Journal of Cell Science* 121.17, pp. 2783–2793. ISSN: 1477-9137. DOI: 10.1242/jcs.023465. URL: <http://dx.doi.org/10.1242/jcs.023465>.
- Flames, Nuria et al. (2004). "Short- and Long-Range Attraction of Cortical GABAergic Interneurons by Neuregulin-1". In: *Neuron* 44.2, pp. 251–261. ISSN: 0896-6273. DOI: 10.1016/j.neuron.2004.09.028. URL: <http://dx.doi.org/10.1016/j.neuron.2004.09.028>.
- Florio, M. and W. B. Huttner (2014). "Neural progenitors, neurogenesis and the evolution of the neocortex". In: *Development* 141.11, pp. 2182–2194. ISSN: 1477-9129. DOI: 10.1242/dev.090571. URL: <http://dx.doi.org/10.1242/dev.090571>.
- Florio, Marta et al. (2015). "Human-specific gene ARHGAP11B promotes basal progenitor amplification and neocortex expansion". In: *Science*, aaa1975.
- Gaiano, Nicholas, Jeffrey S. Nye, and Gord Fishell (2000). "Radial Glial Identity Is Promoted by Notch1 Signaling in the Murine Forebrain". In: *Neuron* 26.2, pp. 395–404. ISSN: 0896-6273. DOI: 10.1016/s0896-6273(00)81172-1. URL: [http://dx.doi.org/10.1016/s0896-6273\(00\)81172-1](http://dx.doi.org/10.1016/s0896-6273(00)81172-1).
- Gal, J. S. (2006). "Molecular and Morphological Heterogeneity of Neural Precursors in the Mouse Neocortical Proliferative Zones". In: *Journal of Neuroscience* 26.3, pp. 1045–1056. ISSN: 1529-2401. DOI: 10.1523/jneurosci.4499-05.2006. URL: <http://dx.doi.org/10.1523/jneurosci.4499-05.2006>.
- Gertz, C. C. and A. R. Kriegstein (2015). "Neuronal Migration Dynamics in the Developing Ferret Cortex". In: *Journal of Neuroscience* 35.42, pp. 14307–14315. ISSN: 1529-2401. DOI: 10.1523/jneurosci.2198-15.2015. URL: <http://dx.doi.org/10.1523/jneurosci.2198-15.2015>.
- Götz, Magdalena and Wieland B. Huttner (2005). "The cell biology of neurogenesis". In: *Nature Reviews Molecular Cell Biology* 6.10, pp. 777–788. DOI: 10.1038/nrm1739. URL: <http://dx.doi.org/10.1038/nrm1739>.
- Govek, Eve-Ellen, Mary E. Hatten, and Linda Van Aelst (2011). "The role of Rho GTPase proteins in CNS neuronal migration". In: *Developmental Neurobiology* 71.6, pp. 528–553. ISSN: 1932-8451. DOI: 10.1002/dneu.20850. URL: <http://dx.doi.org/10.1002/dneu.20850>.

- Halder, G. and R. L. Johnson (2010). "Hippo signaling: growth control and beyond". In: *Development* 138.1, pp. 9–22. ISSN: 1477-9129. DOI: 10.1242/dev.045500. URL: <http://dx.doi.org/10.1242/dev.045500>.
- Hansen, David V. et al. (2010). "Neurogenic radial glia in the outer subventricular zone of human neocortex". In: *Nature* 464.7288, pp. 554–561. ISSN: 1476-4687. DOI: 10.1038/nature08845. URL: <http://dx.doi.org/10.1038/nature08845>.
- Harris, Tony J. C. and Ulrich Tepass (2010). "Adherens junctions: from molecules to morphogenesis". In: *Nature Reviews Molecular Cell Biology* 11.7, pp. 502–514. ISSN: 1471-0080. DOI: 10.1038/nrm2927. URL: <http://dx.doi.org/10.1038/nrm2927>.
- Hartfuss, Eva et al. (2001). "Characterization of CNS Precursor Subtypes and Radial Glia". In: *Developmental Biology* 229.1, pp. 15–30. ISSN: 0012-1606. DOI: 10.1006/dbio.2000.9962. URL: <http://dx.doi.org/10.1006/dbio.2000.9962>.
- Hatakeyama, J. (2004). "Hes genes regulate size, shape and histogenesis of the nervous system by control of the timing of neural stem cell differentiation". In: *Development* 131.22, pp. 5539–5550. ISSN: 1477-9129. DOI: 10.1242/dev.01436. URL: <http://dx.doi.org/10.1242/dev.01436>.
- Haubensak, W. et al. (2004). "Neurons arise in the basal neuroepithelium of the early mammalian telencephalon: A major site of neurogenesis". In: *Proceedings of the National Academy of Sciences* 101.9, pp. 3196–3201. ISSN: 1091-6490. DOI: 10.1073/pnas.0308600100. URL: <http://dx.doi.org/10.1073/pnas.0308600100>.
- Heins, Nico et al. (2002). "Glial cells generate neurons: the role of the transcription factor Pax6". In: *Nature Neuroscience* 5.4, pp. 308–315. ISSN: 1097-6256. DOI: 10.1038/nn828. URL: <http://dx.doi.org/10.1038/nn828>.
- Hevner, Robert F. (2015). "Brain overgrowth in disorders of RTK–PI3K–AKT signaling: A mosaic of malformations". In: *Seminars in Perinatology* 39.1, pp. 36–43. ISSN: 0146-0005. DOI: 10.1053/j.semperi.2014.10.006. URL: <http://dx.doi.org/10.1053/j.semperi.2014.10.006>.
- Hou, Lingmi et al. (2016). "FAT4 functions as a tumor suppressor in triple-negative breast cancer". In: *Tumor Biology* 37.12, pp. 16337–16343. ISSN: 1423-0380. DOI: 10.1007/s13277-016-5421-3. URL: <http://dx.doi.org/10.1007/s13277-016-5421-3>.
- Imai, F. (2006). "Inactivation of aPKC results in the loss of adherens junctions in neuroepithelial cells without affecting neurogenesis in mouse neocortex".

- In: *Development* 133.9, pp. 1735–1744. ISSN: 1477-9129. DOI: 10.1242/dev.02330. URL: <http://dx.doi.org/10.1242/dev.02330>.
- Ishiuchi, Takashi et al. (2009). “Mammalian Fat and Dachshous cadherins regulate apical membrane organization in the embryonic cerebral cortex.” In: *The Journal of cell biology* 185 (6), pp. 959–967. ISSN: 1540-8140. DOI: 10.1083/jcb.200811030.
- Johansson, P. A. et al. (2013). “The transcription factor Otx2 regulates choroid plexus development and function”. In: *Development* 140.5, pp. 1055–1066. ISSN: 1477-9129. DOI: 10.1242/dev.090860. URL: <http://dx.doi.org/10.1242/dev.090860>.
- Jones, Chonnetia and Ping Chen (2007). “Planar cell polarity signaling in vertebrates”. In: *BioEssays* 29.2, pp. 120–132. ISSN: 1521-1878. DOI: 10.1002/bies.20526. URL: <http://dx.doi.org/10.1002/bies.20526>.
- Jossin, Yves and Jonathan A Cooper (2011). “Reelin, Rap1 and N-cadherin orient the migration of multipolar neurons in the developing neocortex”. In: *Nature Neuroscience* 14.6, pp. 697–703. ISSN: 1546-1726. DOI: 10.1038/nn.2816. URL: <http://dx.doi.org/10.1038/nn.2816>.
- Junghans, Dirk et al. (2005). “ β -catenin-mediated cell-adhesion is vital for embryonic forebrain development”. In: *Developmental Dynamics* 233.2, pp. 528–539. ISSN: 1097-0177. DOI: 10.1002/dvdy.20365. URL: <http://dx.doi.org/10.1002/dvdy.20365>.
- Kadoshima, Taisuke et al. (2013). “Self-organization of axial polarity, inside-out layer pattern, and species-specific progenitor dynamics in human ES cell-derived neocortex.” eng. In: *Proc Natl Acad Sci U S A* 110.50, pp. 20284–20289. DOI: 10.1073/pnas.1315710110. URL: <http://dx.doi.org/10.1073/pnas.1315710110>.
- Kadowaki, Masakazu et al. (2007). “N-cadherin mediates cortical organization in the mouse brain”. In: *Developmental Biology* 304.1, pp. 22–33. DOI: 10.1016/j.ydbio.2006.12.014. URL: <http://dx.doi.org/10.1016/j.ydbio.2006.12.014>.
- Kawauchi, T. (2003). “The in vivo roles of STEF/Tiam1, Rac1 and JNK in cortical neuronal migration”. In: *The EMBO Journal* 22.16, pp. 4190–4201. ISSN: 1460-2075. DOI: 10.1093/emboj/cdg413. URL: <http://dx.doi.org/10.1093/emboj/cdg413>.
- Kielar, Michel et al. (2014). “Mutations in Eml1 lead to ectopic progenitors and neuronal heterotopia in mouse and human.” eng. In: *Nat Neurosci* 17.7, pp. 923–933. DOI: 10.1038/nn.3729. URL: <http://dx.doi.org/10.1038/nn.3729>.

- Kosodo, Yoichi et al. (2008). "Cytokinesis of neuroepithelial cells can divide their basal process before anaphase". In: *The EMBO Journal* 27.23, pp. 3151–3163. ISSN: 1460-2075. DOI: 10.1038/emboj.2008.227. URL: <http://dx.doi.org/10.1038/emboj.2008.227>.
- Kriegstein, Arnold R. and Magdalena Götz (2003). "Radial glia diversity: A matter of cell fate". In: *Glia* 43.1, pp. 37–43. ISSN: 0894-1491. DOI: 10.1002/glia.10250. URL: <http://dx.doi.org/10.1002/glia.10250>.
- Kriegstein, Arnold R. and Stephen C Noctor (2004). "Patterns of neuronal migration in the embryonic cortex". In: *Trends in Neurosciences* 27.7, pp. 392–399. DOI: 10.1016/j.tins.2004.05.001. URL: <http://dx.doi.org/10.1016/j.tins.2004.05.001>.
- Kurabayashi, N., M. D. Nguyen, and K. Sanada (2013). "The G protein-coupled receptor GPRC5B contributes to neurogenesis in the developing mouse neocortex". In: *Development* 140.21, pp. 4335–4346. ISSN: 1477-9129. DOI: 10.1242/dev.099754. URL: <http://dx.doi.org/10.1242/dev.099754>.
- Kuta, Anna et al. (2016). "Fat4-Dchs1 signalling controls cell proliferation in developing vertebrae." In: *Development (Cambridge, England)* 143 (13), pp. 2367–2375. ISSN: 1477-9129. DOI: 10.1242/dev.131037.
- Lancaster, Madeline A and Juergen A Knoblich (2012). "Spindle orientation in mammalian cerebral cortical development". In: *Current Opinion in Neurobiology* 22.5, pp. 737–746. ISSN: 0959-4388. DOI: 10.1016/j.conb.2012.04.003. URL: <http://dx.doi.org/10.1016/j.conb.2012.04.003>.
- (2014). "Generation of cerebral organoids from human pluripotent stem cells." In: *Nature protocols* 9 (10), pp. 2329–2340. ISSN: 1750-2799. DOI: 10.1038/nprot.2014.158.
- Lancaster, Madeline A. et al. (2013). "Cerebral organoids model human brain development and microcephaly." eng. In: *Nature* 501.7467, pp. 373–379. DOI: 10.1038/nature12517. URL: <http://dx.doi.org/10.1038/nature12517>.
- Lawrence, Peter A., Gary Struhl, and José Casal (2008). "Do the protocadherins Fat and Dachshous link up to determine both planar cell polarity and the dimensions of organs?" In: *Nature Cell Biology* 10.12, pp. 1379–1382. ISSN: 1476-4679. DOI: 10.1038/ncb1208-1379. URL: <http://dx.doi.org/10.1038/ncb1208-1379>.
- Leventer, Richard J, Renzo Guerrini, and William B Dobyns (2008). "Malformations of cortical development and epilepsy". In: *Dialogues in Clinical Neuroscience* 10.1, pp. 47–62. ISSN: 1958-5969. URL: <http://www.ncbi.nlm.nih.gov/pmc/articles/PMC3181860/>.

- Liu, Judy S. (2011). "Molecular Genetics of Neuronal Migration Disorders". In: *Current Neurology and Neuroscience Reports* 11.2, pp. 171–178. DOI: 10.1007/s11910-010-0176-5. URL: <http://dx.doi.org/10.1007/s11910-010-0176-5>.
- Malatesta, P., E. Hartfuss, and M. Gotz (2000). "Isolation of radial glial cells by fluorescent-activated cell sorting reveals a neuronal lineage". In: *Development* 127.24, pp. 5253–5263. ISSN: 0950-1991. eprint: <http://dev.biologists.org/content/127/24/5253.full.pdf>. URL: <http://dev.biologists.org/content/127/24/5253>.
- Malatesta, Paolo, Irene Appolloni, and Filippo Calzolari (2007). "Radial glia and neural stem cells". In: *Cell and Tissue Research* 331.1, pp. 165–178. ISSN: 1432-0878. DOI: 10.1007/s00441-007-0481-8. URL: <http://dx.doi.org/10.1007/s00441-007-0481-8>.
- Manabe, Naoyuki et al. (2002). "Association of ASIP/mPAR-3 with adherens junctions of mouse neuroepithelial cells". In: *Developmental Dynamics* 225.1, pp. 61–69. ISSN: 1097-0177. DOI: 10.1002/dvdy.10139. URL: <http://dx.doi.org/10.1002/dvdy.10139>.
- Mansour, Sahar et al. (2012). "Van Maldergem syndrome: further characterisation and evidence for neuronal migration abnormalities and autosomal recessive inheritance". In: *European Journal of Human Genetics* 20.10, pp. 1024–1031. ISSN: 1476-5438. DOI: 10.1038/ejhg.2012.57. URL: <http://dx.doi.org/10.1038/ejhg.2012.57>.
- Mao, Yaopan et al. (2011). "Characterization of a Dchs1 mutant mouse reveals requirements for Dchs1-Fat4 signaling during mammalian development." In: *Development (Cambridge, England)* 138 (5), pp. 947–957. ISSN: 1477-9129. DOI: 10.1242/dev.057166.
- Mao, Yaopan et al. (2016). "Dchs1-Fat4 regulation of polarized cell behaviours during skeletal morphogenesis". In: *Nature Communications* 7, p. 11469. ISSN: 2041-1723. DOI: 10.1038/ncomms11469. URL: <http://dx.doi.org/10.1038/ncomms11469>.
- Mariani, Jessica et al. (2015). "FOXP1-Dependent Dysregulation of GABA/Glutamate Neuron Differentiation in Autism Spectrum Disorders". In: *Cell* 162.2, pp. 375–390. ISSN: 0092-8674. DOI: 10.1016/j.cell.2015.06.034. URL: <http://dx.doi.org/10.1016/j.cell.2015.06.034>.
- Marin, O. (2001). "Sorting of Striatal and Cortical Interneurons Regulated by Semaphorin-Neuropilin Interactions". In: *Science* 293.5531, pp. 872–875. ISSN: 1095-9203. DOI: 10.1126/science.1061891. URL: <http://dx.doi.org/10.1126/science.1061891>.

- Marín, Oscar (2013). "Cellular and molecular mechanisms controlling the migration of neocortical interneurons". In: *European Journal of Neuroscience* 38.1, pp. 2019–2029. ISSN: 0953-816X. DOI: 10.1111/ejn.12225. URL: <http://dx.doi.org/10.1111/ejn.12225>.
- Martínez-Martínez, María Ángeles et al. (2016). "A restricted period for formation of outer subventricular zone defined by Cdh1 and Trnp1 levels". In: *Nature Communications* 7, p. 11812. ISSN: 2041-1723. DOI: 10.1038/ncomms11812. URL: <http://dx.doi.org/10.1038/ncomms11812>.
- Matakatsu, H. (2004). "Interactions between Fat and Dachshous and the regulation of planar cell polarity in the Drosophila wing". In: *Development* 131.15, pp. 3785–3794. ISSN: 1477-9129. DOI: 10.1242/dev.01254. URL: <http://dx.doi.org/10.1242/dev.01254>.
- Matakatsu, Hitoshi and Seth S. Blair (2006). "Separating the adhesive and signaling functions of the Fat and Dachshous protocadherins." eng. In: *Development* 133.12, pp. 2315–2324. DOI: 10.1242/dev.02401. URL: <http://dx.doi.org/10.1242/dev.02401>.
- Miyata, T. (2004). "Asymmetric production of surface-dividing and non-surface-dividing cortical progenitor cells". In: *Development* 131.13, pp. 3133–3145. ISSN: 1477-9129. DOI: 10.1242/dev.01173. URL: <http://dx.doi.org/10.1242/dev.01173>.
- Miyata, Takaki et al. (2001). "Asymmetric Inheritance of Radial Glial Fibers by Cortical Neurons". In: *Neuron* 31.5, pp. 727–741. ISSN: 0896-6273. DOI: 10.1016/s0896-6273(01)00420-2. URL: [http://dx.doi.org/10.1016/s0896-6273\(01\)00420-2](http://dx.doi.org/10.1016/s0896-6273(01)00420-2).
- Miyata, Takaki et al. (2015). "Interkinetic nuclear migration generates and opposes ventricular-zone crowding: insight into tissue mechanics". In: *Frontiers in Cellular Neuroscience* 8. ISSN: 1662-5102. DOI: 10.3389/fncel.2014.00473. URL: <http://dx.doi.org/10.3389/fncel.2014.00473>.
- Miyoshi, Goichi and Gord Fishell (2012). "Dynamic FoxG1 Expression Coordinates the Integration of Multipolar Pyramidal Neuron Precursors into the Cortical Plate". In: *Neuron* 74.6, pp. 1045–1058. ISSN: 0896-6273. DOI: 10.1016/j.neuron.2012.04.025. URL: <http://dx.doi.org/10.1016/j.neuron.2012.04.025>.
- Mizutani, Ken-ichi et al. (2007). "Differential Notch signalling distinguishes neural stem cells from intermediate progenitors". In: *Nature* 449.7160, pp. 351–355. ISSN: 1476-4687. DOI: 10.1038/nature06090. URL: <http://dx.doi.org/10.1038/nature06090>.

- Nadarajah, Bagirathy (2003). "Radial glia and somal translocation of radial neurons in the developing cerebral cortex". In: *Glia* 43.1, pp. 33–36. ISSN: 1098-1136. DOI: 10.1002/glia.10245. URL: <http://dx.doi.org/10.1002/glia.10245>.
- Nagano, T. (2004). "Filamin A and FILIP (Filamin A-Interacting Protein) Regulate Cell Polarity and Motility in Neocortical Subventricular and Intermediate Zones during Radial Migration". In: *Journal of Neuroscience* 24.43, pp. 9648–9657. ISSN: 1529-2401. DOI: 10.1523/jneurosci.2363-04.2004. URL: <http://dx.doi.org/10.1523/JNEUROSCI.2363-04.2004>.
- Nakamura, Fumihiko, Thomas P. Stossel, and John H. Hartwig (2011). "The filamins". In: *Cell Adhesion & Migration* 5.2, pp. 160–169. ISSN: 1933-6926. DOI: 10.4161/cam.5.2.14401. URL: <http://dx.doi.org/10.4161/cam.5.2.14401>.
- Noctor, Stephen C. et al. (2001). "Neurons derived from radial glial cells establish radial units in neocortex". In: *Nature* 409.6821, pp. 714–720. ISSN: 0028-0836. DOI: 10.1038/35055553. URL: <http://dx.doi.org/10.1038/35055553>.
- Noctor, Stephen C et al. (2004). "Cortical neurons arise in symmetric and asymmetric division zones and migrate through specific phases". In: *Nature Neuroscience* 7.2, pp. 136–144. ISSN: 1097-6256. DOI: 10.1038/nn1172. URL: <http://dx.doi.org/10.1038/nn1172>.
- Nosten-Bertrand, Marika et al. (2008). "Epilepsy in Dcx Knockout Mice Associated with Discrete Lamination Defects and Enhanced Excitability in the Hippocampus". In: *PLoS ONE* 3.6. Ed. by KenjiEditor Hashimoto, e2473. ISSN: 1932-6203. DOI: 10.1371/journal.pone.0002473. URL: <http://dx.doi.org/10.1371/journal.pone.0002473>.
- Nowakowski, Tomasz J. et al. (2016). "Transformation of the Radial Glia Scaffold Demarcates Two Stages of Human Cerebral Cortex Development". In: *Neuron* 91.6, pp. 1219–1227. ISSN: 0896-6273. DOI: 10.1016/j.neuron.2016.09.005. URL: <http://dx.doi.org/10.1016/j.neuron.2016.09.005>.
- Ohshima, T. et al. (2007). "Cdk5 is required for multipolar-to-bipolar transition during radial neuronal migration and proper dendrite development of pyramidal neurons in the cerebral cortex". In: *Development* 134.12, pp. 2273–2282. ISSN: 1477-9129. DOI: 10.1242/dev.02854. URL: <http://dx.doi.org/10.1242/dev.02854>.
- Ostrem, Bridget E.L. et al. (2014). "Control of Outer Radial Glial Stem Cell Mitosis in the Human Brain". In: *Cell Reports* 8.3, pp. 656–664. ISSN: 2211-1247. DOI:

- 10.1016/j.celrep.2014.06.058. URL: <http://dx.doi.org/10.1016/j.celrep.2014.06.058>.
- Papakrivopoulou, E. et al. (2013). "Planar cell polarity and the kidney". In: *Nephrology Dialysis Transplantation* 29.7, pp. 1320–1326. ISSN: 1460-2385. DOI: 10.1093/ndt/gft484. URL: <http://dx.doi.org/10.1093/ndt/gft484>.
- Paridaen, J. T. and W. B. Huttner (2014). "Neurogenesis during development of the vertebrate central nervous system". In: *EMBO reports* 15.4, pp. 351–364. ISSN: 1469-3178. DOI: 10.1002/embr.201438447. URL: <http://dx.doi.org/10.1002/embr.201438447>.
- Park, Donghyun et al. (2009). "The radial glia antibody RC2 recognizes a protein encoded by Nestin". In: *Biochemical and Biophysical Research Communications* 382.3, pp. 588–592. ISSN: 0006-291X. DOI: 10.1016/j.bbrc.2009.03.074. URL: <http://dx.doi.org/10.1016/j.bbrc.2009.03.074>.
- Pinto, Luisa et al. (2009). "AP2 γ regulates basal progenitor fate in a region- and layer-specific manner in the developing cortex". In: *Nature Neuroscience* 12.10, pp. 1229–1237. ISSN: 1546-1726. DOI: 10.1038/nn.2399. URL: <http://dx.doi.org/10.1038/nn.2399>.
- Qian, Xuyu et al. (2016). "Brain-Region-Specific Organoids Using Mini-bioreactors for Modeling ZIKV Exposure." eng. In: *Cell*. DOI: 10.1016/j.cell.2016.04.032. URL: <http://dx.doi.org/10.1016/j.cell.2016.04.032>.
- Quinn, Jane C. et al. (2007). "Pax6 controls cerebral cortical cell number by regulating exit from the cell cycle and specifies cortical cell identity by a cell autonomous mechanism". In: *Developmental Biology* 302.1, pp. 50–65. ISSN: 0012-1606. DOI: 10.1016/j.ydbio.2006.08.035. URL: <http://dx.doi.org/10.1016/j.ydbio.2006.08.035>.
- R Development Core Team (2008). *R: A Language and Environment for Statistical Computing*. ISBN 3-900051-07-0. R Foundation for Statistical Computing. Vienna, Austria. URL: <http://www.R-project.org>.
- Ragni, Chiara V. et al. (2017). "Amotl1 mediates sequestration of the Hippo effector Yap1 downstream of Fat4 to restrict heart growth". In: *Nature Communications* 8, p. 14582. ISSN: 2041-1723. DOI: 10.1038/ncomms14582. URL: <http://dx.doi.org/10.1038/ncomms14582>.
- Rakic, Pasko (1972). "Mode of cell migration to the superficial layers of fetal monkey neocortex". In: *The Journal of Comparative Neurology* 145.1, pp. 61–83. ISSN: 1096-9861. DOI: 10.1002/cne.901450105. URL: <http://dx.doi.org/10.1002/cne.901450105>.

- Ramos, R. L. (2005). "Heterotopia Formation in Rat but Not Mouse Neocortex after RNA Interference Knockdown of DCX". In: *Cerebral Cortex* 16.9, pp. 1323–1331. ISSN: 1460-2199. DOI: 10.1093/cercor/bhj074. URL: <http://dx.doi.org/10.1093/cercor/bhj074>.
- Reillo, I. et al. (2010). "A Role for Intermediate Radial Glia in the Tangential Expansion of the Mammalian Cerebral Cortex". In: *Cerebral Cortex* 21.7, pp. 1674–1694. ISSN: 1460-2199. DOI: 10.1093/cercor/bhq238. URL: <http://dx.doi.org/10.1093/cercor/bhq238>.
- Saburi, Sakura et al. (2008). "Loss of Fat4 disrupts PCP signaling and oriented cell division and leads to cystic kidney disease." In: *Nature genetics* 40 (8), pp. 1010–1015. ISSN: 1546-1718. DOI: 10.1038/ng.179.
- Sapir, T. (1997). "Reduction of microtubule catastrophe events by LIS1, platelet-activating factor acetylhydrolase subunit". In: *The EMBO Journal* 16.23, pp. 6977–6984. ISSN: 1460-2075. DOI: 10.1093/emboj/16.23.6977. URL: <http://dx.doi.org/10.1093/emboj/16.23.6977>.
- Sasaki, Shinji et al. (2000). "A LIS1/NUDEL/Cytoplasmic Dynein Heavy Chain Complex in the Developing and Adult Nervous System". In: *Neuron* 28.3, pp. 681–696. ISSN: 0896-6273. DOI: 10.1016/s0896-6273(00)00146-x. URL: [http://dx.doi.org/10.1016/s0896-6273\(00\)00146-x](http://dx.doi.org/10.1016/s0896-6273(00)00146-x).
- Schaar, B. T. and S. K. McConnell (2005). "Cytoskeletal coordination during neuronal migration". In: *Proceedings of the National Academy of Sciences* 102.38, pp. 13652–13657. ISSN: 1091-6490. DOI: 10.1073/pnas.0506008102. URL: <http://dx.doi.org/10.1073/pnas.0506008102>.
- Schenk, J. et al. (2009). "Myosin II is required for interkinetic nuclear migration of neural progenitors". In: *Proceedings of the National Academy of Sciences* 106.38, pp. 16487–16492. ISSN: 1091-6490. DOI: 10.1073/pnas.0908928106. URL: <http://dx.doi.org/10.1073/pnas.0908928106>.
- Schindelin, Johannes et al. (2012). "Fiji: an open-source platform for biological-image analysis". In: *Nature Methods* 9.7, pp. 676–682. ISSN: 1548-7105. DOI: 10.1038/nmeth.2019. URL: <http://dx.doi.org/10.1038/nmeth.2019>.
- Schmechel, Donald E. and Pasko Rakic (1979). "A golgi study of radial glial cells in developing monkey telencephalon: Morphogenesis and transformation into astrocytes". In: *Anatomy and Embryology* 156.2, pp. 115–152. ISSN: 1432-0568. DOI: 10.1007/bf00300010. URL: <http://dx.doi.org/10.1007/BF00300010>.
- Schmid, Marie-Theres et al. (2014). "The role of $\hat{I}\pm$ -E-catenin in cerebral cortex development: radial glia specific effect on neuronal migration". In: *Frontiers*

- in Cellular Neuroscience* 8. DOI: 10.3389/fncel.2014.00215. URL: <http://dx.doi.org/10.3389/fncel.2014.00215>.
- Schulze, E. (1987). "Posttranslational modification and microtubule stability". In: *The Journal of Cell Biology* 105.5, pp. 2167–2177. ISSN: 1540-8140. DOI: 10.1083/jcb.105.5.2167. URL: <http://dx.doi.org/10.1083/jcb.105.5.2167>.
- Sessa, A. et al. (2010). "Tbr2-positive intermediate (basal) neuronal progenitors safeguard cerebral cortex expansion by controlling amplification of pallial glutamatergic neurons and attraction of subpallial GABAergic interneurons". In: *Genes & Development* 24.16, pp. 1816–1826. ISSN: 0890-9369. DOI: 10.1101/gad.575410. URL: <http://dx.doi.org/10.1101/gad.575410>.
- Shen, Qin et al. (2002). "Asymmetric Numb distribution is critical for asymmetric cell division of mouse cerebral cortical stem cells and neuroblasts". In: *Development* 129.20, pp. 4843–4853. ISSN: 0950-1991. eprint: <http://dev.biologists.org/content/129/20/4843.full.pdf>. URL: <http://dev.biologists.org/content/129/20/4843>.
- Shimajima, Keiko et al. (2015). "CHCHD2 is down-regulated in neuronal cells differentiated from iPS cells derived from patients with lissencephaly". In: *Genomics* 106.4, pp. 196–203. ISSN: 0888-7543. DOI: 10.1016/j.ygeno.2015.07.001. URL: <http://dx.doi.org/10.1016/j.ygeno.2015.07.001>.
- Singh, Shalini and David J. Solecki (2015). "Polarity transitions during neurogenesis and germinal zone exit in the developing central nervous system". In: *Frontiers in Cellular Neuroscience* 9. ISSN: 1662-5102. DOI: 10.3389/fncel.2015.00062. URL: <http://dx.doi.org/10.3389/fncel.2015.00062>.
- Smart, I H (1972). "Proliferative characteristics of the ependymal layer during the early development of the mouse diencephalon, as revealed by recording the number, location, and plane of cleavage of mitotic figures." In: *Journal of Anatomy* 113.Pt 1, pp. 109–129. ISSN: 1469-7580. URL: <http://www.ncbi.nlm.nih.gov/pmc/articles/PMC1271371/>.
- Srikanth, Priya and Tracy L. Young-Pearse (2014). "Stem Cells on the Brain: Modeling Neurodevelopmental and Neurodegenerative Diseases Using Human Induced Pluripotent Stem Cells". In: *Journal of Neurogenetics* 28.1-2, pp. 5–29. ISSN: 1563-5260. DOI: 10.3109/01677063.2014.881358. URL: <http://dx.doi.org/10.3109/01677063.2014.881358>.
- Stahl, Ronny et al. (2013). "Trnp1 Regulates Expansion and Folding of the Mammalian Cerebral Cortex by Control of Radial Glial Fate". In: *Cell* 153.3, pp. 535–549. ISSN: 0092-8674. DOI: 10.1016/j.cell.2013.03.027. URL: <http://dx.doi.org/10.1016/j.cell.2013.03.027>.

- Stancik, E. K. et al. (2010). "Heterogeneity in Ventricular Zone Neural Precursors Contributes to Neuronal Fate Diversity in the Postnatal Neocortex". In: *Journal of Neuroscience* 30.20, pp. 7028–7036. ISSN: 1529-2401. DOI: 10.1523/jneurosci.6131-09.2010. URL: <http://dx.doi.org/10.1523/JNEUROSCI.6131-09.2010>.
- Tabata, H., S. Kanatani, and K. Nakajima (2009). "Differences of Migratory Behavior between Direct Progeny of Apical Progenitors and Basal Progenitors in the Developing Cerebral Cortex". In: *Cerebral Cortex* 19.9, pp. 2092–2105. ISSN: 1460-2199. DOI: 10.1093/cercor/bhn227. URL: <http://dx.doi.org/10.1093/cercor/bhn227>.
- Tabata, Hidenori and Kazunori Nakajima (2003). "Multipolar Migration: The Third Mode of Radial Neuronal Migration in the Developing Cerebral Cortex". In: *Journal of Neuroscience* 23.31, pp. 9996–10001. ISSN: 0270-6474. eprint: <http://www.jneurosci.org/content/23/31/9996.full.pdf>. URL: <http://www.jneurosci.org/content/23/31/9996>.
- Takai, Yoshimi et al. (2008). "The Immunoglobulin-Like Cell Adhesion Molecule Nectin and Its Associated Protein Afadin". In: *Annual Review of Cell and Developmental Biology* 24.1, pp. 309–342. ISSN: 1530-8995. DOI: 10.1146/annurev.cellbio.24.110707.175339. URL: <http://dx.doi.org/10.1146/annurev.cellbio.24.110707.175339>.
- Tanaka, Teruyuki et al. (2004). "Lis1 and doublecortin function with dynein to mediate coupling of the nucleus to the centrosome in neuronal migration". In: *The Journal of Cell Biology* 165.5, pp. 709–721. ISSN: 1540-8140. DOI: 10.1083/jcb.200309025. URL: <http://dx.doi.org/10.1083/jcb.200309025>.
- Taverna, Elena and Wieland B. Huttner (2010). "Neural Progenitor Nuclei IN Motion". In: *Neuron* 67.6, pp. 906–914. ISSN: 0896-6273. DOI: 10.1016/j.neuron.2010.08.027. URL: <http://dx.doi.org/10.1016/j.neuron.2010.08.027>.
- Thomas, Chloe and David Strutt (2011). "The roles of the cadherins Fat and Dachshous in planar polarity specification in Drosophila". In: *Developmental Dynamics* 241.1, pp. 27–39. ISSN: 1058-8388. DOI: 10.1002/dvdy.22736. URL: <http://dx.doi.org/10.1002/dvdy.22736>.
- Topol, Aaron, Ngoc N Tran, and Kristen J Brennand (2015). "A guide to generating and using hiPSC derived NPCs for the study of neurological diseases." In: *Journal of visualized experiments : JoVE* (96), e52495. ISSN: 1940-087X. DOI: 10.3791/52495.

- Tsai, Li-Huei and Joseph G Gleeson (2005). "Nucleokinesis in neuronal migration." In: *Neuron* 46 (3), pp. 383–388. ISSN: 0896-6273. DOI: 10.1016/j.neuron.2005.04.013.
- Tsai, Jin-Wu et al. (2010). "Kinesin 3 and cytoplasmic dynein mediate interkinetic nuclear migration in neural stem cells". In: *Nature Neuroscience* 13.12, pp. 1463–1471. ISSN: 1546-1726. DOI: 10.1038/nn.2665. URL: <http://dx.doi.org/10.1038/nn.2665>.
- Turner, David A., Peter Baillie-Johnson, and Alfonso Martinez Arias (2015). "Organoids and the genetically encoded self-assembly of embryonic stem cells". In: *BioEssays* 38.2, pp. 181–191. ISSN: 0265-9247. DOI: 10.1002/bies.201500111. URL: <http://dx.doi.org/10.1002/bies.201500111>.
- Tyler, W. A. and T. F. Haydar (2013). "Multiplex Genetic Fate Mapping Reveals a Novel Route of Neocortical Neurogenesis, Which Is Altered in the Ts65Dn Mouse Model of Down Syndrome". In: *Journal of Neuroscience* 33.12, pp. 5106–5119. ISSN: 1529-2401. DOI: 10.1523/jneurosci.5380-12.2013. URL: <http://dx.doi.org/10.1523/JNEUROSCI.5380-12.2013>.
- Vallee, Richard B. et al. (2000). "A role for the lissencephaly gene LIS1 in mitosis and cytoplasmic dynein function." In: *Nature Cell Biology* 2.11, pp. 784–791. ISSN: 1465-7392. DOI: 10.1038/35041020. URL: <http://dx.doi.org/10.1038/35041020>.
- Vierbuchen, Thomas et al. (2010). "Direct conversion of fibroblasts to functional neurons by defined factors". In: *Nature* 463.7284, pp. 1035–1041. ISSN: 1476-4687. DOI: 10.1038/nature08797. URL: <http://dx.doi.org/10.1038/nature08797>.
- Li-Villarreal, Nanbing et al. (2015). "Dachsous1b cadherin regulates actin and microtubule cytoskeleton during early zebrafish embryogenesis." eng. In: *Development*. DOI: 10.1242/dev.119800. URL: <http://dx.doi.org/10.1242/dev.119800>.
- Vladar, Eszter K. et al. (2015). "Observing planar cell polarity in multiciliated mouse airway epithelial cells". In: *Methods in Cell Biology*, pp. 37–54. ISSN: 0091-679X. DOI: 10.1016/bs.mcb.2015.01.016. URL: <http://dx.doi.org/10.1016/bs.mcb.2015.01.016>.
- Walsh, Christopher A (1999). "Genetic Malformations of the Human Cerebral Cortex". In: *Neuron* 23.1, pp. 19–29. ISSN: 0896-6273. DOI: 10.1016/s0896-6273(00)80749-7. URL: [http://dx.doi.org/10.1016/s0896-6273\(00\)80749-7](http://dx.doi.org/10.1016/s0896-6273(00)80749-7).
- Wang, S. et al. (2013). "Nudel/NudE and Lis1 promote dynein and dynactin interaction in the context of spindle morphogenesis". In: *Molecular Biology of*

- the Cell* 24.22, pp. 3522–3533. ISSN: 1059-1524. DOI: 10.1091/mbc.e13-05-0283. URL: <http://dx.doi.org/10.1091/mbc.E13-05-0283>.
- Wynshaw-Boris, Anthony et al. (1998). “Graded reduction of Pafah1b1 (Lis1) activity results in neuronal migration defects and early embryonic lethality.” In: *Nature Genetics* 19.4, pp. 333–339. ISSN: 1061-4036. DOI: 10.1038/1221. URL: <http://dx.doi.org/10.1038/1221>.
- Xie, Zhigang et al. (2007). “Cep120 and TACCs Control Interkinetic Nuclear Migration and the Neural Progenitor Pool”. In: *Neuron* 56.1, pp. 79–93. ISSN: 0896-6273. DOI: 10.1016/j.neuron.2007.08.026. URL: <http://dx.doi.org/10.1016/j.neuron.2007.08.026>.
- Xu, Yingjie et al. (2010). “Filamin A regulates focal adhesion disassembly and suppresses breast cancer cell migration and invasion”. In: *The Journal of Experimental Medicine* 207.11, pp. 2421–2437. ISSN: 1540-9538. DOI: 10.1084/jem.20100433. URL: <http://dx.doi.org/10.1084/jem.20100433>.
- Yamamoto, Hideaki et al. (2015). “Impairment of radial glial scaffold-dependent neuronal migration and formation of double cortex by genetic ablation of afadin.” eng. In: *Brain Res* 1620, pp. 139–152. DOI: 10.1016/j.brainres.2015.05.012. URL: <http://dx.doi.org/10.1016/j.brainres.2015.05.012>.
- Yoon, Ki-Jun et al. (2014). “Modeling a Genetic Risk for Schizophrenia in iPSCs and Mice Reveals Neural Stem Cell Deficits Associated with Adherens Junctions and Polarity”. In: *Cell Stem Cell* 15.1, pp. 79–91. ISSN: 1934-5909. DOI: 10.1016/j.stem.2014.05.003. URL: <http://dx.doi.org/10.1016/j.stem.2014.05.003>.
- Zakaria, Sana et al. (2014). “Regulation of Neuronal Migration by Dchs1-Fat4 Planar Cell Polarity”. In: *Current Biology* 24.14, pp. 1620–1627. DOI: 10.1016/j.cub.2014.05.067. URL: <http://dx.doi.org/10.1016/j.cub.2014.05.067>.
- Zimmer, Geraldine et al. (2008). “Ephrin-A5 acts as a repulsive cue for migrating cortical interneurons”. In: *European Journal of Neuroscience* 28.1, pp. 62–73. ISSN: 0953-816X. DOI: 10.1111/j.1460-9568.2008.06320.x. URL: <http://dx.doi.org/10.1111/j.1460-9568.2008.06320.x>.